REFERENCE ONLY

UNIVERSITY OF LONDON THESIS

Degree MD Year 2006 Name of Author DAVIES M-V.

COPYRIGHT

This is a thesis accepted for a Higher Degree of the University of London. It is an unpublished typescript and the copyright is held by the author. All persons consulting the thesis must read and abide by the Copyright Declaration below.

COPYRIGHT DECLARATION

I recognise that the copyright of the above-described thesis rests with the author and that no quotation from it or information derived from it may be published without the prior written consent of the author.

LOANS

Theses may not be lent to individuals, but the Senate House Library may lend a copy to approved libraries within the United Kingdom, for consultation solely on the premises of those libraries. Application should be made to: Inter-Library Loans, Senate House Library, Senate House, Malet Street, London WC1E 7HU.

REPRODUCTION

University of London theses may not be reproduced without explicit written permission from the Senate House Library. Enquiries should be addressed to the Theses Section of the Library. Regulations concerning reproduction vary according to the date of acceptance of the thesis and are listed below as guidelines.

A. Before 1962. Permission granted only upon the prior written consent of the author. (The Senate House Library will provide addresses where possible).

B. 1962 - 1974. In many cases the author has agreed to permit copying upon completion of a Copyright Declaration.

C. 1975 - 1988. Most theses may be copied upon completion of a Copyright Declaration.

D. 1989 onwards. Most theses may be copied.

This thesis comes within category D.

☑ This copy has been deposited in the Library of UCL

☐ This copy has been deposited in the Senate House Library, Senate House, Malet Street, London WC1E 7HU.

The role of Bone Morphogenetic Protein 7 in the pathophysiology and treatment of vascular calcification associated with chronic renal failure

Matthew Rhys Davies

Thesis submitted in support of the degree of Doctor of Medicine,

University of London

2005

ProQuest LLC
789 East Eisenhower Parkway
P.O. Box 1346
Ann Arbor, MI 48106-1346

Abstract

Vascular calcification (VC) is an important complication of chronic renal failure (CRF), and a risk factor for reduced survival. Osteoblast-like cells in the vessel wall derived from resident vascular smooth muscle cells (VSMC) are considered central to the pathogenesis of VC, which is exacerbated by mineral ion abnormalities inherent in renal osteodystrophy (ROD). Nevertheless, its aetiology is incompletely understood, and no effective therapies exist. Recently, CRF has been characterised as a state of Bone Morphogenetic Protein 7 (BMP7) deficiency, and animal studies have shown that administration of this renal morphogen is efficacious in treating several aspects of renal failure, including progressive renal fibrosis and ROD. The hypothesis of this thesis is that BMP7 deficiency contributes to the pathogenesis of VC, by facilitating the emergence of the osteoblast-like cell, and that exogenous BMP7 administration abrogates it by normalising VSMC behaviour.

This hypothesis was tested in atherosclerotic Low Density Lipoprotein Receptor Null (*ldlr*$^{-/-}$) mice. Uraemia was superimposed surgically to generate VC. Animals received

BMP7 or vehicle over 15 weeks. Untreated uraemic animals had increased VC on histological and chemical grounds, and demonstrated increased expression of the characteristic osteoblast protein osteocalcin was demonstrated in vascular tissues. Both changes were reversed by BMP7 administration. Uraemic animals were shown to have an adynamic form of ROD, also reversed by BMP7 administration, suggesting that normalisation of mineral ion abnormalities may underlie the benefits of BMP7 on VC in CRF. In addition, *in vitro* studies showed that BMP7 can act directly on vascular cells to reduce extracellular calcification under conducive conditions. Finally, in an appendix, preliminary data is presented showing that expression of LRP5, a protein involved in the control of normal bone mineralization, may be increased in *ldlr*$^{-/-}$ animals, suggesting that consequences of this genotype may be important to VC pathogenesis in this model.

Contents

Index of figures and tables

Dedication

For

Huw

"A thing is not proven because no one has ever questioned it.

...Scepticism is the first step towards truth"

Denis Diderot (1713-1784)

Acknowledgements

Firstly, I wish to thank Professor Marc Hammerman for the opportunity to join the Renal Fellowship programme at Washington University School of Medicine, which enabled me to become involved with the project that has resulted in this thesis.

Secondly, I am grateful to my family for their support while I was living in the USA; but they know that.

Third, I'd like to thank Dr Richard Lund, who kindly performed the painstaking bone histomorphometry measurements in this thesis, and who was also a valued friend throughout.

Fourthly, I'd like to thank Professor John Williams, for his perceptive advice on the preparation of this manuscript, and for kindly taking the time to read the text in a critical light.

Fifthly, I am grateful to Professor Leon Fine, for consenting to act as University of London advisor for this thesis, and for his helpful comments during preparation of the text.

Finally, I am immensely grateful to Professor Keith Hruska, for offering me the opportunity to work in his laboratory, and supplying the mentorship without which this thesis would not exist. His enthusiasm was always and continues to be infectious, his knowledge immense, and his critical attention to new developments in an emerging project was invaluable.

Section 1

Overview

Vascular calcification (VC) has recently emerged as an important complication of chronic renal failure (CRF), with serious consequences for morbidity and mortality in patients with end-stage renal disease (ESRD). Current understanding of the aetiology of this widespread problem is incomplete, and no effective therapies are available. However, several recent studies in animal models have shown striking efficacy of the renal morphogen Bone Morphogenetic Protein 7 (BMP7) in treating a number of aspects of renal failure and the uraemic syndrome, including acute ischaemic renal injury, progressive tubulo-interstitial fibrosis, diabetic nephropathy, lupus nephritis and renal osteodystrophy. These results led to the broad hypothesis that BMP7 administration may also be beneficial to VC in the context of CRF, and this hypothesis is the subject of this thesis.

The rationale underlying these beneficial effects of BMP7 administration is that endogenous BMP7 expression in the kidney is decreased soon after renal injury, and that the absence of this important growth factor facilitates progressive renal injury mediated

by other factors, such as Transforming Growth Factor-β (TGFß). Thus CRF has been characterised as a state of relative BMP7 deficiency, and in this setting administration of exogenous BMP7 serves to promote normal end-organ structure and function by restoring the balance between counteracting beneficial and pathological influences.

This paradigm of BMP7 deficiency in CRF may be expanded to explain the aetiology of VC, by extension to vascular smooth muscle cells (VSMCs). VSMCs have emerged to play a central role in the aetiology of VC, and appear to adopt a phenotype reminiscent of osteoblasts through a process of transdifferentiation in this context. Osteoblasts are the major anabolic cells of bone, and function to mineralise their extracellular matrix; VSMCs that have undergone osteoblastic transformation are able to mineralise their own extracellular matrix in an analogous manner, and thereby generate VC. Although the effects of BMP7 on VSMCs are not clearly understood, they derive from the same mesenchymal precursors as other targets of BMP7, and BMP7 is known to play a role in fate-determination and maturation of other cells in this lineage, including osteoblasts. It may therefore be hypothesised on the one hand that BMP7 deficiency in CRF could lead to structural or functional changes in VSMCs, and in particular facilitate their osteoblastic transdifferentiation. Exogenous BMP7 administration in this context would potentially restore normal smooth muscle cell function, and by doing so ameliorate or prevent VC. On the other hand, it is also possible to hypothesise that BMP7 might worsen VC, since it plays a key role in the differentiation and maturation of osteoblasts in normal bone and could therefore potentially accelerate the transdifferentiation of VSMCs to a mineralising phenotype in the vasculature. Such an outcome would clearly outweigh benefits of exogenous BMP7 administration on other aspects of CRF.

This thesis aims to explore these opposing hypotheses, and comprises a review of both current understanding of VC and the role of BMP7 in health and disease of renal tissues, followed by four studies performed to test the hypotheses outlined above. Firstly, two studies are described in an animal model of atherosclerosis and arterial calcification, the Low-Density Lipoprotein Receptor null (*ldlr*$^{-/-}$) mouse, onto which uraemia was superimposed by a surgical procedure. These studies demonstrate through histological, chemical and immunohistochemical techniques that VC is induced in uraemic animals, and that this process is prevented by BMP7 administration. At the same time, abnormalities of bone histology consistent with renal osteodystrophy (ROD) were also apparent in these animals, and these changes too were reversed by BMP7. The interplay between VC, ROD and abnormalities of mineral metabolism inherent in CRF is discussed. Following this is a description of studies performed in an *in vitro* model of VC, the bovine calcifying vascular cell (CVC). These cells are characterised as VSMCs expressing an osteoblastic phenotype, and spontaneously calcify their extracellular matrix. Again, BMP7 administration ameliorated calcification both under basal conditions and also conditions promoting maximal mineralization. The appendix describes an analysis of the vascular expression of LRP5, a protein structurally and functionally related to the LDL receptor that plays an essential role in normal osteoblast development and maturation. The study demonstrates increased expression of LRP5 in the context of the *ldlr*$^{-/-}$ genotype, and suggests a mechanistic link between this lesion and the emergence of VC. The putative interrelationship between this finding and the observed effects of BMP7 is briefly discussed.

The conclusion of the thesis is that the data described support the hypothesis that BMP7 administration prevents VC in CRF, through direct effects on vascular cells as well as indirect effects on bone mineralization, and further that consequences of the *ldlr*$^{-/-}$

genotype may be important to the pathogenesis of VC and its treatment in this setting. More generally, the thesis supports the concept of CRF as a state of relative BMP7 deficiency, and contributes to the hope that new, effective therapeutic options will be developed for the treatment of VC and other aspects of CRF in the future.

Section 2

Introduction to vascular calcification and the role of Bone Morphogenetic Protein 7 in physiology and pathophysiology

2.1 The pathophysiology of vascular calcification

2.1.1 The clinical importance of vascular calcification in chronic renal failure

Registry data from both the USA and Northern Europe have consistently demonstrated an excess mortality in patients with end-stage renal disease (ESRD) [1-3], despite measures to optimise dialysis treatment and pre-dialysis care. Approximately fifty percent of all deaths in such patients are attributable to cardiovascular disease [4], and this problem remains one of the major outstanding issues in clinical nephrology. In an early and influential paper addressing this issue, Lindner *et al* concluded that accelerated atherosclerosis was the major cause of this excess cardiovascular mortality [5]. Given the high incidence of established atherosclerotic risk factors characteristic of the metabolic syndrome in the chronic renal failure (CRF) population [6], such as hypertension, dyslipidaemia, insulin resistance and overt diabetes mellitus, such a conclusion is attractive; however subsequent reports have challenged its validity [7-10], and it remains to be shown conclusively that excess mortality in this setting is caused by accelerated atherosclerosis *per se*. Other factors have therefore been sought to explain the excess

cardiovascular mortality in CRF [11], and included among these is vascular calcification (VC) [12].

VC is prevalent in the general population and has been viewed until recently as characteristic of 'normal' aging. Nevertheless, the presence of coronary artery calcification has clearly been shown to be predictive of cardiovascular mortality in both general and renal populations [13-16], and so VC is likely to have pathological significance. In the CRF population, VC is more extensive than in the general population on both histological [8] and radiological grounds [15, 17]. One radiological study by Goodman *et al* has clearly shown that VC occurs from a young age in patients on dialysis [17], data that is consistent with the extremely high mortality rates seen in such patients [11]. This study also showed that the presence of VC correlated strongly with time on HD, with increased serum calcium and phosphate ion product and with ingestion of increased amounts of calcium-based phosphate binders used in the treatment of renal osteodystrophy (ROD) [17]. Such a link between VC and the abnormalities of mineral metabolism inherent in ROD has come to be seen as centrally important, with large population-based studies independently confirming the association between increased serum phosphate concentrations and VC [4] and subsequently demonstrating that elevation of both serum phosphate and serum calcium concentrations are predictive of increased mortality [18]. Recent data have also demonstrated an increased risk of mortality associated with normal serum calcium concentrations in patients with ESRD, when values at the upper end of the normal range are compared to those at the lower end [14]. Finally, both elevated levels of Parathyroid Hormone (PTH) [18] and the use of Vitamin D analogues for the treatment of secondary hyperparathyroidism [19] have been linked to VC and mortality. In addition to this data focussing on ROD, other studies have also linked VC to diabetes mellitus (DM) [15, 20],

hypertension [8], and duration of renal disease [8]. Taken together, these data suggest that while VC is undoubtedly a product of the uraemic milieu, it may also be in part an iatrogenic disease that occurs as a consequence of current therapies aimed at treating ROD.

At a histological level, two patterns of VC are described. In the context of severe atherosclerosis, calcification is localised to the intimal layer of the vessel wall immediately related to the plaque [21], and nearby vessel wall is usually entirely normal. Alternatively, calcification may be found throughout the medial layer of the arterial tree, particularly at the internal elastic lamina, extending from the proximal aorta to small arteries and even arterioles [22]. This second form of VC, sometimes referred to as Mönckeberg's sclerosis, is confluent and largely unrelated to intimal atherosclerotic disease, which may nevertheless coexist at localised sites. Medial VC of this type is commonly severe enough to be readily visible on plain radiography, and the density of this calcification in vascular tissues may not be dissimilar to that in adjacent bone (Figure 2.1). Extensive medial calcification such as this is particularly characteristic of CRF, although it is also seen in relation to the aging process and in DM in the absence of overt nephropathy [22]. It is worth noting that in these latter cases, in contrast to CRF, most patients will have normal calcium and phosphate homeostasis.

Whether on the one hand these two different histological patterns of VC represent different pathological processes, or whether on the other they represent the same pathological process acting under different circumstances of vascular injury, has not been determined. It is worth noting that the data correlating VC to morbidity and mortality on radiographic grounds [13, 16] do not distinguish between the two different histological - distributions of VC, but instead estimate total vascular calcium load. Thus,

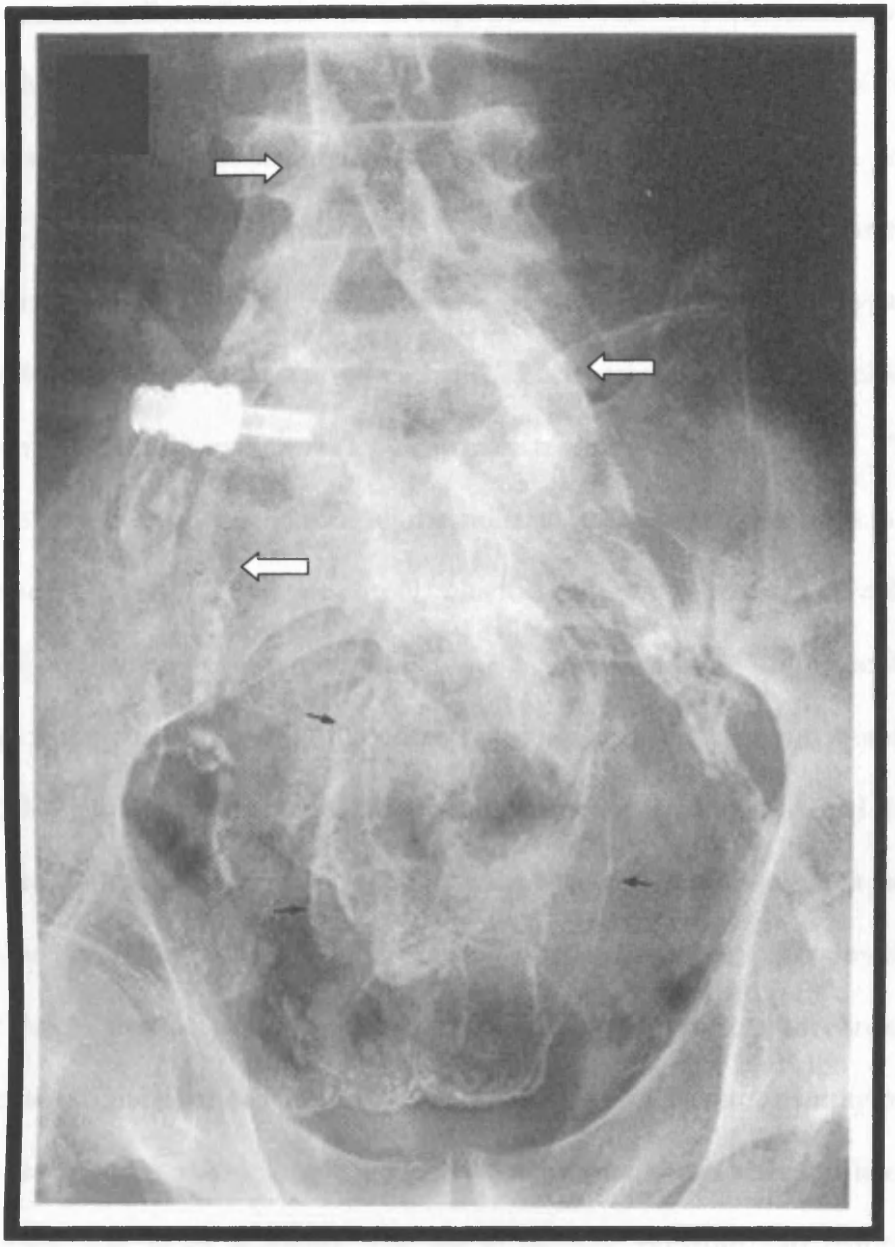

Figure 2.1 Plain abdominal radiograph illustrating extensive calcification of the inferior aorta and iliac arteries in a patient receiving peritoneal dialysis (white arrows). Note that the radiodensity of vascular calcification is similar to that of bone in this example. There is also incidental calcification of the visceral peritoneum (arrows).

the clinical significance of vascular calcification derives from the biophysical alterations it imposes on the vessel wall attributable to both patterns. Focal calcification around atherosclerotic lesions increases plaque fragility, which in turn makes that part of the vessel wall more vulnerable to shear stresses, precipitating acute plaque rupture and thrombosis [23]. This is likely to explain the correlation between coronary artery calcification and mortality [13], and complications after angioplasty [24] and bypass surgery [25]. Medial calcification on the other hand affects cardiovascular morbidity through a different mechanism, which may be clinically more significant in CRF. The main consequence of the confluent nature of the mineralization in this situation is a generalised increase in stiffness of the vessel wall, which is reflected in reduced vascular compliance [26-28] and which has a number of detrimental effects on the cardiovascular system. Widening of the pulse pressure (PP) occurs, reflecting a small increase in systolic blood pressure (SBP) and a more marked fall in diastolic blood pressure (DBP), and this is a stimulus for left ventricular hypertrophy, LVH. LVH is in turn an independent risk factor for cardiac mortality in the ESRD population, and while undoubtedly multifactorial in origin in this patient group (influenced by such factors as chronic anaemia, hypertension, fluid overload, iron overload and the direct effects of parathyroid hormone on cardiac fibrosis), the striking VC that is often present in this setting is likely to play an important role in its aetiology. The fall in diastolic pressure also reduces coronary perfusion, which is predominantly a diastolic process. Thirdly, there is accelerated propagation of the systolic pulse wave through the arterial tree, and an equally accelerated reflection of this wave from the peripheral vascular beds, which arrives back at the LV outflow tract earlier in the cardiac cycle. This in turn causes turbulent flow to occur at the coronary ostia, which further impairs coronary perfusion in diastole [28]. Overall, these changes stimulate the development of LVH and

exacerbate myocardial ischaemia; it is not surprising, therefore that pulse wave velocity (PWV) a measure of arterial stiffening [29], is an independent predictor of all-cause and cardiovascular mortality.

Importantly, human studies have demonstrated the association between these vascular and cardiac changes consequent on the presence of medial VC and mortality in CRF [26-28, 30, 31], and the United States Renal Data System (USRDS) data shows both that pulse pressure is widened in the CRF population compared to the general population [32], and that this change in pulse pressure is related to mortality in such patients [33]. In a recent study by London *et al*, the relative risk of cardiovascular and all cause mortality associated with the presence of arterial media VC was 60- and 46-fold higher than in its absence respectively [34], emphasising the importance of VC as a cardiovascular risk factor.

Thus VC has emerged as an important potential candidate to explain the excess cardiovascular mortality of CRF. Investigations into its pathogenesis are clearly warranted, with the expectation that clearer understanding of this phenomenon might lead to the development of effective therapies that will significantly improve the prognosis for patients with renal failure.

2.1.2 Pathophysiological mechanisms of vascular calcification

Despite being observed at least 150 years ago [35], VC has received little scientific attention until the last decade or so, when assumptions that it is a passive and dystrophic

process of little clinical significance have progressively been undermined. A number of lines of evidence suggest that VC is in fact an active process with strong parallels to normal endochondral bone mineralization [12, 36]. Firstly, clinical and histological descriptions have noted structures strongly resembling bone and containing normal bone marrow elements within the walls of calcified vessels [37, 38]. Secondly, the particular form of calcium phosphate crystal found in vessel walls is hydroxyapatite, the form found in bone [39]. Thirdly, matrix vesicles have been described in calcifying atherosclerotic plaque and aortic tunica media [40, 41]. These sub-cellular structures are the focus of initiation for calcification in normal endochondral bone mineralization, and have been shown to be functionally important in mineralization initiated by calcifying cells of vascular origin *in vitro* [42]. Fourthly, immunohistochemistry and *in situ* hybridisation have demonstrated the expression of a variety of characteristic bone-related proteins in association with calcified atheromatous plaque. These include collagen I [43], the major collagen of bone extracellular matrix, and a number of non-collagenous bone matrix proteins, including Bone Morphogenetic Protein 2a (BMP 2a) [39], Osteopontin [44-48], osteocalcin [36], matrix Gla-protein (MGP) [46], and alkaline phosphatase [36, 37, 49]. While the expression of these proteins could be interpreted as a response to calcification rather than its driving mechanism, data from a number of cell culture models strongly supports the concept that this pattern of gene and protein expression reflects the presence in the vessel wall of a cell expressing an osteoblast-like phenotype, and that this cell is central to the aetiology of VC. It has been further suggested that the expression of key morphogens such as BMP2 may be a critical initiating step in this process.

2.1.2.1 The osteoblast-like cell

Demer's group [39], and subsequently others [50, 51], have isolated primary vascular smooth muscle cell (VSMC) cultures from explants of medial tissue from both normal and diseased aortas which adopt a calcifying phenotype *in vitro*. These cells express the wide array of bone-related proteins mentioned above, and of particular significance is the observation that these calcifying VSMCs, termed calcifying vascular cells or CVCs, follow the critical sequence and timing of expression of these proteins as it occurs in normal mineralising bone [52, 53], albeit over an accelerated time-frame. As cells differentiate into mature osteoblasts in bone the ability to proliferate is lost, while at the same time synthesis of appropriate matrix components begins, predominantly collagen I. In turn, the accumulating matrix signals to the cell to initiate secretion of proteins relating to mineralization, firstly alkaline phosphatase and osteopontin, later osteocalcin and MGP. The synthesis of an appropriate type of matrix critically influences calcification [54]: rapidly calcifying CVCs synthesise a matrix containing high levels of Collagen I and Fibronectin, while more slowly mineralising cells synthesise matrix with less Collagen I and Fibronectin and more Collagen IV. Importantly, when slowly mineralising CVCs are transferred onto matrix synthesised by rapidly mineralising CVCs, their rate of mineralising increased to a comparable level as the rapidly mineralising cells. On the other hand, other VSMC derived from the same bovine vascular tissue never calcified, irrespective of matrix, suggesting that both intrinsic cellular characteristics as well as external environment contribute to the propensity of CVCs to calcify. These influences appear to be mediated, at least in part, through α5 integrins involved in cell/matrix interaction. In addition, CVCs express the transcription factor cbfa1/osf2 [55], a factor both essential and sufficient for differentiation of the mature osteoblast in bone [56]. However, whether the ability to calcify is a characteristic of all VSMCs isn't clear.

Table 2.1 Factors influencing calcification of vascular smooth muscle cells, calcifying vascular cells (CVCs) and pericytes *in vitro*

Factors Increasing Calcification	Factors Decreasing Calcification
cAMP [55]	Autocrine/paracrine PTHrP [64]
Organic phosphate [50, 56]	Osteopontin [51]
Inorganic phosphate [57]	Collagen IV [62]
Alkaline phosphatase [50]	
Corticosteroids [58]	
Vitamin D_3 [59]	
Oestrogens [60]	
Oxidised Lipids [57]	
TGF-β1 [57]	
Advanced Glycation Endproducts [61]	
Collagen I [62]	
? 'Intracrine' PTHrP[63]	

PTHrP, Parathyroid Hormone related peptide

CVC clones calcify spontaneously and rapidly throughout their existence *in vitro*; in contrast other VSMC clones derived from the same vascular explants may never do so [57]. This suggests the existence of either two phenotypically different cell lines in the original tissue, or that certain VSMCs retain sufficient pluripotentiality to change their phenotype. One important characteristic of calcifying clones is their ability to synthesise an appropriate matrix: [54] cell lines that express Fibronectin and Collagen I promote mineralization, whereas those expressing Collagen IV inhibit it. A number of studies have investigated the process of calcification in this cell-line, suggesting it is a cAMP mediated mechanism [55], and influenced by a variety of factors, including Transforming Growth Factor β (TGFß) (Table 2.1) [50, 51, 54, 55, 57-61, 63-65]. While intermittent stimulation of CVCs by cAMP causes a nodular pattern of calcification, continuous stimulation causes a confluent calcification throughout the cell monolayer, strikingly similar to *in vivo* medial calcification seen in CRF [55].

The combination of these *in vivo* and *in vitro* findings suggest that cells normally resident in the vessel wall of healthy aortic tissues have the capacity to adopt a calcifying phenotype under appropriate conditions, and behave extremely similarly to normal osteoblasts. These observations raise the question of the origin of these calcifying cells.

2.1.2.2 The origin of the osteoblast-like cell

The most likely derivation of the osteoblast-like cell in the vessel wall is that is arises by transdifferentiation of vascular smooth muscle cells, which are both the major cell type in the arterial medial layer, and which also migrate into evolving atherosclerotic plaques.

Smooth muscle cells and osteoblasts share a common derivation from bone marrow mesenchymal precursor cells, and whereas osteoblasts are terminally differentiated cells unable to re-enter the cell cycle, smooth muscle cells retain a degree of pluripotentiality that enables them to transdifferentiate into an osteoblastic phenotype, at least *in vitro* [66]. In the setting of smooth muscle cells in culture, changes in protein expression that are consistent with osteoblastic transdifferentiation may be induced by TGFß [67]. In particular, expression of Collagen I, a key component of osteoblastic extracellular matrix, is increased, while expression of both Collagen III, which is characteristic of extracellular matrix synthesised by VSMCs, and α-Smooth Muscle Actin (αSMA), which is a marker of smooth muscle phenotype, are decreased. The precise mechanisms underlying the relationship between these two cell lineages are not clearly understood, but available evidence suggests that Bone Morphogenetic Protein 7 (BMP7) may play a key role, both in defining the two lineages under normal physiological conditions, and also in facilitating the transdifferentiation process by its absence under pathological conditions in CRF (Figure 2.2). While BMP7 is known to be critical for the commitment of precursor cells to the osteoblastic lineage, the factors committing precursors to the VSMC lineage are unknown. However, data from animal studies and from cell culture experiments suggest that BMP7 may be able to contribute to preservation of smooth muscle phenotype in committed cells [67], and prevent the transdifferentiation process, at least when it is driven by TGFß [67]. This point is discussed in more detail below, in section 2.2.

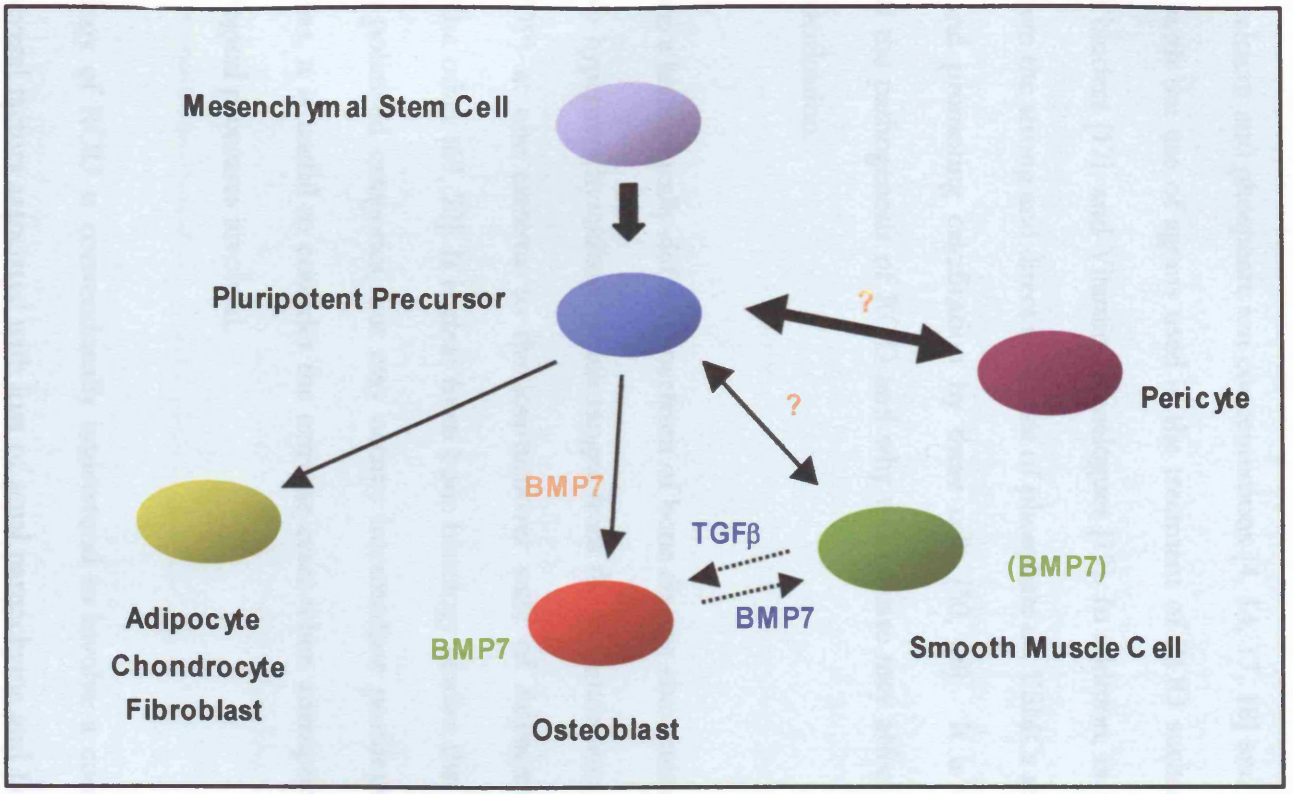

Figure 2.2 Schematic diagram illustrating the relationship between cells of mesenchymal origin relevant to vascular calcification. Bone marrow stem cells differentiate into pluripotent precursors under appropriate stimulation, which in turn differentiate into the mature cell types shown. BMP7 is involved in commitment to the osteoblast lineage (yellow script), and maintenance of mature osteoblastic phenotype (green script); osteoblasts are end-differentiated and unable to re-enter cell cycle (single headed arrow). Factors controlling commitment to smooth muscle cell (SMC) lineage are unknown, but mature SMCs, which retain a degree of pluripotentiality (double-headed arrow) adopt an osteoblastic phenotype under the influence of TGF-β (broken arrow and blue script); this effect is reversed by BMP7 (broken arrow and blue script), and so BMP7 may act to maintain differentiated phenotype of SMCs (green script). Pericytes, which retain considerable pluripotentiality (heavy double-headed arrow), are also resident in the vessel wall in small numbers, although these cells are poorly characterised and the factors involved in their differentiation and maintenance are unknown.

2.1.2.3 Renal osteodystrophy and vascular calcification

As noted previously, clinical studies have associated the presence of VC in patients with CRF with a number of parameters characteristic of the presence of ROD, such as increased calcium and phosphate ion concentrations [4, 14, 17, 18] and PTH levels [18], as well as with the use of agents used in the treatment of ROD such as calcium-based phosphate binders [17], and Vitamin D analogues [19]. In addition, *in vitro* studies have clearly shown the strong and direct influence of phosphate on VSMCs and CVCs in both initiating and promoting calcification by these cells [50, 68]. It is thus relevant to understand the pathogenesis of ROD and why this disease may affect the aetiology of vascular calcification.

ROD forms a histologically-defined spectrum of bone disease characterised by secondary and tertiary hyperparathyroidism, which ranges from the high-turnover state of Osteitis Fibrosa (OF) at one extreme to the low-turnover state of Adynamic Bone Disease (ABD) at the other [69, 70]. It is clear from bone histology studies that not all cases fall into these polarised categories, but may occupy intermediate positions between them. Nevertheless, it is useful to consider the extreme cases when attempting to understand the pathological processes involved.

The aetiology of ROD is conventionally understood to involve a complex interaction between several factors associated with loss of renal parenchyma and falling Glomerular Filtration Rate (GFR) (Figure 2.3a and b). In OF (Figure 2.3 a), reduced synthesis of activated Vitamin D (1, 25 dihydroxy-cholecalciferol) leads to a tendency to hypocalcaemia due to reduced intestinal absorption; in addition, reduced tubular phosphate ion excretion leads to hyperphosphataemia. Hypocalcaemia,

hyperphosphataemia and Vitamin D deficiency all combine to stimulate an increase in Parathyroid Hormone synthesis and secretion, as part of a physiological feedback loop that acts to maintain normal extracellular calcium and phosphate concentrations. The major consequence of this hyperparathyroidism is increased bone turnover, with increased numbers of osteoblasts associated with bone formation rate and osteoid accumulation, as well as increased numbers of osteoclasts associated with bone resorption. Overall, a net bone resorption of bone occurs due to imbalance in the regulation of these processes, tending to increase the concentration of both phosphate and calcium ions in the extracellular fluid. However, the persisting limitation on renal tubular phosphate excretion contributes to ongoing hyperphosphataemia despite hyperparathyroidism, so that even while calcium concentrations may be normal, an increased calcium phosphate ion product occurs. The presence of hyperphosphataemia represents an important link between high-turnover bone disease and VC, since hyperphosphataemia has been shown to be predictive of cardiovascular mortality [4, 18, 71], and phosphate ions have been shown to be able to initiate a calcifying phenotype in VSMCs [50, 68] as well as promoting mineralization by CVCs. In addition, it has been speculated that high levels of parathyroid hormone itself may act to promote VC [71].

In contrast to OF, ABD is characterised by low numbers of osteoblasts, with normal or reduced numbers of osteoclasts. Mineralization proceeds at a normal rate, and osteoid thickness may be normal or decreased [72, 73], but overall bone turnover is low. It is interesting to note that such a low turnover state has been observed in a murine model of CKD treated with Vitamin D in the context of normal calcium, phosphate and PTH levels, at a stage when GFR is approximately 60 % normal [74]. This indicates that there may be a decrease in bone anabolism early in the course of CKD, before abnormal phosphate or PTH levels are demonstrable. Since BMP7 is known to be an anabolic

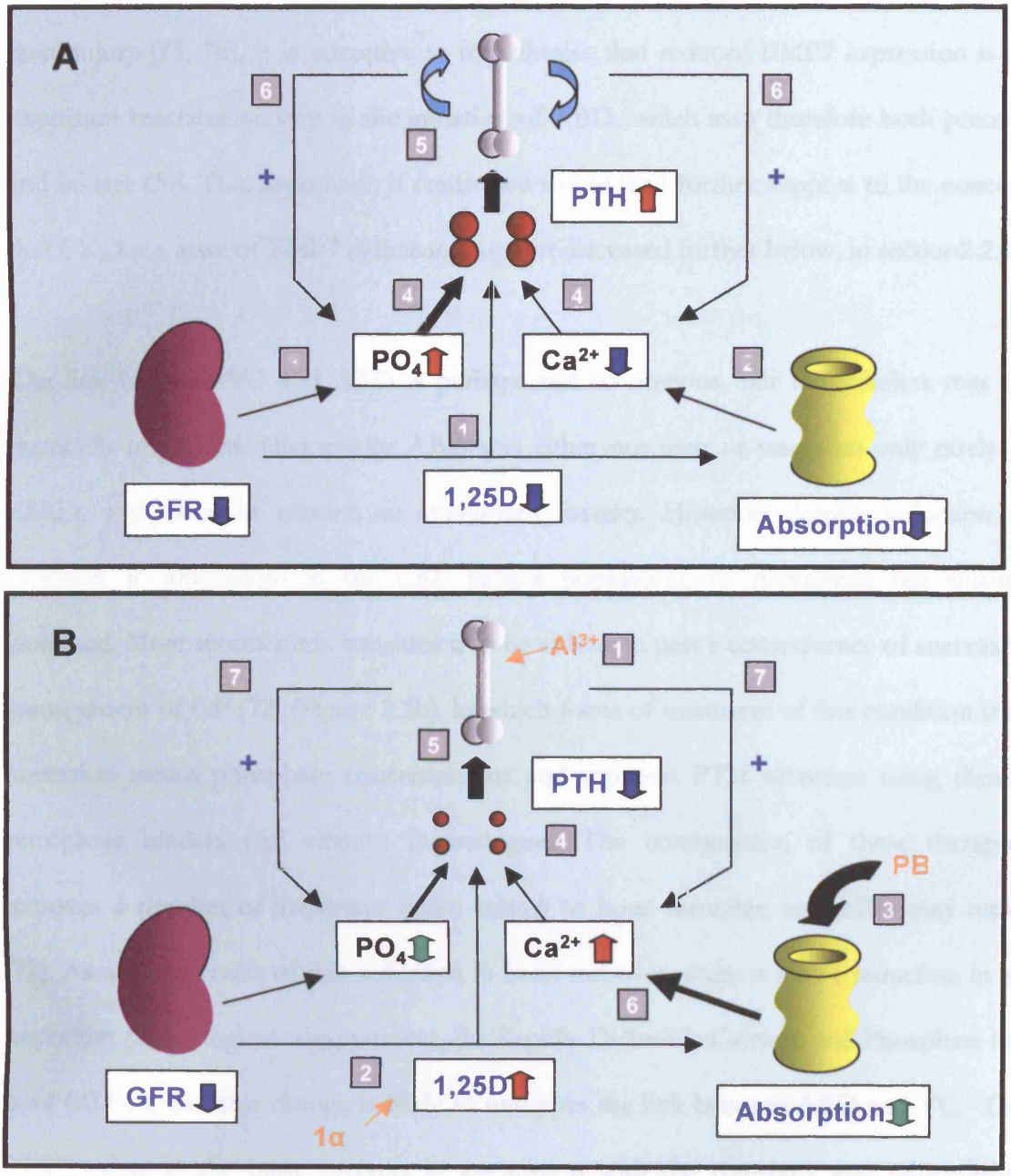

Figure 2.3 **Classical paradigm of the aetiology of renal osteodystrophy (ROD). A,** In high turnover ROD, loss of functional renal tissue reduces activated Vitamin D (1,25D) synthesis **(1),** causing reduced intestinal Ca^{2+} absorption and hypocalcaemia **(2).** Reduced renal PO_4 excretion leads to hyperphosphataemia **(3).** Hypocalcaemia, hyperphosphataemia and 1,25 D deficiency combine to stimulate Parathyroid Hormone (PTH) synthesis (secondary hyperparathyroidism, 2HPT) **(4),** causing increased bone turnover **(5)** and peritrabecular fibrosis (Osteitis Fibrosa, OF). Net bone resorption increases extracellular PO_4 and Ca^{2+} concentrations **(6);** persisting limitation of renal PO_4 excretion contributes to ongoing hyperphosphataemia despite hyperparathyroidism. **B,** Adynamic bone disease often derived from aluminium (Al^{3+}) toxicity **(1).** More recently it is a consequence of over-treatment of 2HPT with both 1,25D analogues (1α) **(2),** and dietary binders (PB) used reduce PO_4 absorption **(3).** Both suppress PTH synthesis **(4)** and reduce bone turnover **(5).** Paradoxically 1,25D analogues promote intestinal Ca^{2+} and PO_4 absorption **(6),** particularly when Ca^{2+}-containing binders are used. In addition, reduced bone turnover reduces capacity to buffer extracellular Ca^{2+} and PO_4 **(7),** causing persistent abnormalities of mineral metabolism.

factor in healthy bone and since the renal expression of this protein is reduced early after renal injury [75, 76], it is attractive to hypothesise that reduced BMP7 expression is an important mechanistic step in the initiation of ABD, which may therefore both precede and initiate OF. This hypothesis if confirmed would lend further support to the concept that CKD is a state of BMP7 deficiency, a point discussed further below, in section2.2.3.

The link between VC and ABD is perhaps not so obvious, but nevertheless may be extremely important. Historically, ABD was either not seen or was seen only rarely in ESRD, and often in relation to aluminium toxicity. However despite reduction in exposure to aluminium in the CRF patient population, its prevalence has steadily increased. More recently it is considered to be at least in part a consequence of successful management of OF [72] (Figure 2.3b), in which focus of treatment of this condition is to normalise serum phosphate concentrations and suppress PTH secretion using dietary phosphate binders and vitamin D analogues. The combination of these therapies removes a number of important major stimuli to bone turnover, and ABD may result [72]. As a direct result of this reduction in bone turnover, there is also a reduction in an important physiological compartment, the Rapidly Diffusible Calcium and Phosphate ion pool (RDIP), and this change is likely to underpin the link between ABD and VC. The RDIP exists at the bone surfaces in association with the resorbing and mineralising fronts, and although it does not have any strict anatomical definition, its size varies in proportion to the amount of bone turnover [77]. In addition to accommodating the ions involved in bone turnover, one of the key functions of the RDIP is that it serves to buffer extracellular calcium and phosphate ion concentrations over short time-frames, for instance in the immediate post-prandial period. This allows the body to maintain tightly controlled levels of these ions over shorter periods of time than can be achieved via buffering by bone mineral itself or by adjustments in renal tubular ion fluxes. Thus,

while patients with ABD may have satisfactory ion levels for most of the time, they are prone to peaks of ion concentrations after meals, and since pulses of phosphate have been shown to be able to induce a mineralising phenotype in VSMCs *in vitro* [68], this may have important consequences for the aetiology of VC. In support of this concept, a recent study has shown a clear association between the presence of VC detected radiologically and ABD diagnosed on bone biopsy in the same patients [78].

It can therefore be seen that ROD of whichever type will contribute to disturbances of calcium and phosphate homeostasis that are likely to contribute to the pathogenesis and progression of VC, and by doing so contribute to the excess cardiovascular mortality of CRF.

2.2 Bone Morphogenetic Protein 7

The role of BMP7 in the aetiology of aspects of the uraemic syndrome, and its emergence as a potentially useful therapeutic agent in this setting, is central to the current thesis. It is thus worth taking time to discuss the biology of this protein in health and disease in order to understand its role in pathophysiology and treatment of vascular calcification in CRF.

2.2.1 Structure and function

The Bone Morphogenetic Proteins (BMPs) are a large subgroup of the TGFß super-family of cytokines, comprising at least 30 members throughout the animal kingdom, which are highly conserved throughout evolution [79, 80]. They are named for their osteo-inductive properties, since they are able to recapitulate formation of endochondral

bone as well as haematopoetic marrow elements at extra-skeletal sites [81]. However, their nomenclature is an accident of the circumstances of their discovery, and BMPs are clearly not functionally limited to bone development. Indeed, they are widely expressed throughout embryonic development, and play an essential role in organogenesis and axial patterning in addition to skeletal development, influencing processes as diverse as proliferation, differentiation and apoptosis in doing so [79].

BMPs are synthesised as large precursor proteins which form dimers and are subsequently cleaved at a consensus Arg-X-X-Arg sequence to yield mature carboxy-terminal dimers. This process occurs before secretion. X-ray crystallography has demonstrated that BMP monomers are characterised by an invariant motif, a cystine knot comprising six cysteine residues; in addition, virtually all BMP family members have a seventh cysteine residue, involved in disulphide bonding in the dimerization process [79].

Interactions between secreted dimers and their receptors are complex, but follow a general paradigm of all TGFß superfamily members [79] (Figure 2.4). Ligands bind to one of a number of type II transmembrane serine-threonine kinase receptors, which then forms a heterodimer with one of a number of type I receptors, also a transmembrane serine-threonine kinase. The type I receptor is then phosphorylated and activated by the type II receptor, and initiates further signal transduction via the Smad pathway, in common with TGFß super-family signalling as a whole, leading to appropriate modification of gene expression [79]. Each protein may interact with a number of Type I and Type II receptors, leading to considerable promiscuity in these ligand/receptor relationships. This allows an individual ligand to transduce several effects

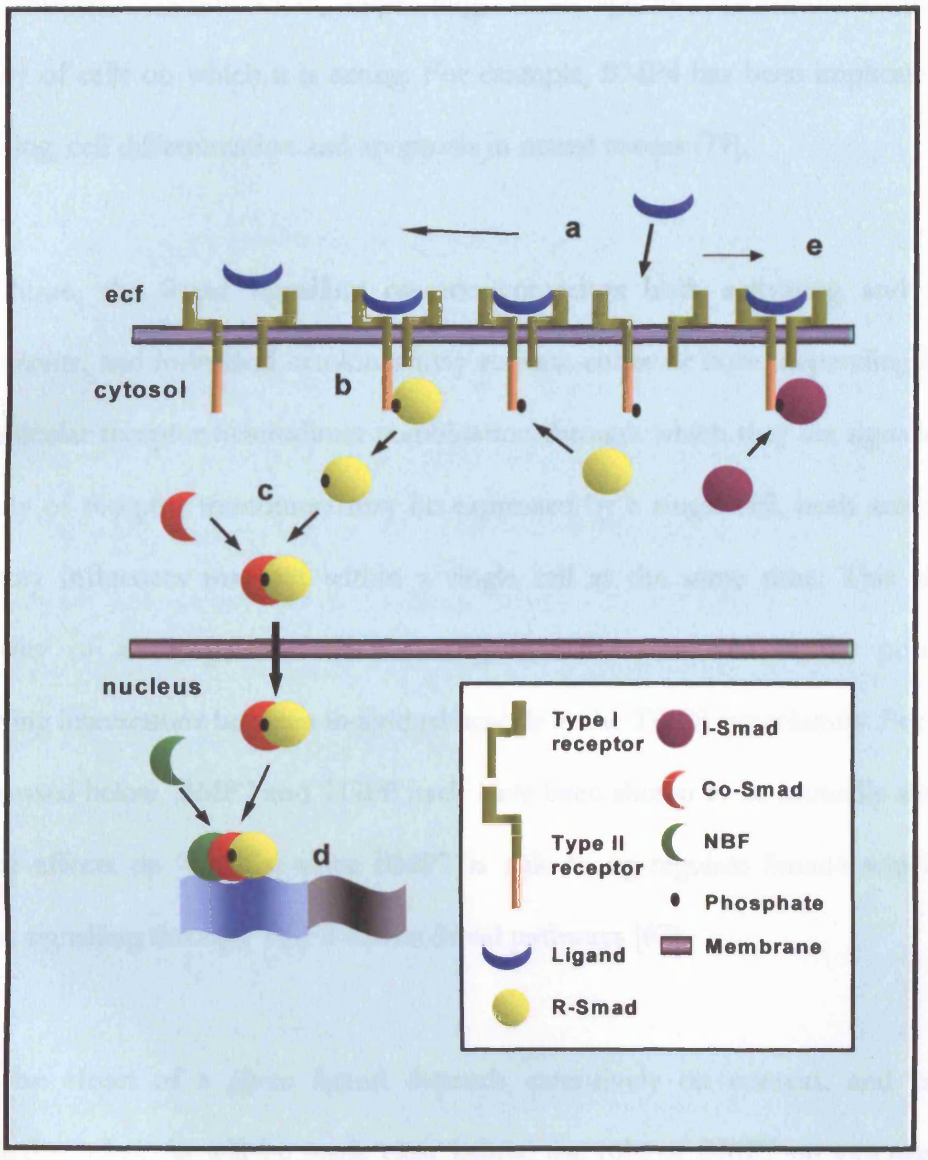

Figure 2.4 **Transforming Growth Factor β superfamily signal transduction.** Extracellular ligand binds to a type I receptor, which forms a heterodimer with a type II receptor **(a)**. R-Smads (Smads 1,2,3,5 or 8) interact with the cytosolic tail of the type II receptor, becoming phosphorylated and active **(b)**. Activated R-Smads combine with Co-Smad (Smad 4) **(c)**, and translocate to the nucleus, where the combine with Nuclear Binding Factors (NBF), bind to DNA and regulate gene expression **(d)**. Inhibitory Smads (I-Smad, Smads 6 and 7) bind to type II receptors and competitively inhibit phosphorylation of R-Smads **(e)**.

under different circumstances, depending on its specific environment and on the maturity of cells on which it is acting. For example, BMP4 has been implicated in axial patterning, cell differentiation and apoptosis in neural tissues [79].

In addition, the Smad signalling cascade comprises both activating and inhibiting components, and individual cytokines may activate either or both, depending largely on the particular receptor heterodimer combination through which they are signalling. Since a variety of receptor monomers may be expressed by a single cell, both activating and inhibitory influences may act within a single cell at the same time. This allows the possibility of auto-regulation of some ligand effects, as well as the potential for modifying interactions between individual ligands in the TGFß superfamily. For example, as discussed below, BMP7 and TGFß itself have been shown to be mutually antagonistic in their effects on VSMCs, since BMP7 is able to up-regulate Smad6 which in turn inhibits signalling through TGFß driven Smad pathways [67].

Thus the effect of a given ligand depends extensively on context, and cannot be predicted *a priori*. As will be made clear below, the role of BMP7 on vascular smooth muscle cells and bone marrow osteoblasts in the uraemic milieu is particularly important to the pathogenesis and potential treatment of VC.

2.2.2 Role in embryonic development and post-partum health

Bone Morphogenetic Protein7 (BMP7), also know as Osteogenic Protein-1 (OP-1), is widely expressed in a number of embryonic tissues [82], and plays an important role in skeleton, eye, kidney [83-86] and cardiovascular system [87, 88] development. In the kidney, BMP7 primarily coordinates the interaction between the condensing mesenchyme of the emerging metanephros and the branching morphogenesis of the ureteric bud [83, 84], while in the skeleton BMP7 plays a role in committing mesenchymal stem cells to the osteoblastic lineage, thus facilitating bone mineralization. Expression of BMP7 in the eye is implicated in the coordinated development of mature structures. Cardiac expression of BMP7 is widespread in the developing heart throughout embryonic development.

The relative importance of these roles of BMP7 is illustrated by studies of genetically mutant animals. The essential nature of BMP7 expression in renal development and the inherent redundancy of BMP signalling is clear from the phenotype of the *bmp7*$^{-/-}$ mouse, which is characterised by markedly reduced nephron mass at birth, and perinatal death from uraemia [83]. While failure of eye development also occurs in this genetic setting, skeletal abnormalities in the *bmp7*$^{-/-}$ mouse are relatively minor, and no cardiovascular abnormalities are apparent at time of death. Nevertheless, the importance of BMP7 expression to cardiovascular development is illustrated by the phenotype of two double genetic mutants. In *bmp5*$^{-/-}$/ *bmp7*$^{-/-}$ mice [87] cardiac development does not progress, with failure of chamber septation and endocardial cushion formation being fatal at about 10.5 days post conception (dpc). In *bmp6*$^{-/-}$/*bmp7*$^{-/-}$ mice [88], defects of chamber septation together with delay in formation of outflow-tract cushion formation and consequent defects in valve morphogenesis are lethal at 10.5 to 15.5 dpc. Due to the

lethality of these lesions, the influence of BMP7 on cardiovascular development in later life is not currently defined.

In mature animals, BMP7 expression is almost exclusively confined to renal collecting tubules, with expression also documented in glomerular podocytes as well as renal artery adventitia [75]. The role of BMP7 in the kidney appears to be to preserve the differentiated phenotype of glomerular and tubulo-interstitial cell types, by autocrine and paracrine mechanisms [89]. In addition, the ongoing importance of BMP7 in osteoblast development suggests a hormonal role for renal BMP7, since no expression is documented in skeletal tissues in the adult. However, no role is clearly defined for BMP7 in the adult cardiovascular system at present. This issue is discussed further in section 2.2.4 below.

2.2.3 Role in the aetiology and therapy of chronic renal failure and uraemic syndrome

Parallels have been drawn between the processes involved in embryonic development of the kidney and those involved in renal healing after injury. This view is undoubtedly overly simplistic, since some degree of progressive fibrosis and anatomical destruction is the hallmark of most renal injury, rather than a process of complete recovery. Nevertheless, the specificity of BMP7 to embryonic renal development led to the hypothesis that BMP7 therapy might improve renal recovery and healing after injury, by supporting a more complete embryological program of gene expression. This concept is supported by observations in rodent models of DM and acute ischaemic renal injury that

tubular BMP7 expression is reduced early in the disease process following the initiating injury [75, 76], which characterise uraemia as a state of BMP7 deficiency in these settings. As a result, the hypothesis that BMP7 therapy may be beneficial in the healing of renal injury has been tested in several animal models.

Initial experiments looked at a model of ischaemic nephropathy, and showed that animals receiving BMP7 therapy had less marked deterioration in renal function as well as faster recovery following injury than control animals [90].

Following this, an important study investigated the effect of BMP7 on tubulo-interstitial fibrosis (TIF) [91]. TIF is an important entity since it is a final common pathological pathway of virtually all renal diseases. This study used the Unilateral Ureteric Obstruction (UUO) model of progressive TIF, in which angiotensin II-stimulated TGFß expression causes progressive interstitial fibrosis following transient surgical ureteric obstruction. BMP7 administered for the duration of the obstruction preserved renal function, prevented tubular atrophy and markedly diminished the activation of tubulo-interstitial inflammation and fibrosis. In addition to demonstrating the efficacy of BMP7 in the therapy of a common pathological condition in kidneys, and thereby supporting the general concept of chronic renal disease as a condition of BMP7 deficiency, this study also emphasises that BMP7 signalling has the potential to antagonise processes mediated by TGFß; this in turn has parallels with the interaction between these two cytokines in VSMCs, as described above [67].

Subsequently, studies have looked at the effects of BMP7 in models of diabetic nephropathy [92] (in which TIF undoubtedly plays a critical pathological role), and lupus nephritis, with similarly beneficial effects being seen [93]. In addition, studies particularly

relevant to this thesis have examined the effect of BMP7 in renal osteodystrophy [94, 95]. As discussed above, ROD comprises a spectrum of disease entities, ranging from the high bone-turnover state of Osteitis Fibrosa (OF) at one extreme, to low turnover Adynamic Bone Disease (ABD) at the other. The abnormalities of osteoblast function implicit in these disease states together with the role of BMP7 in normal osteoblast development suggest that the down-regulation of renal BMP7 expression seen in renal injury [75] may be an important contributor to the aetiology of ROD, and that BMP7 therapy may therefore be beneficial in this context. This has proved to be the case in a study of high turnover ROD [94], where uraemic mice treated with BMP7 had reduced bone resorption, reduced fibrosis and normalised osteoblast characteristics compared to untreated controls. In a second study of adynamic bone disease in a similar model BMP7 therapy again normalised osteoblastic function and improved bone turnover [95]. As noted above, there is an increasing amount of clinical data to link biochemical consequences of ROD with the aetiology of VC, and this in turn suggests the hypothesis that BMP7 may be beneficial in the treatment of this important component of the uraemic syndrome.

2.2.4 Role in cardiovascular biology and potential influence on vascular calcification

As noted in section 2.2.2, BMP7 is expressed in the cardiovascular system during embryonic development [82], and comparison of mice genetically null for BMP7 alone [83-86] or BMP7 in conjunction with either BMP6 or BMP5 [87, 88] shows that this protein plays an important but not essential role in early embryonic cardiac development. Unfortunately, the early lethality of these double null animals limits their usefulness in understanding the role of BMP7 at later stages of cardiac development, and its role in adult cardiovascular biology is not well understood. However, investigations using different genetic techniques offer some support for the concept that BMP signalling is important in later cardiac development and function [96]. Cre/lox technology allows tissue-specific gene deletion limited both spatially and temporally. Studies using this technique involving cardiac-limited expression of the Type II BMP receptor ALK3 in mice have demonstrated the importance of the integrity of BMP signalling pathways in several aspects of mid-gestational cardiac development, including cardiomyocyte survival, formation of the interventricular septum and the development of the atrioventricular cushion [96]. In addition, other studies have used the over-expression of the BMP antagonist Noggin to investigate similar pathways in chicks [96]. However, none of these investigations have assessed the role of BMP signalling in cardiovascular tissues beyond the embryological environment, nor do they address its role in any peripheral vasculature.

Nevertheless, recent studies in humans have linked BMP signalling to normal arterial structure and function in the pulmonary circulation. BMPR2 is a type II TGFß superfamily receptor specific to BMP signalling, and deletions in the gene for this receptor have been linked to Primary Pulmonary Hypertension (PPH) in a large

proportion of both familial and sporadic cases [97-99]. This condition is characterised by hypertrophy of the medial layer of the pulmonary arterial tree due to an imbalance between proliferation and apoptosis of pulmonary arterial smooth muscle cells [99, 100], which in turn leads to increased pulmonary artery pressure, and ultimately to right ventricular failure and death. The genetic lesions of BMPR2 are generally predicted to lead to truncated non-functioning proteins, a fact which suggests that BMP signalling is required for normal control of smooth muscle cell development and function, at least in the pulmonary circulation. It is important to note that there is currently no evidence to suggest which ligand of the BMPR2 is predominantly affected in this setting, and it is also important to note that patients with PPH have no defined pathological phenotype of the systemic circulation [96].

Nevertheless, a number of further lines of evidence from *in vitro* and *in vivo* studies support the hypothesis that BMP7 signalling may have specific importance in normal VSMC biology, in the aetiology of vascular calcification and in its treatment. First, in primary cultures of VSMCs, cells can be induced to calcify under the influence of TGFß, as noted previously [67], this effect is accompanied by a shift in gene expression by these cells consistent with transdifferentiation into an osteoblastic phenotype. In this setting, BMP7 is able to reverse these effects of TGFß and re-establish gene expression consistent with the normal VSMC phenotype by increasing expression of the inhibitory Smad, Smad6 [67], which is capable of directly inhibiting TGFß signalling through the stimulatory Smads 2 and 3. The concept that BMP7 signalling through Smad 6 is important in the maintenance of normal VSMC phenotype and the prevention of VC *in vivo* is supported by the observation that the *smad6*$^{-/-}$ mouse is characterised by spontaneous aortic calcification in the postnatal period [101]. The relevance of this putative effect of BMP-7 in sustaining VSMC phenotype is additionally supported by

data from a study described above investigating the effect of BMP7 treatment in acute ischaemic nephropathy [90], which shows that αSMA expression was induced in peritubular blood vessels in the kidneys of animals treated with BMP7 when compared to controls.

Taken together, these lines of evidence suggest that BMP signalling in general and BMP7 signalling in particular have important roles to play in normal cardiac development and vascular smooth muscle physiology. Furthermore, disruption of these pathways leads to lethal abnormalities of cardiac development *in utero*, and to significant pathology in the adult human. In addition, evidence exists to link BMP7 signalling with the prevention of vascular calcification in cellular and animal models. Thus, the occurrence in uraemia of both down regulation of BMP7 expression on the one hand together with the presence of vascular calcification and high cardiovascular mortality on the other, suggests that BMP7 may be an important factor in the body's defence against VC in health.

2.3 Hypotheses

The hypotheses to be tested in the following studies derive from the data outlined in the previous sections, and are as follows:

- that administration of exogenous BMP7 will reduce or prevent the development of vascular calcification in the context of chronic kidney disease.
- that administration of exogenous BMP7 will improve pathological changes in bone structure and function in the context of chronic kidney disease, in parallel with benefits to vascular calcification.
- that administration of exogenous BMP7 will prevent pathological transdifferentiation of vascular smooth muscle cells towards an osteoblastic phenotype, and directly act to reduce their tendency to mineralise their extracellular matrix.

2.4 Summary

In summary, it has emerged that BMP7 is a critical renal factor both in embryological development and in maintenance of structural integrity in the adult, that expression of this factor is down-regulated in response to renal injury, and that BMP7 has beneficial effects when given as therapy in models of several common renal diseases, as well as some extra-renal complications of uraemia. The direct effects of BMP7 on smooth muscle cells of vascular origin as well as its benefits on the pathophysiology of renal osteodystrophy suggest that BMP7 may also have beneficial effects on vascular calcification, since the aetiology of vascular calcification in turn depends on abnormalities of vascular smooth muscle cell biology that may be promoted by a number of pathophysiological components of renal osteodystrophy. If this turns out to be the case, it is likely to have important consequences for the morbidity and mortality associated with chronic renal failure, since vascular calcification has emerged as an important risk factor for excess death in this setting.

Section 3

The effects of exogenous Bone Morphogenetic Protein 7 on vascular calcification in a murine model of chronic renal failure and atherosclerosis

3.1 Aims

As outlined above in section 2, the aetiology of VC is not clearly understood, whether as a component of the uraemic syndrome or in other clinical contexts. In part, this relates to a lack of a suitable animal model. The study described in this section aimed to establish such a model, building on the particular association between VC and both atherosclerosis and uraemia by superimposing chronic kidney disease on an established murine model of atherosclerosis. In addition, the relationship between VC and renal failure was investigated by assessing the effect of exogenous BMP7 on VC in this model, since evidence supports the concept of CKD as a state of BMP7 deficiency, which can in turn be hypothesised to increase the propensity of vascular smooth muscle cells to adopt a calcifying, osteoblastic phenotype in the vasculature. Thus, the study has three main aims:

- to characterise VC in the context of CKD in a murine model of atherosclerosis, using histological assessment.

- to identify the presence of cells expressing an osteoblastic phenotype in the pathogenesis of VC in this model, by analysing expression of osteocalcin in vascular tissues.

- to assess the influence of BMP7 on both these factors.

3.2 Introduction

3.2.1. The animal model

The Low-Density Lipoprotein Receptor null (*ldlr*$^{-/-}$) mouse in a C57/Bl6 background was selected as a suitable model for this study, as animals of this genotype have been documented to develop VC spontaneously in the context of atherosclerosis when fed a high fat, high cholesterol 'Western'-style diet [102].

Vascular calcification is generally difficult to model in laboratory animals. Most rodents, which are the most convenient animals to work with experimentally, are resistant to this disease process, and unlike humans do not commonly develop spontaneous VC even in extreme old age. However, in a comparison of several in-bred mouse strains commonly used experimentally, the C57/Bl6 mouse developed age-related VC the most commonly, with an incidence of about 25% [103].

While models of VC exist that use pharmacological manipulation to induce VC, for example with low-dose Warfarin regimes [104, 105] or high doses of Vitamin D [106,

107], such approaches were not felt to be attractive for the current study since they do not translate easily to human settings, where no consistent data exist linking these pharmacological treatments to VC [12]. While Warfarin use has been associated with some cases of the rare disease calciphylaxis (or calcific uraemic arteriolopathy) [108], in which patients with end-stage renal failure develop extensive medial-layer calcification in small calibre arterial vessels, this is not a ubiquitous finding and it remains to be shown that this is a truly causative relationship. In addition, no current human data has linked Warfarin use to calcification of larger vessels or in other settings. Given the widespread use of Warfarin in the clinical arena, there is unlikely to be any large uncharacterised pro-calcific effect of Warfarin yet to be discovered in humans. Vitamin D on the other hand has been related to VC in humans in clinical studies [19, 109], although, paradoxically, low Vitamin D levels have been correlated with the presence of coronary artery calcification [110, 111]. In addition, *in vitro* studies have shown that Vitamin D is able to up-regulate Matrix Gla protein (MGP) expression by rat vascular smooth muscle cells, a change which is likely to reduce the tendency of such cells to calcify their extracellular environment, and thus potentially reduce VC in rodents [107]. Further, it was felt that any such pharmacological model of VC would introduce an additional potential confounding factor into the study, since the possibility would exist for pharmacological interaction between agents used to set up the model on the one hand, and the BMP7 used in the treatment arm of the study on the other.

In addition to developing spontaneous VC, the *ldlr*$^{-/-}$ model is attractive since is genetically homologous to Familial Hypercholesterolemia in humans, and the atherosclerotic phenotype can be accentuated by feeding the animals a simulation of a 'westernized' human diet [102]. These animals also exhibit persistent hyperglycaemia when fed this atherogenic diet, evidenced by mild elevations of serum glucose

concentrations. This combination of atherosclerosis, glucose intolerance, dyslipidaemia and uraemia in one model therefore has the attraction of reflecting several aspects of the complex clinical milieu found in patients with renal failure in the context of type II diabetes mellitus, one of the commonest causes of CKD in the clinical setting, and one that continues to increase its prevalence.

3.2.2. The model of chronic renal failure

Several models of uraemia have been developed in rodents, variously using surgical, immunological, genetic or metabolic strategies. We decided to impose uraemia by a surgical technique using destructive electrocautery of one kidney followed by contralateral nephrectomy two weeks later, to give a decrease in renal function analogous to the 5/6 nephrectomy model in rats. This model is technically feasible in mice, and has been established to give reproducible amounts of renal injury [112, 113]. One advantage of this model, which has previously been used in studies of BMP7 and renal osteodystrophy discussed above [94], is that the permanent loss of nephron mass gives a fixed reduction in renal function that is not amenable to recovery under the influence of the BMP7 treatment, ensuring that any effects of therapy seen on VC are independent of changes in glomerular filtration rate. On the other hand, the studies described in section 2.2.3 above indicate that using other uraemic strategies to investigate VC might be confounded by the possible beneficial effects of BMP7 therapy on the underlying renal lesion itself, through modification of progressive fibrosis inherent in their aetiology.

3.2.3 Assessment of calcification

There is currently no established gold standard technique for analysing calcification histologically. We had initially planned to use one of two techniques. Firstly, histomorphometry is a well-established technique used to analyse bone mineralization in health and disease [114, 115], but can be laborious to perform where many small areas of calcification need to be defined and analysed, and as will become clear, the punctate nature of calcification seen in the vascular tissues in this study made it impractical to use. Secondly, a method of calcium quantification based on the elution Alizarin Red-S from appropriately stained tissues has been successfully used in an osteoblast cell culture system [116], but we were unable to successfully transfer this technique to whole tissue preparations. We therefore developed our own scoring system based objectively on the presence or absence of calcification, described below.

3.2.4 Assessment of osteoblastic cells in vascular tissues

To assess the role of cells expressing an osteoblastic phenotype, we decided to analyse osteocalcin (OC) expression by tissue immunohistochemistry. OC is a gamma-glycosylated (Gla-) protein expressed in normal endochondral bone mineralization, and regarded as pathognomonic of mature osteoblastic function and phenotype [119,151]. If the hypothesis that transdifferentiation of vascular smooth muscle cells to an osteoblastic

phenotype were correct, we would expect to find localised OC expression by cells in close association with areas of calcification, but not in normal non-calcifying tissues.

3.3 Methods

3.3.1 Animals and experimental procedures

Animals and diets. All experimental protocols involving animals were approved by the Washington University Animal Care committee (http://medicine.wustl.edu/~acu). *ldlr*$^{-/-}$ mice in a C57Bl/6 background were a gift from Dr C Semenkovich (Division of Atherosclerosis Nutrition and Lipid Research, Washington University School of Medicine, St Louis). Animals were allocated to experimental groups as shown in figure 3.1. Mice were weaned at three weeks to a standard laboratory chow diet. At 10 weeks, animals either continued chow or started a high cholesterol (0.15%) diet containing 42% calories as fat ('Fat' ; Harlan Teklad, Madison WI, Product No.TD88137) [102]. Animals had access to water *ad libitum.*

Surgical Procedures. We used a two-step surgical procedure to create animals with renal impairment [112] (Figure 3.2). In the first procedure, a 2 cm flank incision was made and the right kidney mobilised. Perirenal fat and the adrenal gland

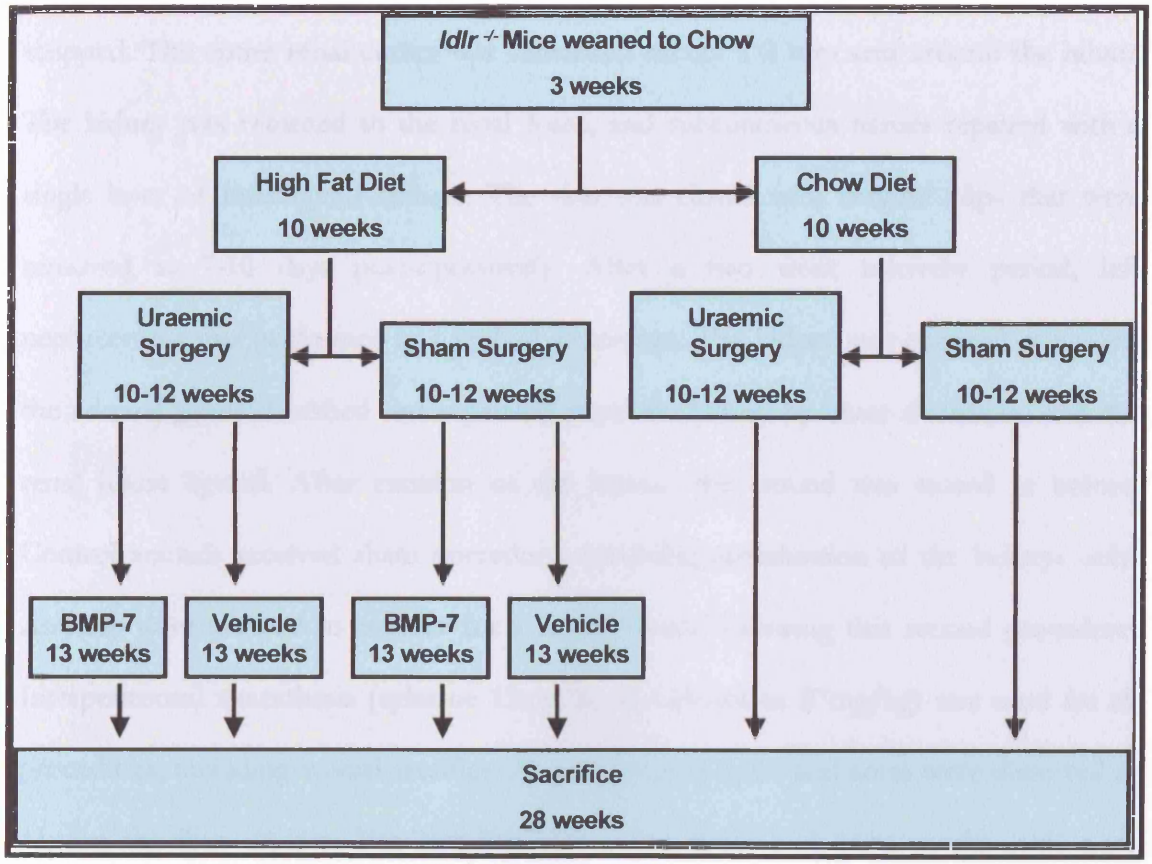

Figure 3.1 **Study design.** Animals were sequentially entered into experimental groups on the basis of diet, uraemic surgery and treatment. Experimental diets were commenced at the same time as the first uraemic surgery at 10 weeks. Second uraemic surgery was performed at 12 weeks. Experimental treatments were started one week after this, to allow animals to adequately recover from the surgical process. See text for full description.

were separated form the kidney by blunt dissection and the capsule of the kidney stripped. The entire renal cortex was cauterised except a 2 mm area around the hilum. The kidney was returned to the renal fossa, and subcutaneous tissues repaired with a single layer of interrupted sutures. The skin was closed with surgical clips that were removed at 7-10 days post-operatively. After a two week recovery period, left nephrectomy was performed in a second procedure. The kidney was exposed as before, the adrenal gland identified and separated from the kidney by blunt dissection, and the renal hilum ligated. After excision of the kidney, the wound was closed as before. Control animals received sham operations, involving mobilisation of the kidneys only. Animals were allowed to recover for a further week following this second procedure. Intraperitoneal anaesthesia (xylazine 13mg/kg and ketamine 87mg/kg) was used for all procedures, including animal sacrifice. At sacrifice, the heart and aorta were dissected *en bloc,* to the iliac arteries. For histological analysis, heart and aorta to the arch were separated from more distal aorta, and for chemical analysis, the aorta was separated from the heart at the level of the aortic valves, then further processed in its entirety.

Blood tests. Saphenous vein blood samples were taken one week following the second surgery, prior to initiation of therapy, and further samples were drawn by right ventricular puncture at the time of sacrifice. Serum was separated from all blood samples on the day of blood draw, stored at –80 ^{0}C and assayed variously for blood urea nitrogen (BUN), cholesterol and glucose by standard laboratory methods.

Treatment groups. This study was structured in two parts. Firstly, animals were entered into a protocol to assess vascular calcification in the context of CRF in *ldlr*$^{-/-}$ mice fed the high cholesterol diet. Animals in certain groups of this protocol received

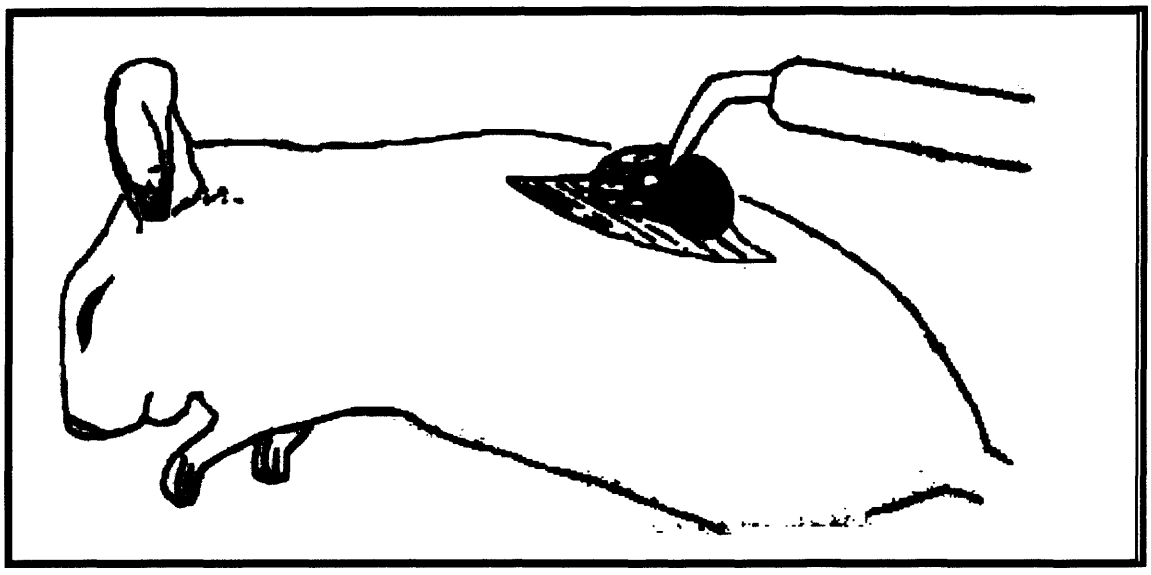

Figure 3.2 **Surgical approach.** The kidney is mobilized through a 2 cm flank incision, perirenal fat and the adrenal gland are separated from the kidney by blunt dissection, and the adrenal gland preserved. The capsule of the kidney is stripped, and the entire renal cortex cauterized, except a 2 mm area around the hilum, using an electrocautery probe as shown.

BMP7 treatment in addition. Blood samples of these animals were used to characterise various biochemical parameters in different treatment groups, and aortic tissues were assessed histologically for atherosclerosis and vascular calcification. To avoid unnecessary animal sacrifice, no chow-fed animals were treated with BMP7, as they were not expected to develop significant VC. Immunohistochemistry for osteocalcin was then performed on these same tissues. Secondly, in order to confirm aspects of the findings concerning osteocalcin expression, a small number of additional animals were given the various dietary options without surgery or BMP7 treatment for a shorter period of time, and at sacrifice various organs were removed for RNA extraction. Osteocalcin expression in these tissues was then assessed by Reverse Transcription PCR.

We allocated animals to six groups: Chow fed animals receiving either sham ('Chow Sham', Group 1) or uraemic ('Chow Sham', Group 2) surgery; high cholesterol-fed animals receiving sham ('Fat Sham' Groups 3 and 5) or uraemic ('Fat CRF', Groups 4 and 6) surgery, and each of these groups received either intraperitoneal BMP7 (Curis Inc, Cambridge MA) 10μg/kg in 100 μl vehicle (20mM acetate, 5% mannitol at pH 4.5) once weekly (Groups 5 and 6), or 100 μl vehicle alone Groups 3 and 4). This dose was selected by extrapolation from previous studies involving rats after discussion within the laboratory and with the manufacturers. This treatment began on the day after post-surgical phlebotomy.

3.3.2 Tissue processing and analysis

Tissue preparation. For histological analysis, we fixed resected specimens in formalin, and then divided as follows: the heart and proximal aorta up to and including

the arch were separated from the descending aorta, and bisected sagittally through the aortic outflow tract. 5 μm thick slices were stained with Alizarin Red and Von Kossa. Samples were stored at – 80 °C until assayed. For RNA extraction, we flash-froze resected tissues in dry ice/ethanol slurry, and stored at - 80 °C until processed.

Calcification score. In the absence of an accepted histological method of VC quantification, we developed the following. For each animal, we scored each of three slides stained with Alizarin Red for the presence or absence of calcification in two areas, the Intimal and Medial compartments of the proximal aortic sections. We derived a Total Vascular score by combining the individual compartment scores for each animal. To maximize objectivity in this scoring system, no attempt was made to grade the degree of calcification; the system is thus more sensitive in differentiating between no calcification and some calcification than it is at differentiating between various degrees of calcification where present. The scoring system was developed by the author, and one independent investigator (RJ Lund) scored all sections in a blinded fashion. Correlation between these two scorers was 0.9. Where differences arose, an arithmetic mean was taken.

Immunohistochemistry. Sections were deparaffinised in xylene, rehydrated in graded ethanols, incubated in 3% Hydrogen Peroxide to block endogenous peroxidase activity and in a solution of casein in PBS ('Background SNIPER', Biocare Medical, Walnut Creek CA). For OC, antigen retrieval with 5 minute incubation in citrate buffer ('Decloaker' Biocare Medical, Walnut Creek CA) at 100 °C was performed. Tissue slides were incubated with polyclonal antibodies raised against mouse OC in goats (Biogenesis Inc, Brentwood NH) diluted 1: 200 (in 2% BSA and 0.04% sodium azide in PBS as per manufacturer's instructions) overnight; then developed with a biotin-streptavidin-horseradish peroxidase system (all reagents, Biocare Medical, Walnut Creek CA) before

counterstaining with Haematoxylin. For anti-α-smooth muscle actin staining, slides were incubated with monoclonal primary antibodies (Sigma, St Louis MO) at a dilution of 1:300 in 2% BSA and 0.04% sodium azide in PBS with anti-mouse immunoglobulin secondary antibody ('Universal Link', Biocare Medical, Walnut Creek CA) overnight at 40 °C [117] to form immune complexes, which were applied to sections prepared as before overnight at 40 °C, then processed as above. Negative control slides were prepared in an identical way in the absence of primary antibody, and in addition, slides of mouse tibiae were stained for OC as positive control.

Statistical Analysis Comparisons across all groups together were performed with ANOVA, and where significant trends were detected, significance was allocated to a specific group or groups by comparison to the control (Chow Sham) group using Dunnetts post hoc test of ANOVA. Comparisons between individual pairs of groups used student's t-test. Data are presented as mean ± SD. Analyses was performed on Instat statistical software.

3.3.3 Analysis of osteocalcin gene expression

Animals and diets. Six 10 week old *ldlr*$^{-/-}$ mice were given either chow diet or high fat diet for four weeks. At sacrifice under anaesthesia, organs were removed and flash-frozen in dry ice and ethanol slurry, then stored at -80 °C.

Reverse transcription polymerase chain reaction (RT-PCR). Messenger RNA (mRNA) was isolated using the RNAqueous-4PCR kit (Ambion), according to

manufacturer's instructions. RT-PCR used the Onestep RT-PCR Kit (Qiagen, Valencia CA) according to manufacturer's instructions, using the following primers for Murine osteocalcin: Sense: 5' –CAAGTCCCACACACAGCAGCTT- 3'; Antisense: 5' – AAAGCCGAGCTGCCAGAGCTGCCAGAGTT- 3'. Reaction conditions were: 50 °C for 30 min, 95 °C for 15 min, then 35-40 cycles of 94 °C for 1 min, 60 °C for 1 min & 72 °C for 1 min, then 72 °C for 10 min. Negative control reactions were prepared by substituting an appropriate volume of deionised sterile water in place of RNA template.

3.4 Results

3.4.1 Animals and groups

The study was designed to sequentially enter animals into six groups (Table 3.1) as follows: 5 animals in a chow-fed sham operated group (Group 1) as controls, and 10 animals in each of five further groups (groups 2-6), receiving uraemic surgery (Groups 2, 4 and 6), high fat diet (Groups 3-6) or BMP7 treatment (Groups 5 and 6). However, when some animals in groups 2, 3 and 4 (2, 3 and 1 respectively) did not survive surgery, it was decided to enter 12 animals in the final two groups (Groups 5 and 6). Two animals did not survive surgery in group 5, but all animals survived in group 6. This led to uneven numbers in each group. The higher than expected mortality was attributable to the surgical program, and may have reflected initial surgical inexperience of the researcher, but not to either the treatment regime or diet (Table 3.1). Approximately equal numbers of male and female animals were entered into each group to increase the applicability of results to the clinical environment. Initial weights were comparable across all groups (Table 3.1). Untreated uraemic animals (Groups 2 and 4) tended to have a

	Group 1	Group 2	Group 3	Group 4	Group 5	Group 6
Diet	Chow	Chow	Fat	Fat	Fat	Fat
Surgery	Sham	CRF	Sham	CRF	Sham	CRF
Rx	-	-	Vehicle	Vehicle	BMP-7	BMP-7
n (Males)	5 (2)	8 (5)	7 (4)	9 (4)	10 (5)	12 (6)
Pre-Surgical Weight (g)	19.8 ±3.4	22.1 ±2.3	19.3 ±2.6	24.4 ±4.2	22.0 ±1.1	20.5 ±3.3
Sacrifice Weight (g)	24.8 ±4.0	22.3 ±2.1	25.0 ±3.9	26.2 ±5.4	[a]34.8 ±2.8	25.8 ±6.0
Post-Surgical BUN (mg/dl)	24.2 ±5.2	[b]69.8 ±16.2	21.5 ±8.3	[b]86.0 ±12.1	23.8 ±5.0	[b]63.5 ±16.4
Sacrifice BUN (mg/dl)	23.0 ±5.0	[c]76.5 ±11.0	25.5 ±6.6	[c]88.0 ±10.5	29.0 ±6.0	[c]71.9 ±21.3
Total Cholesterol (mg/dl)	261 ±28	168 ±24	[d]1071 ±370	[d]940 ±386	[d]871 ±192	[d]1097 ±348
Glucose (mg/dl)	172 ±31	183 ±21	192 ±23	190 ±46	211 ±66	197±59

Table 3.1 **Biochemical parameters of *ldlr*$^{-/-}$ mice by experimental group.** All values are mean ± SD. BUN Cholesterol and Glucose are expressed as mg/dl. [a] Group 5 Sacrifice weight was higher than Group 1. [b] The CRF Groups 2, 4 & 6 had significantly higher Post Surgical BUNs than Group 1 ($P<0.01$). [c]Groups 2, 4 & 6 have significantly higher sacrifice BUNs than Group 1 ($P<0.01$). [d]Groups 3 – 6 had significantly higher Cholesterols than Group 1 ($P<0.01$).

smaller weight gain than untreated non-uraemic animals (Groups 1 and 3), but these differences were not significant. Weight gain in the BMP7 treated Fat Sham animals (Group 5) was significantly greater than in other groups. Weight gain in BMP7 treated Fat CRF animals (group 6) did not differ from either untreated Fat CRF animals (Group 4) or Chow Sham animals (Group 1). We did not observe any toxicity attributable to BMP-7 therapy.

3.4.2 Biochemical data

All animals undergoing uraemic surgery developed significant renal impairment, and there were no significant differences in the degree of renal failure in CRF groups (Groups 2, 4 and 6) (Table 3.1). Renal function deteriorated during the treatment period, as evidenced by a rise in BUN between surgery and sacrifice (Median 5mg/dl, range –16 to +75mg/dl); however the increment was small, and similar in magnitude to that in sham-operated animals (1mg/dl, range –5 to +14mg/dl). Animals fed the high cholesterol diet (Groups 3-6) were significantly hypercholesterolaemic compared to Chow fed animals (Table 3.1), and where observed to have dramatic atherosclerotic plaque formation in the proximal aorta compared to chow-fed animals. All animals had mild glucose intolerance, but this did not vary significantly across the groups.

3.4.3 Histology

All of the *ldlr*$^{-/-}$ animals fed the high fat diet developed an increase in the number and size of atheromatous plaques of the proximal aorta and aortic arch. No difference was observed between male and female animals. Punctate calcification was seen in the aortic intima and media in all untreated groups (Figure 3.3 A-D). The high cholesterol diet produced severe atherosclerosis and calcification of aortic intima and media (Figure 3.3 C and D). Addition of CRF increased the number of punctate calcium deposits detected by the histological stain (Figure 3.3 E) compared to chow sham, group 1 ($p<0.01$, Table 3.2). Calcification was strikingly reduced in BMP7-treated, Fat CRF animals (Group 6) (Figure 3.3. G and H). The extent of atherosclerosis (the number and size of atheromatous plaques) remained unchanged by BMP7 treatment. Scoring of the histological slides for the presence or absence of calcification confirmed these findings (Table 3.2). Total Calcification scores and scores for the Intimal vascular compartment were significantly higher in untreated Fat CRF animals (Group 4) than for Chow Sham animals (Group 1). These scores for Fat CRF animals treated with BMP7 (Group 6) demonstrate significantly less calcification than either Fat CRF vehicle-treated animals (Group 4) or Chow Sham animals (Group 1). Scores for the medial compartment revealed that BMP7 treated Fat CRF animals have significantly less calcification here than either untreated Fat CRF or Chow sham animals (Groups 4 & 1). There was a tendency towards reduction of vascular calcification by BMP7 on Fat Sham animals (Group 5 versus group 3), but this did not reach statistical significance. Our scoring system did not measure differences in size or number of calcifications between groups where calcification was present. In particular, the effect of the fat diet to increase size of medial calcifications (Figure 3.3 C and D), and of CRF to increase the number of medial calcifications (Figure 3.3 E) were not measured in the scoring system, but this was

	Group1	Group2	Group3	Group4	Group5	Group 6
Diet	Chow	Chow	Fat	Fat	Fat	Fat
Surgery	Sham	CRF	Sham	CRF	Sham	CRF
Rx	-	-	Vehicle	Vehicle	BMP-7	BMP-7
n	5	8	7	9	10	12
[A]Total Score	3.6 ±1.6	3.8 ±1.0	4.4 ±2.1	[a]5.7 ±0.4	2.9 ±2.9	[b]0.5 ±0.5
[B] Intimal Score	1.0 ±1.3	1.2 ±0.9	2.0 ±1.3	[c]2.8 ±0.4	1.5±1.5	[d]0.1 ±0.2
[C]Medial Score	2.6 ±0.4	2.6 ±0.4	2.4 ±1.0	[f]2.9 ±0.2	1.4 ±1.4	[e]0.4 ±0.5

Table 3.2 Effect of BMP-7 on aortic calcification scores by group. The maximum Total calcification score is six, the sum of the maximum Intimal and medial scores. Three sections were analysed from each animal for the presence (one) or absence (zero) of calcification, yielding a maximal score of three for each compartment. All values are mean ± SD, in arbitrary units (see text). [a] Total Score for group 4 is significantly higher than for group 1 ($P<0.01$); [b] Total Score for group 6 is significantly lower than for group 1 ($P<0.01$) and group 4 ($p<0.0001$). [c] Intimal Score for Group 4 is significantly higher than for Group 1 ($P<0.01$). [d] In addition, the Intimal Score for group 6 is significantly lower than Group 4 ($P<0.0002$). [e] Medial Score for Group 6 differs from Group 1 ($P<0.01$). [f] Groups 4 & 6 differ from each other, $P=0.0003$.

nevertheless the most objective system for scoring the effect of BMP7, which was to eliminate calcification (Figure 3.3 G-H, Table 3.2). Since no attempt was made to grade the severity of calcification histologically, specimens with a few small punctate lesions would score similarly to large areas of confluent calcification.

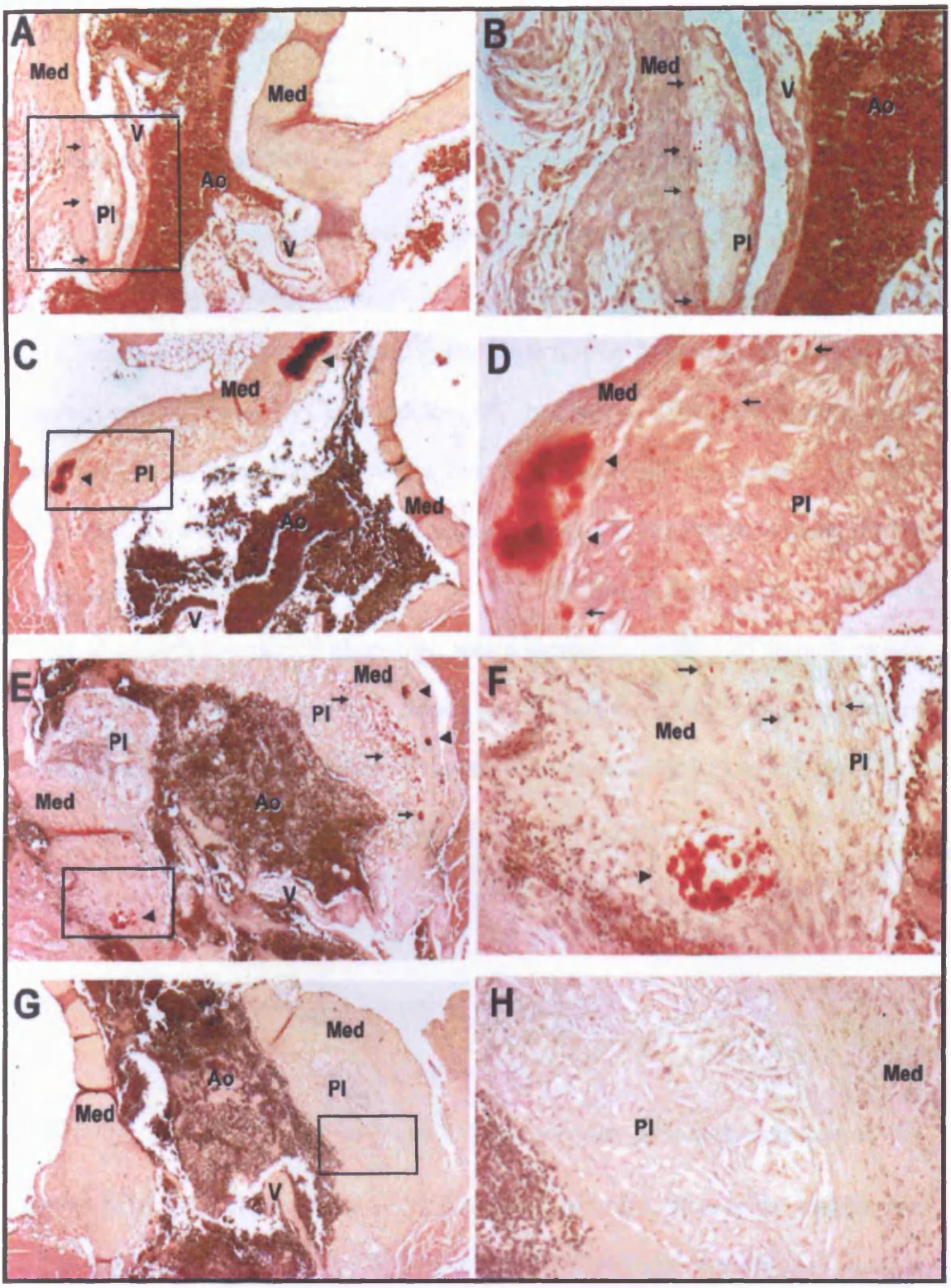

Figure 3.3 Effect of chronic renal failure (CRF) and bone morphogenetic protein–7 (BMP7) treatment on proximal aortic calcification. Aortic outflow tract sections defined by two vascular walls and intervening aortic valves stained for calcification (Alizarin Red-S). Boxes in left-hand panels show area enlarged in corresponding right-hand panel. (A and B) Punctate intimal calcification in an area of plaque (arrows) in chow sham animal (group 1). (C and D) Intimal (arrows) and medial (arrowheads) calcification in fat sham animal (group 3). (E and F) Intimal (arrows) and medial (arrowheads) calcification in fat CRF vehicle animal (group 4). (G and H) Absence of intimal or medial calcification in Fat CRF BMP-treated animal (group 6). Magnifications: 5 in A, C, E, and G; 10 in B; 20 in D, F, and H. Ao, aortic lumen; Pl, intimal plaque; Med, layer; Va, Valve leaflet.

3.4.4 Immunohistochemistry

Osteocalcin is regarded as a marker of the osteoblastic phenotype. Immunohistochemistry demonstrated low-grade baseline staining of vascular tissues in Chow Sham animals (Group 1) (Figure 3.4 B), compared to negative control (Figure 3.4 A). OC staining was diffusely increased in Fat Sham (Group 3, not shown) and Fat CRF animals (Group 4, Figure 3.4 C). In addition, OC staining was also noted on other tissues fortuitously on the same slides, including lung and oesophagus (not shown). In BMP7 treated Fat CRF animals (Group 6), OC staining was greatly reduced in vascular (Figure 3.4 D) and other tissues (not shown). This is in contrast to expression of αSMA, a marker of smooth muscle cell phenotype, which remained confined to smooth muscle layers in pulmonary and oesophageal tissues (not shown), for which immunostaining of vascular tissues was consistent across all experimental groups (Figure 3.4 E-H).

3.4.5 Reverse transcription polymerase chain reaction

To confirm the finding of widespread extra-osseous osteocalcin expression, we extracted RNA from the organs of 14 week old *ldlr*$^{-/-}$ mice fed chow or the high fat diet for four weeks, and performed RT-PCR. Osteocalcin mRNA was detectable in a number of organs in *ldlr*$^{-/-}$ animals, and was found to be more widespread in fat fed animals (Figure 3.5). This confirmed the immunohistochemistry results that a previously unknown component of the *ldlr*$^{-/-}$ phenotype is loss of tissue-specific expression of osteocalcin, which was restored by BMP7 therapy. However, tissues were not available

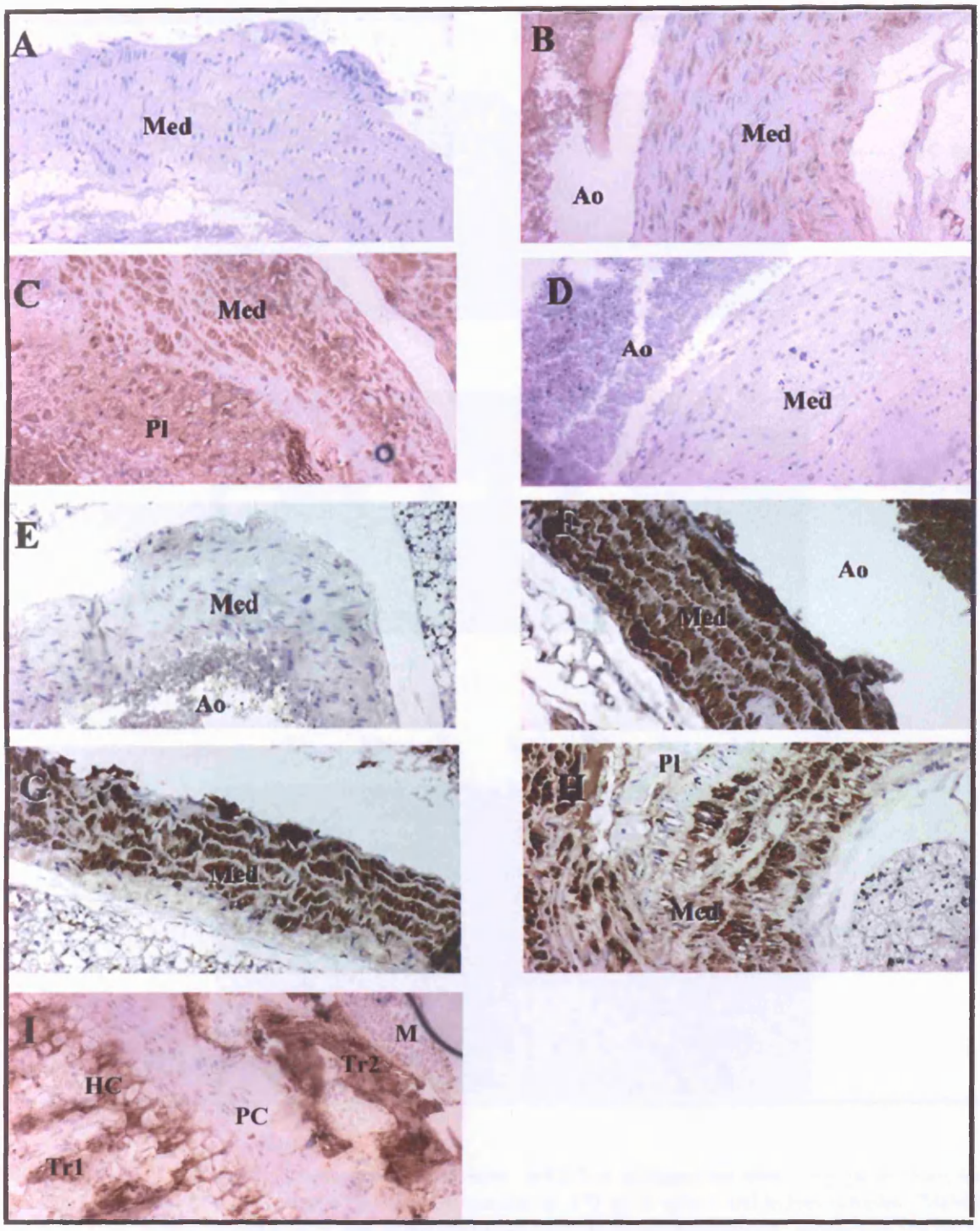

Figure 3.4. Effect of BMP7 on osteocalcin (OC) expression. Immunohistochemistry of proximal aortic sections for OC (A through D, I) and α-smooth muscle actin (SMA)(E through H). (A) Negative control (vascular media, wild-type mouse); (B) medial OC expression (brown staining) in chow sham animal; (C) more intense medial and plaque OC staining in fat CRF animal; (D) striking reduction in medial and plaque OC staining in fat CRF BMP7-treated animal; (E) negative control for SMA. (F through H) Consistent medial SMA staining in chow sham (F), fat CRF (G), and fat CRF BMP7–treated animals (H). (I) Positive control: endochondral bone of ENAC overexpressing mouse tibial plateau, showing normal OC staining of mineralized primary and secondary spongiosa trabeculae and around hypertrophic chondrocytes, but not prehypertrophic chondrocytes or marrow space (I). Magnification, x20. Med,medial layer; Pl, intimal plaque; Ao, aortic lumen. Tr1, trabeculum in primary spongiosa; Tr2, trabeculum in the secondary spongiosum; HC, hypertrophic chondrocyte; PC, prehypertrophic chondrocyte; M, marrow.

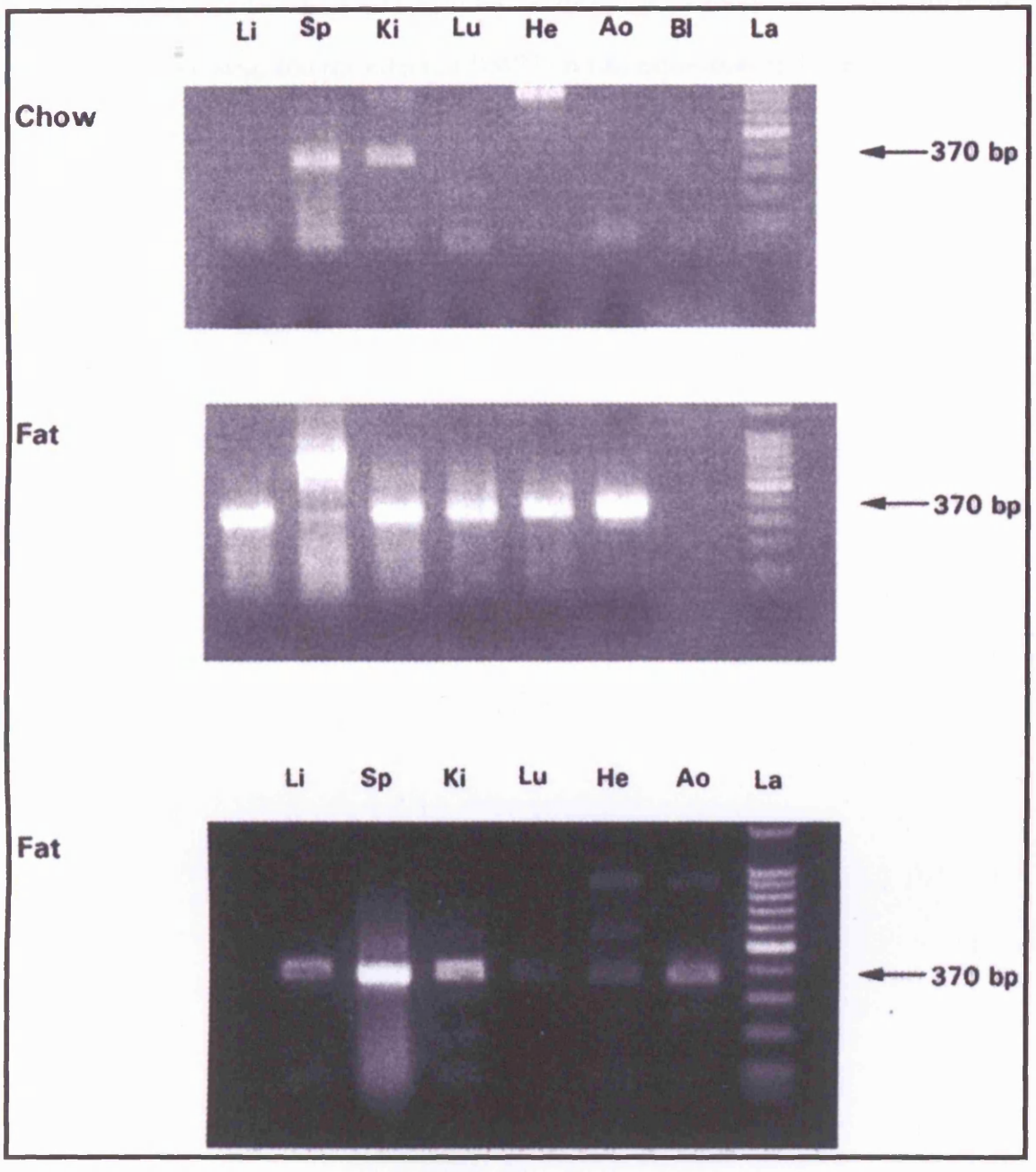

Figure 3.5 RT-PCR demonstrates Osteocalcin mRNA at extraosseous sites. (Top panel) Samples from a chow-fed LDLR-/- mouse showing OC product at 370 bp in spleen and kidney samples. (Middle and bottom panels) Samples from two cholesterol-fed LDLR-/- mouse showing OC product at 370 bp in liver, spleen, kidney, lung, heart, and aorta. Li, liver; Sp, spleen; Ki, kidney; Lu, lung; He, heart; Ao, aorta; Bl, blank; La, 100-bp ladder.

to extend these results to CKD animals as these had already been committed to histological processing, and the effect of BMP7 on OC expression at the level of mRNA in this setting is not known.

3.5 Discussion

This study shows that the *ldlr*$^{-/-}$ genotype in the C57/Bl6 mouse background is a suitable model for the investigation of vascular calcification in the context of CRF, without the need for pharmacological manipulations used in other models [104-107]. While it is clear that atherosclerosis in this model is dependant on dietary manipulation, the diet used is nevertheless similar in composition to a 'Western' high fat diet, containing 0.15% cholesterol weight for weight and 42 % of calorific content as fat. The surgical technique used is analogous to the 5/6 nephrectomy model in rats [112], and has previously been used to model renal osteodystrophy in mice. In contrast to other models of uraemia, it is relatively stable over time: it is debatable whether the small but statistically significant increase in BUN during the study is clinically significant, since a similar increase was observed in non-uraemic animals. In addition, the study shows that BMP7 is an efficacious treatment of Vascular Calcification in the context of CRF and atherosclerosis, an effect that appears to be general to both medial and intimal calcification, although BMP7 treatment does not affect the extent of atherosclerosis. The data concerning

osteocalcin expression show that this osteoblastic protein is expressed in increased amounts in the calcifying milieu, and that its expression is reduced by BMP7 treatment.

However, the histological data contains some inconsistencies that need explanation. Firstly, it appears that in Fat-fed CRF animals (Group 6), BMP7 was able to reduce VC to levels lower than under non-uraemic baseline conditions (groups 1 and 3). There is no obvious biological rationale for this finding, and it is likely to reflect limitations of the calcification scoring system. The system is based simply on the presence or absence of calcification, but makes no attempt to grade different degrees of calcification where present, in order to maximise objectivity, and a consequence of this is that the difference in score between samples with small amounts of calcification, such as group 1, and samples with extensive calcification, such as groups 3 or 4, was minimized, but the difference between groups with small amounts of calcification and nearly none (Groups 1 and 6) was exaggerated. The scoring system may also be prone to sampling errors that are difficult to quantify or control for. These limitations were therefore addressed in a further study, described below, in which total vascular calcification was quantified using a chemical technique.

A further inconsistency was the apparent lack of effect of BMP7 on vascular calcification in the absence of uraemia (Group 3 versus Group5). It is possible that the mechanisms underlying the calcification in the uraemic and non-uraemic situations may differ, with only uraemia-related disease amenable to BMP7 therapy, but it is also possible that the pharmacokinetics of BMP7 may be importantly different in the two setting. Firstly, animals in group 5 appeared to put on more weight than other groups, for reasons that aren't clear (Table 3.1). Second, BMP7 therapy was given via the intraperitoneal route, and since it has been shown that peritoneal permeability is increased in uraemia [79], it is

possible that uraemic animals absorbed a larger proportion of the delivered dose. Thirdly, BMP7 in the circulation is bound to α2-macroglobulin, which is in turn removed from the circulation in the liver by the receptor LRP1. Expression of this receptor has been shown to be increased in the context of the *ldlr*$^{-/-}$ genotype in the absence of uraemia, and so BMP7 may be removed from the circulation more rapidly in this setting. Since the dose used was a small one, it may be that the combination of these factors has rendered the dose sub-therapeutic in non-uraemic *ldlr*$^{-/-}$ animals. Further work is needed to clarify these issues.

Given the available data supporting the presence of a cell expressing an osteoblastic phenotype in the vessel wall [12, 39, 57, 118], it may seem paradoxical that a bone morphogenetic protein should reduce VC, given the known role of BMP7 in osteoblast biology. However it is clear that the effects of individual BMPs are highly dependent on the target cell type, the type of receptors that cell expresses, and its state of differentiation and maturity [79]. In this respect the nomenclature of these proteins based on their skeletal effects may be superficially confusing. Nevertheless, BMPs are critical morphogens in a wide range of tissue differentiation events, and BMP5, -6 and -7are clearly collectively critical for cardiovascular development. Important to understanding the data in this study is the data presented above that BMP7 has a positive influence on VSMC differentiation, and overall this study supports the hypothesis that transdifferentiation of VSMCs is the first critical step in the aetiology of vascular calcification. However, beneficial effects of therapy could be explained by other mechanisms such as secondary benefits of improved osteodystrophy, calcium phosphate homeostasis or perhaps nutrition in these uraemic animals, and these issues are also investigated further in the studies described below.

The data on osteocalcin expression are also somewhat unexpected. We chose to study osteocalcin because it is regarded as a marker of mature osteoblastic phenotype, and we anticipated that immunohistochemistry would reveal localised expression in relation to areas of calcification. However, the finding of widespread osteocalcin expression on IHC was supported by analysis of RNA from various tissues of the *ldlr*$^{-/-}$ mice (Figure 3.4). We observed that osteocalcin was increased in fat-fed animals, in parallel with increased vascular calcification, and that both osteocalcin expression and VC are strikingly suppressed by BMP7 treatment. This suggests that the interpretation of osteocalcin expression as a unique marker for osteoblast function is overly simplistic. In fact the findings are consistent with the concept of osteocalcin as an endogenous limiter of calcification, expressed late in the osteoblastic gene program after mineralization has been initiated. The data presented above are consistent with an extended role beyond bone to other tissues including but not limited to the vasculature, with increased expression occurring under certain pro-calcific circumstances such as CRF, LDLR deficiency and high fat diet. Established data support this interpretation. In the mouse, osteocalcin exists in a three-gene cluster, OC1 and OC2, and the OC-related gene or ORG, which codes for the protein Nephrocalcin [119]. It has been shown that OC1 is strongly expressed in bone, and that OC2 and ORG are expressed elsewhere, albeit at lower levels. High structural homology between these proteins is consistent with functional homology, and they may be regarded as isoforms. All three bind to calcium ions via gamma-carboxylated residues, and act to limit the size of crystal formation. The phenotype *oc* $^{-/-}$ mouse includes an enlarged but otherwise normal skeleton [120], and Nephrocalcin expression by cells in the kidney tubule serves to limit renal stone formation [121]. Their high structural homology also makes it impossible to distinguish between the three gene products by conventional IHC or RT-PCR [122]. It is thus likely that the data in this study show an increase in expression of extra-osseous isoforms of

OC in the face of the *ldlr*$^{-/-}$ genotype and a pro-calcific environment caused by hypercholesterolaemia, atherosclerosis and CRF, and that BMP7 administration reduces expression of OC by ameliorating that pro-calcific tendency, by modifying the uraemic environment or preventing the initiation of the osteoblastic process. In this analysis, calcification of the vasculature in CRF represents a special circumstance, homologous to endochondral bone formation, where pro-calcific influences orchestrated by osteoblasts or osteoblast-like cells outweigh local anti-calcific mechanisms represented by osteocalcin and related proteins.

In summary, this study shows that BMP7 is an effective treatment of VC in the context of a murine model of atherosclerosis and CRF, but raises a number of further issues, including the relationship between vascular calcification and renal osteodystrophy, which are addressed below.

Section 4

The relationship between vascular calcification and renal osteodystrophy in a murine model of atherosclerosis and chronic renal failure, and of the effect of exogenous Bone Morphogenetic Protein 7 on these conditions

4.1 Aim

The study described in the previous section establishes the uraemic *ldlr*$^{-/-}$ mouse as a model of vascular calcification in chronic renal failure. However, as described above, the use of a histological system to assess vascular calcification is semi-quantitative at best, and the conclusions of the study would be strengthened by corroboration with alternative, quantitative methods. It is also clear that the effects of BMP7 on vascular calcification may be interlinked with its effects on bone. Thus, the present study was designed with the following specific aims:

- to quantify the degree of vascular tissue calcification previously defined histologically in section 4, using an analysis based on chemical quantification of total tissue calcium content.
- to define the characteristics of renal osteodystrophy seen in the murine *ldl*$^{-/-}$ model of atherosclerosis, uraemia and vascular calcification.
- to define the effect of BMP7 on both these pathologies in this setting.

4.2 Introduction

4.2.1 Background and hypothesis

In the previous study, vascular calcification (VC) was shown to increase when CRF was superimposed on a murine model of atherosclerosis. In addition, this increase in VC was successfully ameliorated by intraperitoneal administration of exogenous BMP7. However, as discussed above, there are a number shortcomings inherent in assessing calcification by a histological scoring system, and it became clear that these results needed to be validated using a quantitative method. Thus, the intention of the present study was to assess VC using a chemical assay [104] to quantify total tissue calcium content in aortic tissues of *ldlr*$^{-/-}$ mice exposed to the same experimental conditions.

A further aim was to assess the nature of renal osteodystrophy (ROD) in this model of VC. Abnormalities of calcium and phosphate ion homeostasis associated with VC such as hyperphosphataemia and elevated calcium/phosphate ion product (CaXP) are also characteristic of ROD. In addition, therapies used in the treatment of ROD, such as vitamin D analogues and calcium-containing phosphate binders, are also associated with

the presence of VC [4, 17]. It is thus reasonable to hypothesise a pathophysiological link between these two conditions. As noted above in Section 2.1.2.3, ROD comprises a spectrum of histological abnormalities, ranging from Osteitis Fibrosa characterised by high bone turnover, to Adynamic Bone Disease (ABD) characterised by low turnover [69]. While both forms of ROD may be associated with biochemical abnormalities relevant to the aetiology and progression of VC, it is likely that they do so by different mechanisms. While evidence now exists that BMP7 is effective in the treatment of both high [94] and low [74] turnover ROD in rodent models, this evidence with respect to ABD was not apparent at the time of design of the study. In any case, it was important to characterise the precise nature of ROD occurring in the present model if we were to fully understand the pathological processes involved in both the aetiology of VC, and the mechanism of action of BMP7 therapy in controlling VC in this setting. To do this, femurs and tibias were retrieved form experimental animals at sacrifice, and analysed by standard bone histomorphometric techniques that enable precise histological characterisation of ROD to be made in this model.

4.2.2 Bone remodelling

In order to understand the histomorphometric analysis, it is important to understand normal processes involved in trabecular bone remodelling [115].

Normal trabecular bone is involved in a continuous process of remodelling, allowing renewal of trabecular structures and the maintenance of architectural integrity even after overall bone growth has ceased. This allows the skeleton to respond to external

mechanical stresses by strengthening appropriate areas, but also contributes importantly to calcium, and to a lesser extent phosphate, homeostasis. Bone resorption occurs through the actions of multinucleated osteoclasts derived from monocyte precursors, and new bone matrix is synthesised and subsequently mineralised by osteoblasts derived from mesenchymal precursors. In health, these processes are in balance, a situation orchestrated at the cellular level by osteoblasts through direct regulation of osteoclast maturation and function. Coordinated groups of osteoblasts and osteoclasts are referred to as a bone remodelling unit (BRU), which in turn acts to remodel a defined section of bone referred to as a bone structural unit (BSU). The BSU consists of a disc-like structure on the trabecular surface. Osteoclasts initially erode a pit at the leading edge of the BSU, and subsequently pre-osteoblasts migrate into the pit before differentiating into mature osteoblasts. These mature osteoblasts then synthesise osteoid, which they subsequently mineralise. The remodelling process may thus be divided into erosion and formation periods, separated by a quiescent period. Resorption is a more rapid process than formation. Approximately 4% of trabecular surface is undergoing resorption, 16% formation and 80% of trabecular bone is not involved in either process at any one time. In humans, the erosion period lasts approximately 43 days, the quiescent period 7 days and the formation period 145 days, giving a total of approximately 200 days for the whole process.

The total amount of bone remodelling occurring at any given time depends not only on osteoblast and osteoclast activity, but also on the total number of BRUs. The rate at which BRUs are formed is known as the activation frequency (Acf). This parameter is highly variable in bone diseases, and may have a large influence on overall bone turnover.

4.2.3 Bone histomorphometry

Bone histomorphometry is an established histological technique used to analyse static and dynamic bone parameters in metabolic bone diseases of various types, through quantification of both directly measured and derived parameters of trabeculated and cortical bone. A detailed discussion of this technique is beyond the scope of this thesis, but a summary of the methodologies involved is included here and supported by a number of publications [114, 115, 152]. These measurements at a single point in time allow reconstruction of the recent remodelling cycle, through resorption, quiescence and then formation, a period of approximately three years in healthy human bone. For static parameters, histological sections of bone are stained in a standard way, to demonstrate the relevant cell types and structures, for example using Masson's or Goldner's trichrome. For dynamic measurements, the mineralising front is labelled at two points separated by a known period, and the spatial difference between the two labels assessed. Tetracycline is a commonly-used label as it autofluoresces, and dynamic measurements are thus made on unstained sections in this setting. Sections are then viewed under high power, through a superimposed grid, which intersects tissue structures in a random fashion. Morphometric methods used to analyse the sections rely on the application of probability theory and geometry, and use estimates rather than precise measurements. However, repeated counting ensures these estimates are highly accurate and robust. Defined tissue areas can be determined by point counting techniques, and measurements of distances or surfaces are made using the linear intercept method. These values are repeated then averaged over a number of sections. (See section 4.3.2 of specific methodology). While counting, measurement and calculation are carried out by computer, but the definition of structures to be assessed is a manual process. As such,

bone histomorphometry is a meticulous and time consuming technique requiring thorough training and expertise for consistent results. Thus, for reasons of quality and consistency, sections in this study were analysed by an investigator already experienced in the technique. Nomenclature and definition of the various parameters have been standardised by The American Society of Bone and Mineral Research, and these terms will be used in this thesis [114].

Tables 4.1 and 4.2 summarize some of the terms used, although this list is not exhaustive. Primary indices are directly measured, and include dynamic parameters measured from tetracycline or calcein double-labelling. These primary indices are then used to calculate secondary indices. As can be seen from Table 4.1, some parameters are quoted in both two- and three-dimensional formats. The rationale for this is that, while all measurements are actually performed in two dimensions, well-validated correlations exist between related two- and three-dimensional parameters, for example area and volume; thus a measurement in two-dimensional space can be confidently extrapolated to three dimensions. This allows appropriate ratios between different parameters to be derived: for instance the number of osteoblasts seen, NOb, can be related to bone perimeter, BPm, in two-dimensions, giving the parameter NOb/BPm, while the osteoblast surface, ObS, can be related to Bone Surface, BS, in three dimensions (ObS/BS).

Changes in bone histomorphometry seen in ROD are well described [69]. Osteitis Fibrosa is characterised by an increase in both bone formation rate and bone resorption, with an imbalance of osteoclastic activity leading to net bone resorption. As well as increased cellular activity, increased numbers of osteoblasts and osteoclasts are also seen, and there is evidence of peritrabecular fibrosis generated by functionally abnormal osteoblasts that have adopted a fibroblastic phenotype. Increased osteoblast activity also

Index Type	Measured parameter	Name of Index	Abbreviation 3D	2D
Area & Volume	Area	Bone Volume	BV	BAr
		Osteoid Volume	OV	OAr
		Mineralised Volume	MdV	MdAr
		Tissue Volume	TV	TAr
Perimeter & Surface	Length	Bone Surface	BS	BPm
		Osteoid Surface	OS	Opm
		Eroded Surface	ES	EPm
		Osteoblast Surface	ObS	ObPm
		Osteoclast Surface	OcS	OcPm
		Labelled Surface	LS	LPm
		(single, double)	sLS, dLS	sLPm, dLPm
Width & Thickness	Distance between points or lines	Mineralised Thickness	MdTh	MdWi
		Osteoid thickness	OTh	OWi
		Wall thickness	WTh	WWi
		Label thickness	LTh	LWi
Number	Number	Osteoblast number	-	NOc
		Osteoclast number	-	NOb

Table 4.1 Primary Indices in Bone Histomorphometry. See text for further explanation of terms

Index Type	Name of measurement	Abbreviation
Structural	Trabecular Number	TbN
	Trabecular Separation	TbS
Kinetic	Mineralising Surface	MS
	Mineral Apposition Rate	MAR
	Osteoid Apposition Rate	OAR
	Bone Formation Rate	BFR
	Formation Period	FP
	Quiescent Period	QP
	Activation Frequency	Acf

Table 4.2 **Derived Indices in Bone Histomorphometry.** See text for further explanation of terms.

results in the presence of extensive unmineralised osteoid. A number of abnormal parameters, including the increased erosion surface, osteoclast number and extent of fibrosis all correlate to circulating parathyroid hormone levels, which are characteristically elevated in OF. Adynamic Bone Disease on the other hand is characterised by reduced bone formation rate and reduced osteoblast numbers. Osteoclast numbers and activity may be low or normal in this setting. ABD is differentiated from osteomalacia, another low-turnover bone disease sometimes seen in CRF, by the extent of unmineralized osteoid present: while osteoid dimensions are increased in Osteomalacia, they are usually normal in ABD. Clinically, some heterogeneity exists, and biopsies fall into a spectrum of diagnosis between these extreme points. In addition, serial biopsy studies have shown that individual patients may move from one condition to another during the course of their illness.

To enhance reliability and consistency, bone histomorphometry in this study was performed by a single operator (Dr R J Lund) blinded to the experimental grouping of the histological slides.

4.2.4 The animal model and the model of chronic renal failure

The model of *ldlr*$^{-/-}$ model atherosclerosis, CRF and vascular calcification was unchanged from the previous study, and CRF was generated by the same surgical technique. It was expected that untreated uraemic mice fed the high cholesterol diet would develop OF, since their diet contained normal amounts of calcium and phosphate (1.0 and 0.65 %

respectively) and the consequent secondary hyperparathyroidism would remain untreated.

4.3 Methods

4.3.1 Animals and experimental procedures

Animals and diets. Experimental protocols involving animals and diets are as described in section 3.3.1.

Surgical Procedures. Animals were rendered uraemic as described previously in section 3.2 [112](Figure 3.2). Control animals underwent sham operations, and intraperitoneal anaesthesia (xylazine 13mg/kg and ketamine 87mg/kg) was used for all procedures, including sacrifice. At sacrifice, the heart and aorta were dissected *en bloc,* to the iliac arteries. For chemical analysis, the aorta was separated from the heart at the level of the aortic valves, and then
further processed in its entirety. Both femurs and tibias were removed by dissection, and fixed in 70% ethanol at 4 ^{0}C.

Treatment groups. We allocated animals to five groups (Table 4.2, Figure 4.1): Chow fed animals receiving sham surgery ('Chow Sham', Group 1); high cholesterol-fed animals receiving sham surgery('Fat Sham', Groups 2 and 4)); and high cholesterol-fed animals receiving uraemic surgery ('Fat CRF', Groups 3 and 5). Groups other than control received either intraperitoneal BMP-7 (Curis Inc, Cambridge MA) 10μg/kg in 100 μl vehicle once weekly (Groups 3 and 5), or 100 μl vehicle alone Groups 2 and 4). This treatment began on post-surgical day eight, the day after phlebotomy. The Chow sham group was included to define the bone parameters in the *ldlr*$^{-/-}$ genotype under unmodified conditions. In contrast to the previous study, no chow fed animals were rendered uraemic. This avoided unnecessary sacrifice of animals, since it was felt that this group would be unlikely to contribute significantly to the interpretation of the study.

Blood tests. Blood samples were taken for biochemical assays prior to initiation of BMP7 or vehicle therapy, and again at sacrifice, as above in section 3. In addition samples were taken at sacrifice for intact Parathyroid hormone assay. Serum was separated and stored at –80 C and assayed variously for blood urea nitrogen (BUN), cholesterol, calcium, phosphate, and glucose by standard laboratory methods. Intact Parathyroid Hormone levels were measured using a two-site immunoradiometric assay (IRMA) using a commercially available kit. (Immutopics, San Clemente, CA, USA).

Statistical analysis. Comparisons across all groups together were performed with ANOVA, and where significant trends were detected, significance was allocated to a specific group or groups by comparison to the control (Chow Sham) group using Dunnetts post hoc test of ANOVA. Comparisons between individual pairs of

groups used student's t-test. Data are presented as mean ± SD. Analyses was performed on Instat and SAS statistical software.

4.3.2 Tissue processing and analysis

Chemical quantification of aortic calcification. Aortic tissue from the outflow tract to the iliac bifurcation was desiccated overnight at 55° C, weighed and crushed in a pestle and mortar. Calcium was eluted from this crushed tissue using 10% Formic acid (10:1 v/w) for 24 hours at 4° C. The eluate was stored at -80° C until assayed. The calcium content of the eluate was assayed used a Cresophthalein-Complexone method (Calcium Kit, Sigma, St Louis), according to manufacturer's instructions, and values were then corrected for dry tissue weight [104].

Bone Histomorphometry. For dynamic measurements, *in vivo* fluorescent labelling of the mineralising front was achieved by intraperitoneal calcein injections, giving 20 mg/kg seven and two days prior to sacrifice. Femoral and tibial bone samples were dissected and fixed as above, and embedded undecalcified in a plastic embedding kit H7000 (Energy Beam Sciences Inc, Agawam, MA USA) Tissues were sectioned in a frontal plane in 5 um sections, with a JB-4 Microtome, (Energy Beam Sciences, Inc) and stained with Goldner's Stain for trabecular and cellular analysis. Tartrate-Resistant Acid

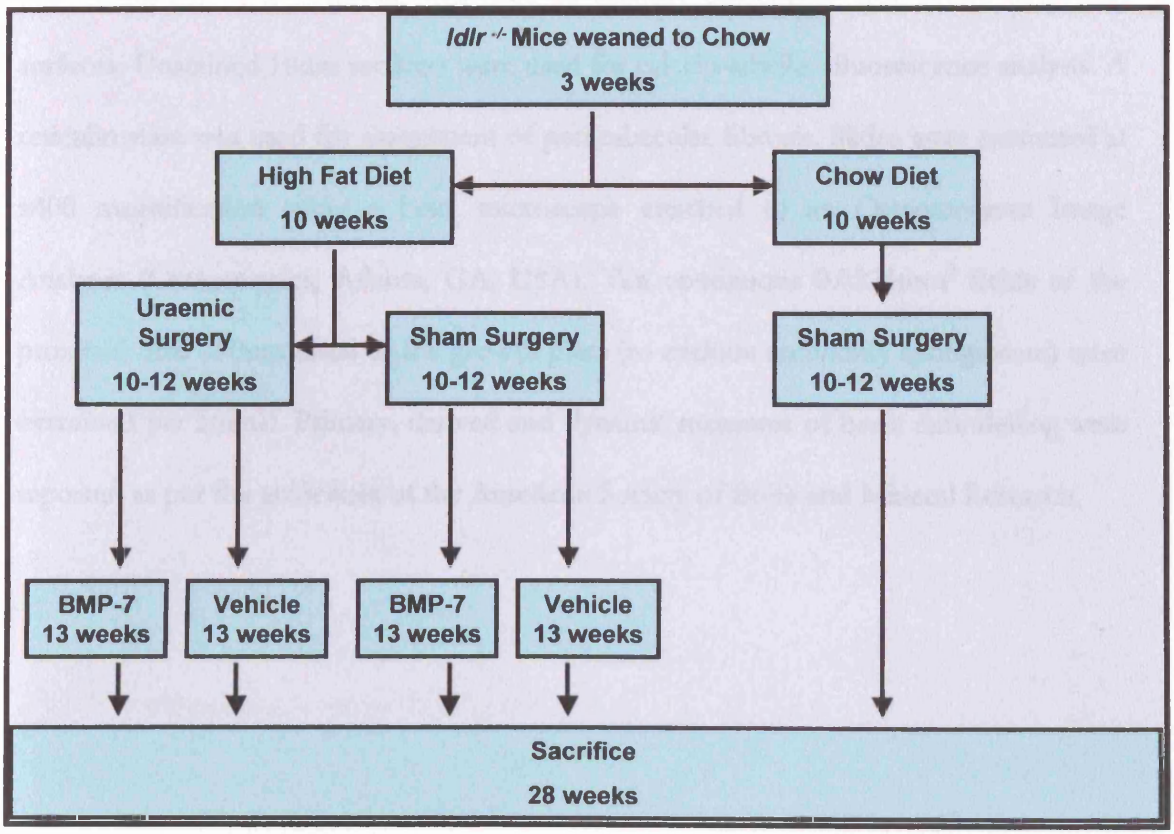

Figure 4.1 **Study design.** Animals were sequentially entered into experimental groups on the basis of diet, uraemic surgery and treatment. Experimental diets were commenced at the same time as the first uraemic surgery at 10 weeks. Second uraemic surgery was performed at 12 weeks. Experimental treatments were started one week after this, to allow animals to adequately recover from the surgical process. See text for full description.

Phosphatase (TRAP) staining was used to identify osteoclasts and define osteoclast surfaces. Unstained 10um sections were used for calcein-labelled fluorescence analysis. A reticulin stain was used for assessment of peritrabecular fibrosis. Slides were examined at x400 magnification using a Leitz microscope attached to an Osteomeasure Image Analyser (Osteometrics, Atlanta, GA, USA). Ten contiguous 0.0225mm^2 fields of the proximal tibia 150um distal to the growth plate (to exclude secondary spongiosum) were examined per animal. Primary, derived and dynamic measures of bone remodelling were reported as per the guidelines of the American Society of Bone and Mineral Research.

4.4 Results

4.4.1 Animals and groups: biochemical data

Five animals were entered into each group in this study. All animals survived the surgical procedures and experimental protocol, likely to reflect improved surgical technique. There were small non-significant differences in weight gain throughout the study between groups. No toxicity attributable to BMP-7 therapy was observed.

All animals undergoing uraemic surgery developed significant renal impairment, and there were no significant differences in the degree of renal failure in CRF groups (Groups 4 and 5) (Table 4.3). Renal impairment was maintained throughout the study period in these groups. Animals fed the high cholesterol diet (Groups 2-5) were significantly hypercholesterolaemic compared to chow fed animals (Table 4.3). All animals had mild glucose intolerance, but this did not vary significantly across the

	Group 1	Group 2	Group 3	Group 4	Group 5
Diet	Chow	Fat	Fat	Fat	Fat
Surgery	Sham	Sham	Sham	CRF	CRF
Rx	-	Vehicle	BMP7	Vehicle	BMP-7
n	5	5	5	5	5
Pre-Surgical Weight (g)	21.7 ±2.2	21.1 ±2.2	20.3 ±2.9	21.6 ±2.7	23.7 ±2.3
Sacrifice Weight (g)	22.6 ±2.6	24.7 ±5.7	20.7 ±3.7	21.4 ±3.4	23.3 ±3.6
Post-Surgical BUN (mg/dl)	26.9 ±7.4	25.4±5.6	34.3 ±6.8	[a]95.7±22.8	[a]77.9 ±10.1
Sacrifice BUN (mg/dl)	36.9 ±5.4	26.4 ±6.7	53.2 ±56.9	73.1±2.6	102.5 ±35.5
Total Cholesterol (mg/dl)	494.3 ±40.5	[c]2249.8 ±816.8	[c]1784.8 ±476.7	[c]1462.0 ±51.5	[c]1986.0 ±1120.7
Glucose (mg/dl)	289.3 ±91.6	209.0 ±63.6	219.0 ±67.1	240 ±107.1	194.5 ±44.7
Calcium (mg/dl)	8.4 ±1.5	8.2 ±1.5	10.2 ±1.7	9.8 ±0.6	10.5 ±4.7
Phosphate (mg/dl)	9.4 ±0.4	12.2 ±4.2	11.1 ±0.7	12.4 ±2.8	10.2 ±1.0
PTH (pg/dL)	30.0 ±26.7	28.4 ±28	85.2 ±159.9	209.6 ±187.7	268.6 ±335.7.

Table 4.3 Biochemical parameters of *ldlr*$^{-/-}$ mice by experimental group. Values are expressed as mean ± SD. [a] The CRF Groups 4 & 5 had significantly higher Post Surgical BUN values than Group 1 ($P<0.01$). [b] Groups 4 & 5 had significantly higher sacrifice BUN values than Group 1 ($P<0.01$). [c] Groups 2-5 had significantly higher Cholesterol values than Group 1 ($P<0.01$).

groups. Calcium and phosphate data showed variability between groups; however, wide confidence intervals mean that no differences were significant. This may reflect sample size. Animals with CRF (groups 4 and 5) had higher PTH levels than non uraemic animals, but once again, wide confidence intervals mean that these differences are not significant (Table 4.3). In fact, with respect to PTH the most striking change in these animals with CKD is the increase in range and variability of values measured (Figure 4.2).

4.4.2 Chemical quantification of aortic calcification

This assay quantifies total tissue calcium content. We assumed that intracellular calcium content was identical in all groups, and that differences detected between groups reflect differences in extent of extracellular calcium deposition. Baseline levels of calcification were defined in Chow Sham animals (Group 1) (Fig. 4.3), and a non-significant two-fold increase was detected in Fat Sham animals (Group 2). BMP-7 therapy had no effect on calcification in Fat Sham animals (Group 3). The aortas of the Fat CRF animals (Group 4) had a significant increase in calcification, approximately 6 fold over Chow Sham animals. BMP-7 therapy of Fat CRF animals reduced calcification (Group 5), and calcium levels in this group are not different statistically from Chow Sham animals (Group 1).

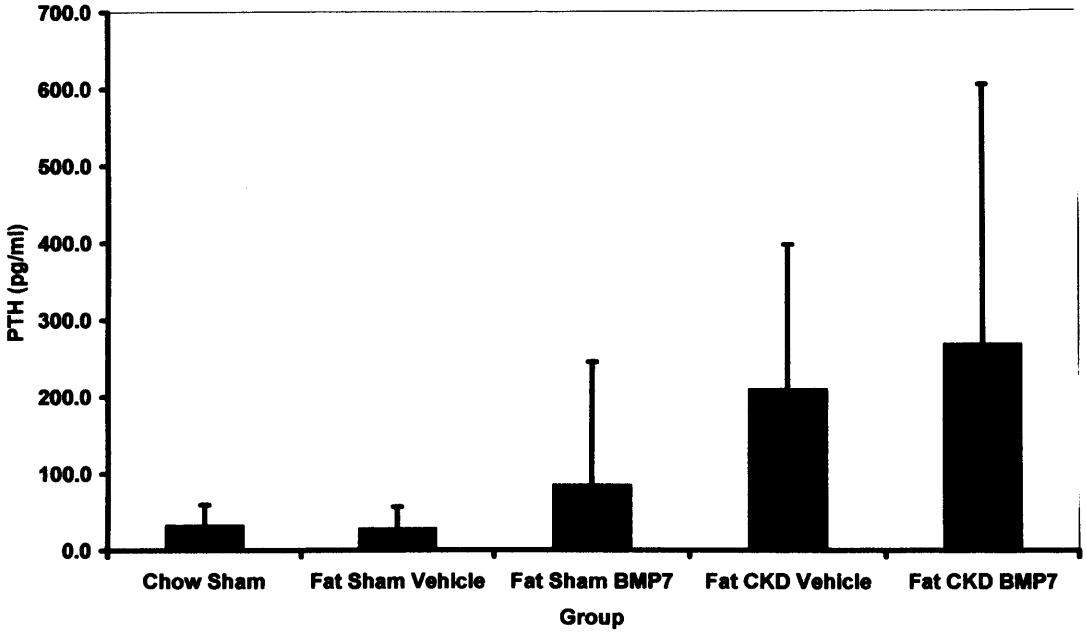

Figure 4.2 **Parathyroid Hormone levels in *ldlr*$^{-/-}$ mice.** Serum Parathyroid Hormone level at sacrifice by group (mean ± SD). No significant differences between groups

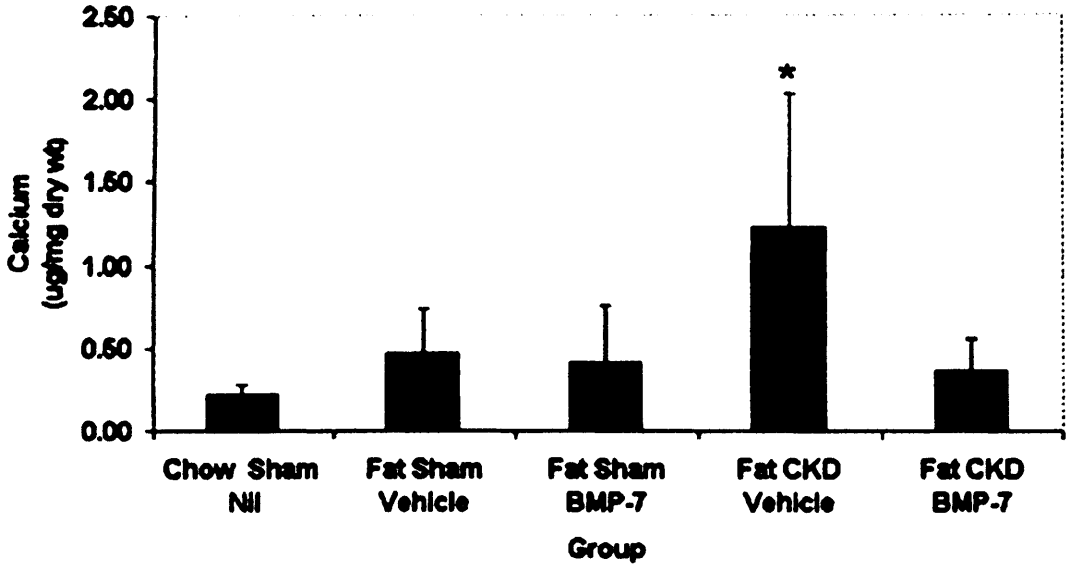

Figure 4.3 Chart showing chemical assessment of effect of BMP-7 on vascular calcification by treatment group. Total aortic calcium content measured in a 10% formic acid eluate of crushed desiccated aorta. Data are mean ± SD. Trend is significant by ANOVA, $P = 0.008$. * Fat-fed uraemic animals treated with vehicle have significantly higher levels than chow-fed sham controls. ($P < 0.01$, by Dunnetts post hoc test.) Fat-fed uraemic animals treated with BMP-7 are indistinguishable statistically from control (chow sham animal).

4.4.3 Bone histomorphometry

The most striking bone histomorphometric findings concerned osteoblast-related bone formation parameters in uraemic animals receiving vehicle (Group 4). The number of osteoblasts per field (NOb) was significantly reduced compared to control animals (Group1) (Figure 4.4A), and this remained true when expressed in relation to the defined tissue area (NOb/Tar) (Figure 4.4 B), or bone perimeter (NOb/BPm) (Figure 4.4 C). Consistent with this, the osteoblast surface as a proportion of bone surface (ObS/BS) (Figure 4.5A) was reduced, and indices of the bone formation component of the remodelling cycle were appropriately perturbed: the proportion of bone surface that is mineralising (MS/BS) (Figure 4.5 B) and calcein-labelled (LS/BS, Figure 4.5 C) were both reduced, and the formation period (FP) and quiescent period (QP) were both lengthened (Figure 4.6 A & B). Measures of overall bone structure reflect this reduction in bone formation: Bone perimeter (BPm) (Figure 4.6 C) and trabecular number (TbN) are reduced, and trabecular separation (TbS) is increased (Figure 4.7 A & B). The total amount of bone surface in relation to the tissue volume (BV/TV) was also reduced (Figure 4.7C).

In contrast, Osteoclast numbers (NOc) were not significantly different between groups, and nor were parameters of bone resorption such as Activation frequency (Acf) or eroded surface in relation to bone surface (ES/BS) (Table 4.4). Osteoid parameters, such as thickness, volume and proportion of bone surface (OTh, OV/BV, and OS/BS) were also indistinguishable from control (Table 4.4). These findings are all consistent with an Adynamic Bone Disease.

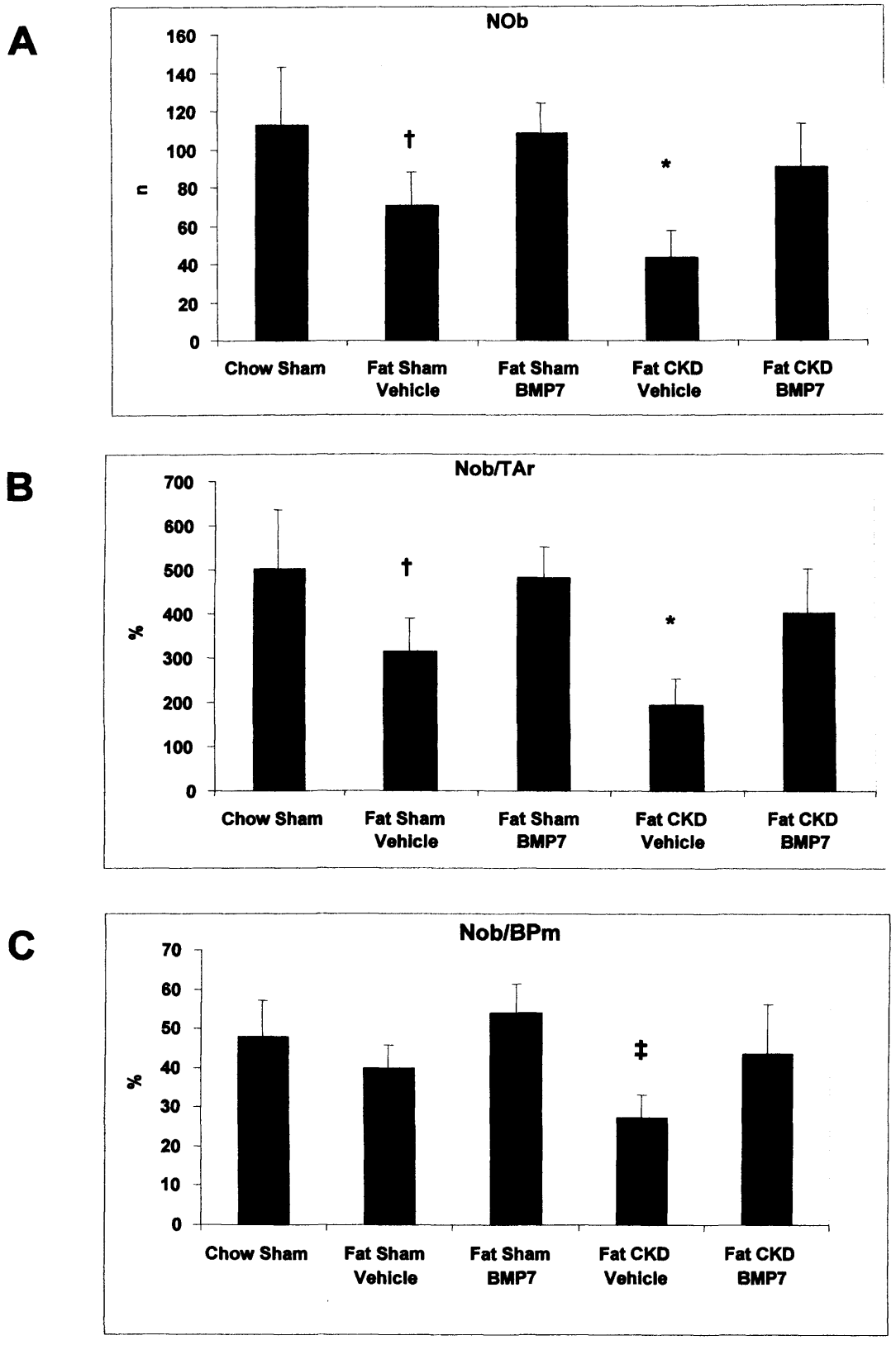

Figure 4.4 Bone histomorphometry: comparison between groups of osteoblast numbers expressed alone (A), related to tissue area (B) and bone perimeter (C) (mean ± SD). * $p < 0.001$; † $p < 0.02$; ‡ $p < 0.005$ versus Chow Sham.

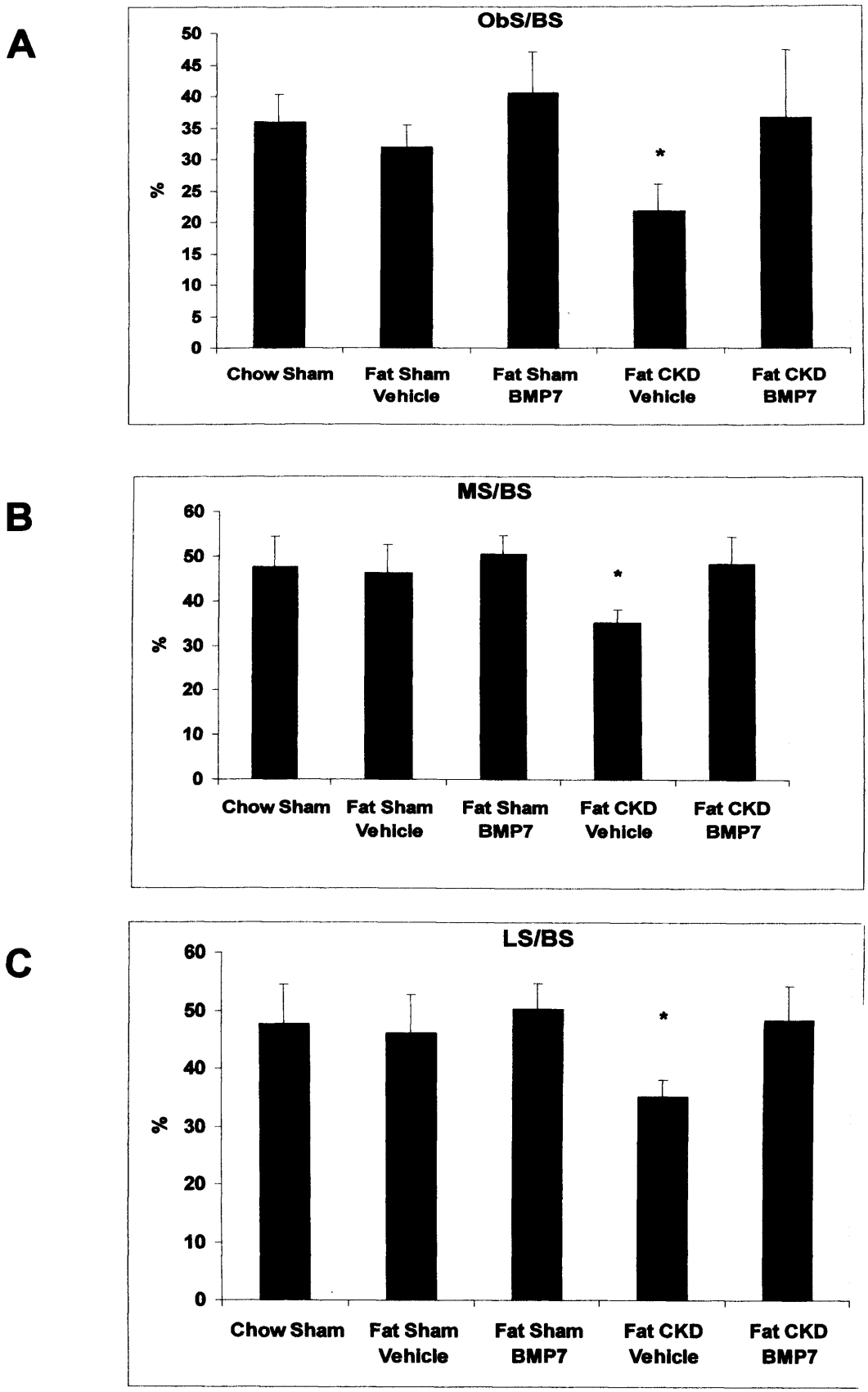

Figure 4.5 **Bone histomorphometry in *Idlr*$^{-/-}$ mice.** Comparison is made between experimental groups of osteoblast surface (A), mineralising surface (B) and labelled surface (C), all related to bone surface (mean ± SD). * $p < 0.01$ versus Chow Sham

With respect to the effects of BMP7 in this setting, it is notable that in the fat CRF group treated with BMP7 (Group 5), none of the parameters that are abnormal in the untreated group (Group 4) are significantly different from control (Group 1) (Figures 4.4-4.6, Table 4.4), suggesting that in this setting BMP7 prevents ABD.

Data in groups 1-3 define the baseline bone histomorphometry of the fat-fed animals without CRF, and their response to BMP7. In considering parameters related to bone formation (Figure 4.3), NOb and NOb/TAr are reduced in untreated fat-fed animals (Group 2).While osteoblast number expressed in relation to bone perimeter (NOb/BPm) is also less than control, the difference does not reach statistical significance (Figures 4.3 C). While a number of other parameters differ from control in a manner consistent with an adynamic state (ObS/BS, BPm, TbN and BS/TV are reduced; FP, QP, and TbS are increased (Figures 4.4-4.6)), none of these differences are statistically significant. Parameters relating to Osteoclasts and bone resorption, as well as osteoid parameters are also no different to control (Table 4.4) in these non-uraemic groups. Taken together, these findings in the fat-fed untreated animals with normal renal function are consistent with a mild adynamic condition, although caution is needed in drawing this conclusion.

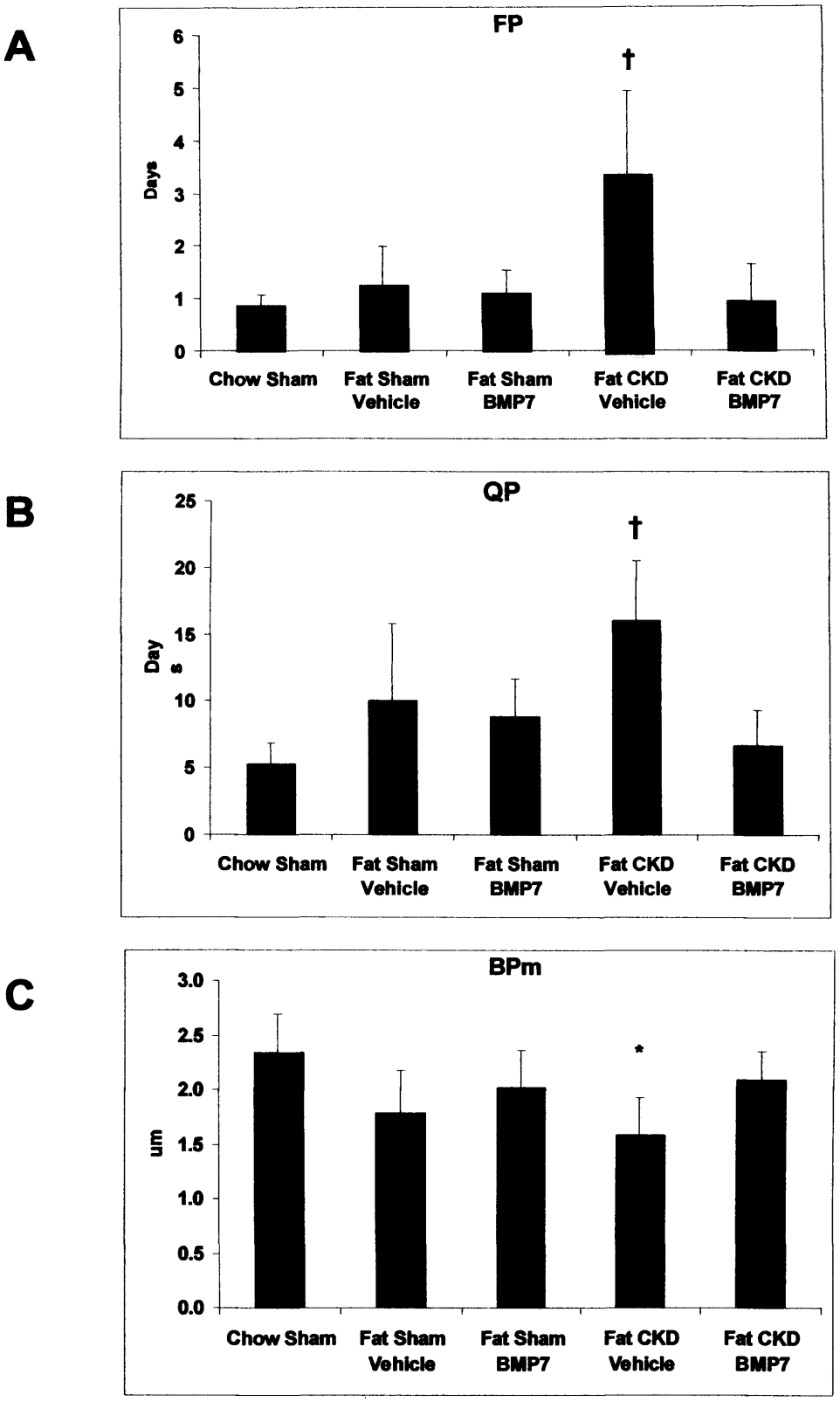

Figure 4.6 **Bone histomorphometry in *ldlr*$^{-/-}$ mice**: comparison between experimental groups of formation period (A), quiescent period (B) and bone perimeter (C) (mean ± SD). † $p = 0.001$, * $p < 0.01$ versus Chow Sham.

A

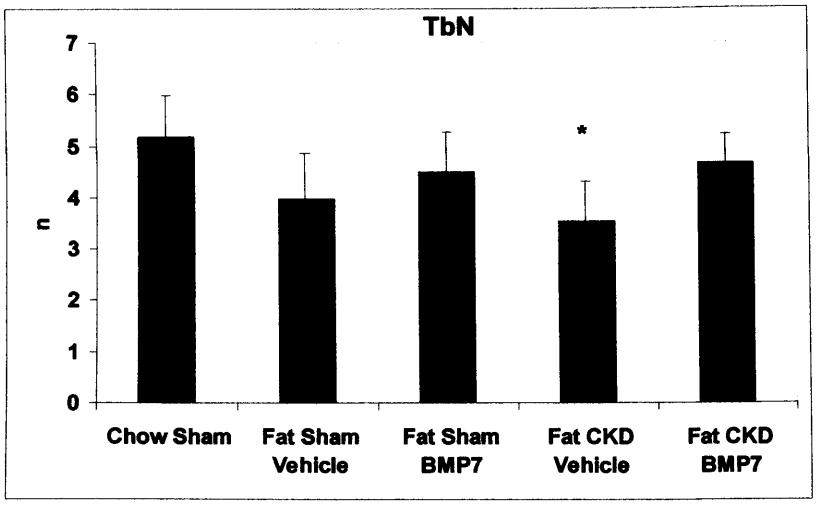

B

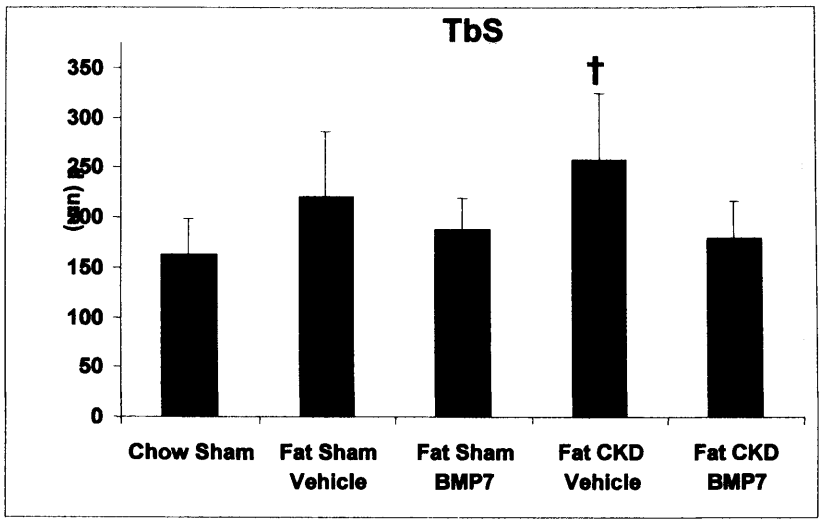

C

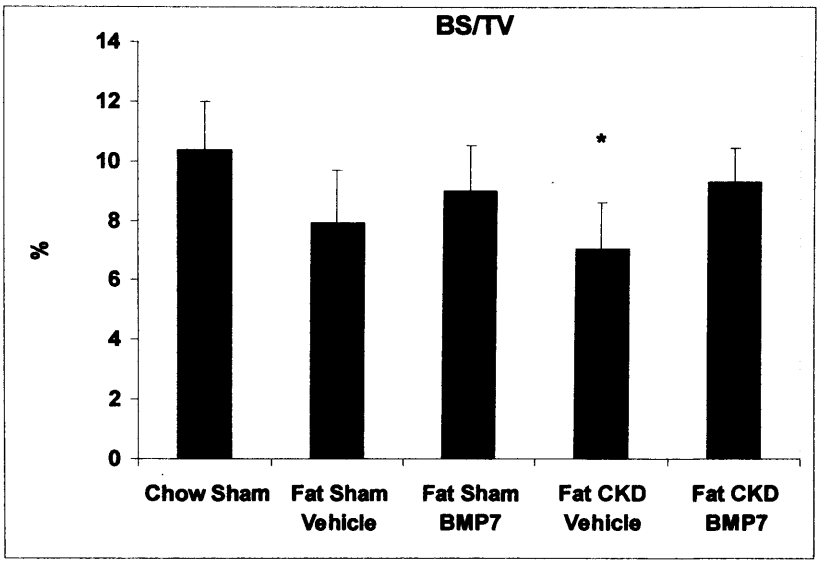

Figure 4.7 **Bone histomorphometry in *Idlr*$^{-/-}$ mice**: comparison between groups of trabecular number (A), trabecular surface (B) and bone surface related to tissue volume (C) (mean ± SD). † p= 0.02, * p < 0.01 versus Chow Sham.

Parameter	Group 1	Group 2	Group 3	Group 4	Group 5
Diet	Chow	Fat	Fat	Fat	Fat
Surgery	Sham	Sham	Sham	CRF	CRF
Rx	-	Vehicle	BMP7	Vehicle	BMP-7
NOc (n)	6.0 ±1.2	5.8 ±0.5	6.2 ±1.6	5.2 ±1.58	6.0 ±0.7
ES/BS (%)	12.3 ±4.5	17.3 ±5.9	10.2 ±3.0	12.5 ±4.8	8.4 ±2.0
OTh (uM)	1.3 ±0.3	1.3 ±0.2	1.2 ±0.3	2.1 ±0.7	1.5 ±0.9
OV/BV(%)	1.0 ±0.4	0.7 ±0.4	0.6 ±0.3	2.0 ±1.4	1.0 ±0.7
OS/BS(%)	13.2 ±5.2	9.0 ±3.4	10.0 ±3.5	15.5 ±7.8	12.3 ±9.7
Acf (t^{-1})	54.1 ±11.1	43.4 ±43.0	35.8 ±11.1	17.6 ±5.3	48.6 ±17.2

Table 4.4 **Results of selected bone histomorphometric parameters.** Data expressed as mean ± SD. There are no significant differences between groups for these parameters.

4.5 Discussion

4.5.1 Vascular calcification

The results of the current study complement the findings described in Section 3. They confirm firstly that VC is significantly increased in the context of CRF in this model, and also confirm the important finding that BMP7 therapy is able to prevent this change. The methodology used in this study is quantitative, and entirely objective. Whereas the histological data presented above concentrated on the proximal aorta from the aortic valves to the beginning of the descending aorta, the current data reflects the state of calcification of the whole aorta from the aortic valves to the iliac bifurcation. Thus, these findings counter concerns that the previous histological results might have been subject to either sampling errors or observer errors by the scorers. We have assumed that intracellular calcium is identical in all samples, and that changes measured in tissue calcification reflect differences in extracellular mineralisation. While evidence shows that changes in extracellular calcium and phosphate concentrations may promote expression of the osteoblastic phenotype in these cells, it has not been shown that intracellular ion changes are essential to this. While it is therefore possible that the measured changes in

tissue calcium content in VC include a component of intracellular change that thus far remains unquantified, it is nevertheless likely, given the striking histological changes seen and the density of calcium ions in hydroxyapatite, that the majority of the measured changes do indeed reflect extracellular mineralisation.

4.5.2 Bone histomorphometry and renal osteodystrophy

The bone histomorphometry data in this study clarify the nature of renal bone disease in the *ldlr*$^{-/-}$ model of vascular calcification and uraemia, and clearly show that uraemic animals fed a high fat, high cholesterol diet have a low-turnover bone turnover state characterised by reduced osteoblast numbers and function (Group 4). These histomorphometric findings are highly congruent with changes seen in adynamic bone disease in humans [69]. It is interesting to note that even in animals with normal renal function (group 2), a number of findings in osteoblastic parameters suggest that there may be a tendency to a low turnover state in *ldlr*$^{-/-}$ mice fed a high fat diet, when these animals are compared to chow-fed controls. These are unexpected findings. The initial assumption when this study was being designed was that untreated uraemic animals would have a high-turnover bone disease consistent with OF and secondary hyperparathyroidism, since this is found in other mouse models of uraemia [94], and is the commonest histological diagnosis noted in early bone biopsy series in uraemic human subjects [69, 72]. While rodent models of adynamic bone disease do exist, these involve additional intervention beyond the imposition of uraemia itself, such as either Vitamin D therapy [74] or dietary supplementation with calcium to act as a phosphate binder [123]. The animals in the present study received no supplementary Vitamin D,

and the calcium content of the high fat diet is comparable with standard laboratory chow; thus other explanations of this finding need to be sought. In this respect, it is worth considering that not all human subjects with untreated uraemia develop high turnover bone disease. A percentage of subjects in biopsy studies have adynamic bone disease [72], and the factors responsible for this are not clearly known. However, it is likely that this heterogeneity in bone disease reflects underlying metabolic and genetic heterogeneity in the population studied, and therefore the particular genetic and metabolic phenotype of the *ldlr*$^{-/-}$ mouse model may include a combination of factors that predispose to the occurrence of an adynamic bone disease in the context of uraemia. Certainly diabetes mellitus has been linked to ABD, and also to low bone turnover states in the absence of uraemia, and undoubtedly fat-fed *ldlr*$^{-/-}$ mice are glucose intolerant. In addition, it is possible that the dyslipidaemia seen in this model may be important to the aetiology of ABD since Demer and colleagues have proposed a link between elevated oxidised lipid fractions, in particular LDL, and the presence of osteoporosis [124], another bone disease characterised by low bone turnover. Clearly in the *ldlr*$^{-/-}$ model, LDL fractions will be elevated, and in the context of uraemia, these are likely to be oxidised, since this process is increased in uraemia.

Undoubtedly, further investigation is needed to clarify these issues. Nevertheless, on the evidence of this study the *ldlr*$^{-/-}$ uraemia mouse is characterised as a model of spontaneous adynamic bone disease without the need for further manipulation beyond the imposition of uraemia.

The second important finding of the histomorphometry data is that the low-turnover state seen in fat uraemic animals is entirely reversed by BMP7. This is consistent with known functions of BMP7 in the normal differentiation and maturation of osteoblasts

[80, 125], given that the histomorphometric abnormalities in ABD are predominantly of osteoblastic parameters and bone formation. This is an important finding, and complements previous results showing that BMP7 is an effective therapy of high turnover bone disease [94] and an alternative model of the ABD [74] in mice. This finding emphasises that both types of bone disease are characterised by abnormalities of osteoblast function. In OF, dysregulation of OB function leads to over-activity of osteoclastic bone resorption and marrow fibrosis, while in ABD the failure of osteoblasts to differentiate and mature, leads to low bone turnover. Importantly, both studies demonstrate that normalising osteoblast function permits normal bone turnover and structural integrity, strongly suggesting that the documented osteoblast abnormalities are initiating events, rather than consequences of other pathological processes. It is interesting to note that this benefit occurred without clearly improving hyperphosphataemia or hyperparathyroidism in these animals and this indicates that the processes of secondary hyperparathyroidism and ROD may not be inextricably linked. This raises the possibility of alternative therapeutic approaches to the problem of ROD in the clinical arena in the future.

4.5.3 Bone biochemistry and parathyroid hormone

The presence of adynamic bone disease is important when analysing bone chemistry and PTH data. The mean PTH level is increased in uraemic animals (Groups 4 and 5), but wide confidence intervals are seen, and differences between these groups and control are not significant. Perhaps the most striking finding is the wide range of values: some are elevated, some nearly normal. This finding largely reflects the known clinical condition of

ABD, where PTH levels are not as consistently elevated as they are in OF, and may be normal in some subjects. It should be noted that there is no clear difference for PTH levels between groups 4 and 5, suggesting that the beneficial effects of BMP7 on bone histomorphometric parameters are independent of any changes in parathyroid hormone levels.

With respect to calcium and phosphate levels, it is difficult to make out a clear pattern of variation, and confidence intervals are again wide. A number of factors may be relevant to this finding, including the presence of ABD. As noted previously, one consequence of the presence of a low bone turnover state is the reduction in size of the rapidly exchangeable ion pool, which has important consequences for buffering serum calcium and phosphate levels. This may be particularly important in the post-prandial setting. Animals in this study were not fasted prior to sacrifice, and so it is possible that the variability seen reflects underlying lability of serum concentrations of these ions. This on the other hand may be important in the aetiology of vascular calcification, in that the initiation of osteoblastic transdifferentiation of VSMCs has been linked to phosphate concentrations [50, 68], and peak phosphate concentration may be as detrimental as steady state level in this context. Secondly, heterogeneity in PTH levels and hyperparathyroidism may contribute to the variance observed in these ion levels. A third factor is that no assessment has been made of Vitamin D status of these animals. The uraemic animals are presumed to be deficient of Vitamin D, in keeping with the extent of their renal failure, but levels were not measured to confirm this. It is therefore possible that the differences in the extent of renal impairment between individual animals within groups 4 and 5 could lead to physiologically different levels in Vitamin D, leading to variance in serum calcium and phosphate levels. A final issue relevant to variability in phosphate levels in particular is the possibility of haemolysis during blood sample

retrieval by ventricular stabbing. Haemolysis releases intracellular contents, including phosphate, and a small amount of haemolysis is likely to occur even in carefully drawn samples, particularly in uraemic subjects in whom red cell fragility is increased. However, this factor was not obvious on inspection of plasma after separation, and although difficult to quantify, is likely to be small. Since all uraemic groups have blood drawn under similar conditions irrespective of BMP7 therapy, this effect is controlled for.

In summary, the present study addresses three issues. Firstly, it confirms the histological data presented in section 3, showing that aortic calcification is increased in the context of CRF superimposed on atherosclerosis in the *ldlr*$^{-/-}$ mouse. This confirmation, using an established chemical assay of whole-tissue calcium content, is entirely quantitative and therefore these data are more robust than in the previous study. Secondly, this study defines the nature of the renal osteodystrophy associated with CRF in this model, and characterises it as an adynamic bone disease. Thirdly, the study demonstrates that exogenous BMP7 administration is able both to counteract the vascular calcification and to prevent the osteodystrophy observed in this setting. This finding lends further support to the concept of chronic kidney disease as a state of BMP7 deficiency, and to the idea that many of the clinical manifestations of the uraemic syndrome derive directly from this.

Section 5

The effect of Bone Morphogenetic Protein 7 on calcifying vascular cells, an *in vitro* model of vascular calcification

5.1 Aim

The findings described in Sections 3 and 4 have established that exogenous BMP7 administration prevents vascular calcification (VC) in uraemic *ldlr*$^{-/-}$ mice. At the same time, BMP7 is able to ameliorate the adynamic renal osteodystrophy (ABD) inherent in this model by normalising osteoblast function. This effect may in part explain the beneficial effects of BMP7 on VC through its consequent effects on extracellular calcium and phosphate concentrations. Nevertheless, other lines of evidence suggest that BMP7 may have direct beneficial effects on vascular smooth muscle cell (VSMC) biology that serve to reduce VC independent of its effects on bone mineralization. Thus, the studies in this chapter aim to test this hypothesis in an established *in vitro* model of VC, the Calcifying Vascular Cell (CVC).

5.2 Introduction

5.2.1 Background

As previously discussed in Section 2, the transdifferentiation of VSMCs into an osteoblastic phenotype has emerged as a central mechanism in the pathophysiology of VC. Several studies have documented increased expression of osteoblastic proteins in vascular tissues in the context of VC [36, 37, 39, 43-49], and similar expression patterns have been demonstrated in smooth muscle cells derived from healthy vascular tissues when studied *ex vivo* under various conditions[52, 53]. In one study, Dorai showed in VSMCs that TGFβ is able to increase expression of the Collagen I gene [67], a protein associated with osteoblast but not smooth muscle extracellular matrix. At the same time, expression of genes for typical smooth muscle proteins collagen III and α Smooth Muscle Actin (αSMA) was decreased [67]. Importantly, these changes were prevented by co-administration of BMP7 in a Smad6-dependant manner, suggesting that BMP7 may play a role in maintaining the normal integrity of VSMCs and that its absence may facilitate the emergence of an osteoblastic phenotype in these cells conducive to VC. This may particularly be so under conditions of inflammation when increased levels of

TGFβ may be present. Several other lines of evidence exist supporting this concept that imbalance between TGFβ and BMP7 may be important in the osteoblastic transformation of VSMCs and their subsequent ability to mineralize their extracellular matrix. Firstly, TGFβ has been shown to promote extracellular mineralization by CVCs *in vitro* [57]. As discussed previously in Section 2.1.2.1, these cells have been derived from the medial layer of arteries from healthy animals in a number of species, and share characteristics of both osteoblasts and smooth muscle cells. Thus CVCs putatively represent a subgroup of VSMCs that have undergone a process of transdifferentiation, and have emerged as a useful *in vitro* model of vascular calcification. Nevertheless, not all VSMC have this propensity, although the reasons for this are not clear. Secondly, *smad6*$^{-/-}$ mice develop spontaneous aortic calcification, which supports the concept that the interaction between BMP7 and Smad6 is physiologically important in maintaining VSMC integrity and preventing VC [101]. Thirdly, VC is highly prevalent in CKD, and this setting is increasingly becoming characterised as one of relative BMP7 deficiency. This is based on the observation that BMP7 expression is decreased soon after renal injury [75, 76, 90], and supported by data from studies showing that exogenous BMP7 administration improves a number of aspects of renal failure and uraemic syndrome in animals with renal impairment [74, 90-92, 94, 126, 127].

However, there are no studies to date looking at the effects of BMP7 on calcification itself by vascular cells *in vitro*, and the studies described in this chapter aimed to address this issue.

5.2.2 The model

The derivation and investigation of CVCs were first described by Demer's group [39], and have subsequently been extensively studied by other investigators [50, 51] (see section 2.1.2.1). Cells are derived from explants of the medial layer of aortic tissue from healthy adult animals of various species, and propagated by standard cell culture techniques. Cells are identified as VSMCs rather than other cells of vascular origin on morphological and immunohistochemical grounds, and are not associated with extracellular calcification. Once these VSMC cultures have progressed to confluence, cells draw themselves up into a characteristic hill-and-valley morphology, and nodules of calcification typically appear on the summits of these hills of cells over a period of two to three weeks in standard culture conditions. The cells associated with the calcified nodules are then separated from uncalcified areas of the culture, as well as from the nodules themselves, and may be further propagated. Subsequent generations of these cells continue to calcify their extracellular matrix spontaneously and express the range of osteoblastic genes previously discussed. It is these cells that are termed CVCs. Thus, CVCs are effectively VSMCs selected preferentially for their ability to calcify their extracellular matrix, and which show evidence of having transdifferentiated into an osteoblastic phenotype.

CVCs are relatively easy to derive, and can be sustained in culture in straightforward media such as Dulbecco's Modified Eagle Medium (DMEM) with 10 - 15% serum, without the need for supplementation with growth factors. They have been extensively investigated in a number of studies that have characterised the conditions under which calcification occurs (summarised in Table 2.1), as well as the nature of osteoblastic transformation of these cells in terms of gene expression. Included among the factors

causing increased calcification by CVCs are TGFß [57] and both organic and inorganic phosphate [50, 58, 68]. Since hyperphosphataemia is a common finding in CKD which has been correlated to the presence of VC, and since increased TGFß expression is implicated in the progression of a number of renal diseases, these findings suggest that CVCs are a suitable model of VC in CKD in which to investigate the role of BMP7. While CVCs have been derived from a number of different species including humans, bovine cells have emerged as pre-eminent due to their ease of derivation and stability in culture up to 20 passages, and are the species studied in most of the studies noted above. Bovine CVCs were thus chosen for these experiments.

5.3 Methods

5.3.1 Cell culture and media

Bovine CVCs were a gift from the laboratory of Dr Linda Demer (UCLA), and derived from aortic media of healthy adult cows as previously described [39, 57]. Cells were stored in liquid nitrogen until required for use. Cells were used between passage 13 and 18, propagated in T75 flasks under aseptic conditions, and incubated at 37 °C in an atmosphere supplemented with 5% CO_2. Cells were passaged at confluence by incubation in 0.5% trypsin in0.2% EDTA for 3-5 minutes at 37 °C followed by filtration of the cell suspension through a 40 μm pore filter (Fisher Scientific, Pittsburgh) to remove calcified nodules, before either storing at -80 °C, seeding further flasks as above split in a ratio of 1:7. For experimental protocols, cells were seeded into 12 well plates at a density of 10^5 cells/cm^2. For immunohistochemistry, cells were grown on sterilised glass cover-slips placed in the wells.

Basic media used for cell propagation and as control medium in experimental protocols was DMEM with 0.45% glucose (Product D5648, Sigma, St Louis), supplemented with

10% Foetal Bovine Serum, 1mM Sodium Pyruvate, Penicillin 100 units/ml and Streptomycin 100 μg/ml. Media was routinely changed every second or third day. In experimental protocols, 10 mM β-glycerophosphate (βGP) was added to the culture medium as an organic source of phosphate ions ('Calcifying medium'). Previous studies have shown that βGP promotes mineralization by CVCs in a dose-dependant fashion up to a concentration of 10 mM [51], and has been widely used to promote extracellular calcification of osteoblastic cultures [116]. Where indicated, BMP7 was diluted to concentrations of 0.1, 1.0 and 10 ng/ml in manufacturer's specified vehicle (20mM acetate, 5% Mannitol at pH 4.5) and added to the basic or calcifying culture medium immediately prior to its application to cells. In addition, vehicle was added to media, where indicated, to act as a treatment control. Media was changed every second day during experimental protocols, and BMP7 or vehicle added at the same time. Each treatment was performed on six samples per experiment, and repeated twice.

5.3.2 Calcification assays

For histological assessment of calcification, cell layers were stained with Alizarin Red-S. Cells were washed in PBS after removal of culture medium, and fixed in 4% formaldehyde freshly prepared in PBS for 30 minutes. Cells were further rinsed in PBS, washed in deionised water, and then incubated with Alizarin Red-S 5 mg/ml titrated to pH 4.2 at room temperature for 15 minutes. Cells were rinsed again in deionised water, before the stain was developed in PBS for 20 minutes. Finally, cells were dehydrated in 100% ethanol and allowed to air dry.

Calcification was quantified by chemical assay of total extracellular calcium deposited on cell layers, and corrected for total protein content. Culture media was aspirated at the end of each experiment and unfixed cells were washed in phosphate-buffered saline (PBS), and then incubated in 0.6N Hydrochloric Acid (HCl) overnight at 4 °C to elute calcium. This eluate was removed and stored at -80 C until assayed using the Complexone assay system (Calcium Kit, Sigma, St Louis) according to manufacturer's instructions. Following removal of the calcium-containing eluate, cells were further washed and solubilized in 0.1 N Sodium Hydroxide (NaOH)/ 0.1% SDS. This lysate was also stored at -80 °C until assayed for protein content using the DC Protein assay kit (Biorad) according to manufacturer's instructions.

5.3.3 Immunohistochemistry

Cells were washed in PBS and fixed in fresh 4% formaldehyde, as above. After rinsing in PBS, cells were incubated with 50mM freshly made Ammonium Chloride (NH_4Cl) for 15 minutes at room temperature to quench aldehyde groups and reduce background tissue fluorescence, then rinsed again in PBS. To expose intracellular epitopes (eg αSMA) cells were permeabilized by incubation with 0.2% Triton X-100 in PBS for 15 minutes at room temperature. Non-specific antibody binding was blocked with a 30 minute incubation with 2% bovine serum albumin (BSA) and 0.04% sodium azide in PBS at room temperature, or 2% BSA, 0.04% sodium azide and 0.1% Triton X-100 in PBS if cells had previously been permeabilized. Cells were incubated with primary antibody diluted 1:200 (αSMA) and 1:300 (3G5) in 2% BSA and 0.04% sodium azide in PBS for 1 hour at room temperature, washed in PBS, then incubated with secondary antibody

(Indocarbocyanine (Cy3)-conjugated Immunoglobulin G (IgG)) diluted to 1:200 in 2% BSA and 0.04% sodium azide in PBS for a further hour. Cells were washed in PBS and mounted on microscope slides with Aqua Polymount, then viewed on a Zeiss Fluorescent Microscope, and results recorded digitally. Control cells were incubated as above in the absence of primary antibody. Primary murine monoclonal antibodies against α-SMA were obtained from Sigma and 3G5 antibodies (human monoclonal antibodies against CD44v3) from R&D Systems

5.4 Results

CVCs showed characteristic stellate morphology, formed hills and valleys, and developed calcifying nodules (Figure 5.1 A, B) over a period of 10 to 20 days. Cells expressed α-SMA extensively, and were also positive for 3G5, as previously described [57] (Figure 5.2 and 5.3A). Calcified nodules spontaneously fluoresced in the absence of antibody staining, as seen in control conditions (Figure 5.3A), but cells did not. CVCs spontaneously calcified when cultured in basic growth medium, and addition of BMP7 at 1.0 and 10 ng/ml significantly reduced the amount of calcification seen over 20 days but Vehicle and BMP7 at 0.1ng/ml did not (Figure 5.4). The extent of reduction of calcification did not appear to vary with different effective doses of BMP7, suggesting an all-or-nothing effect over this range of doses, although further dose titration between these effective doses would be needed to demonstrate this. When grown in medium supplemented with 10mM βGP, there was greater total calcification by CVCs (Figure 5.5). BMP7 at 0.1, 1.0 and 10 ng/ml significantly reduced this, although not to levels seen in the absence of βGP. Again, vehicle alone had no effect.

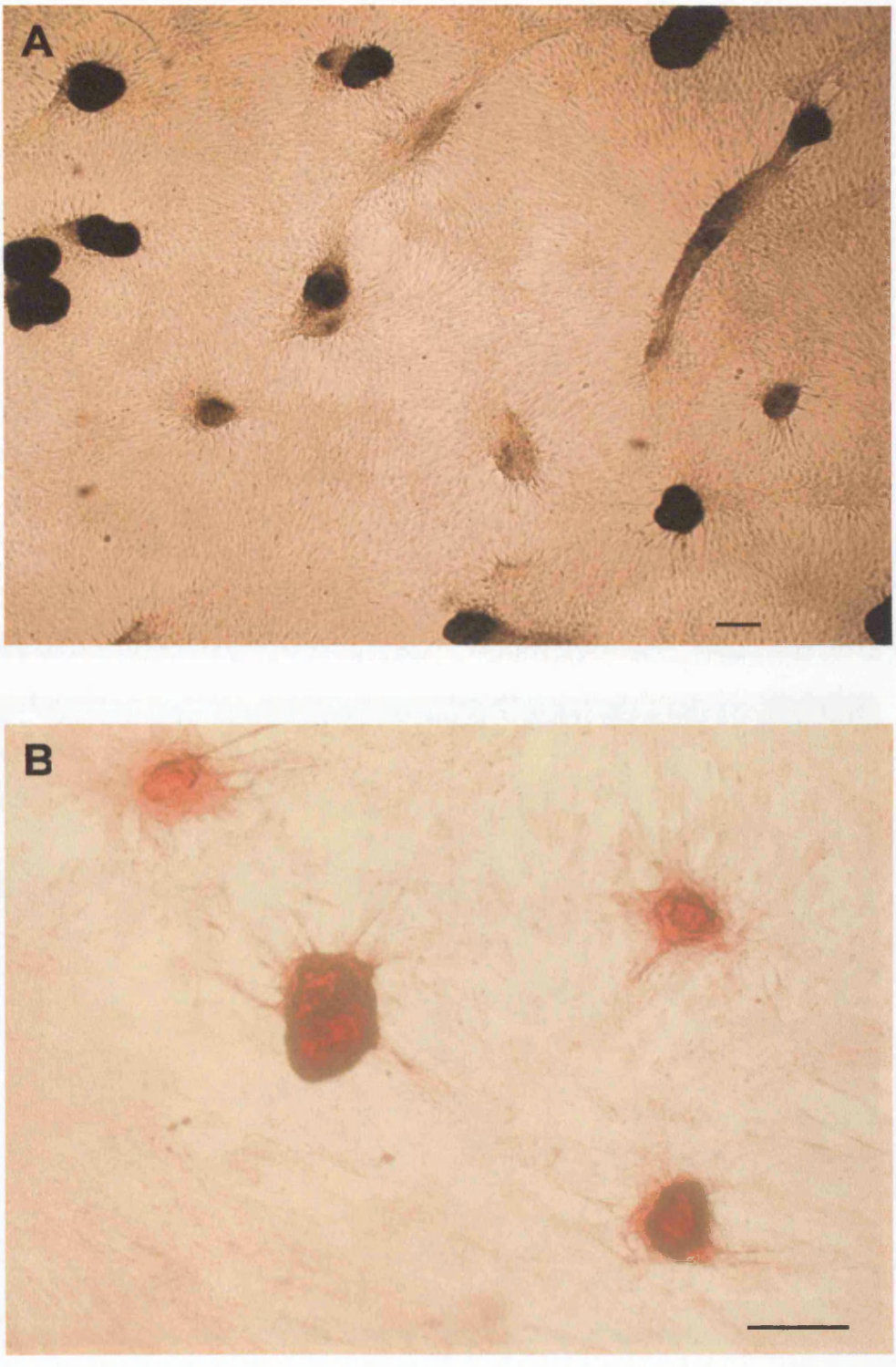

Figure 5.1 **Calcification associated with calcifying vascular cells.** Nodules of calcification are shown on layers of cells arranged in a 'hill and valley' pattern(phase-contrast, unstained (A), and stained with Alizarin Red-S (B)). Bars = 150 μm

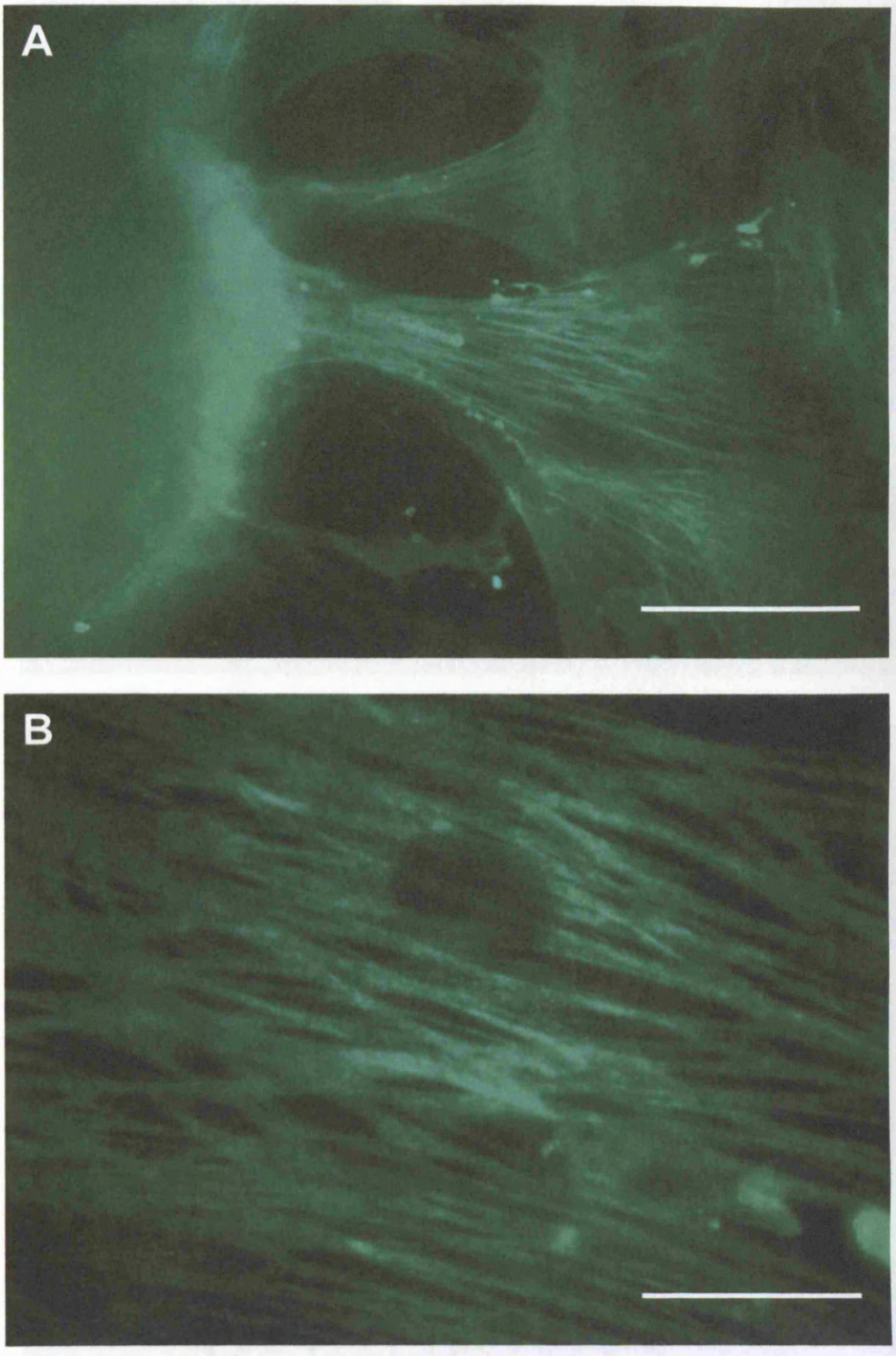

Figure 5.2 Calcifying vascular cells stain with antibodies for α-Smooth muscle actin. A nodule is showing auto-fluorescence to the left of panel (a, x40, bar = 50μm), with adherent smooth muscle cells to the right. Staining clearly defines myofibrils within the cells (b, x400, bar = 5μm).

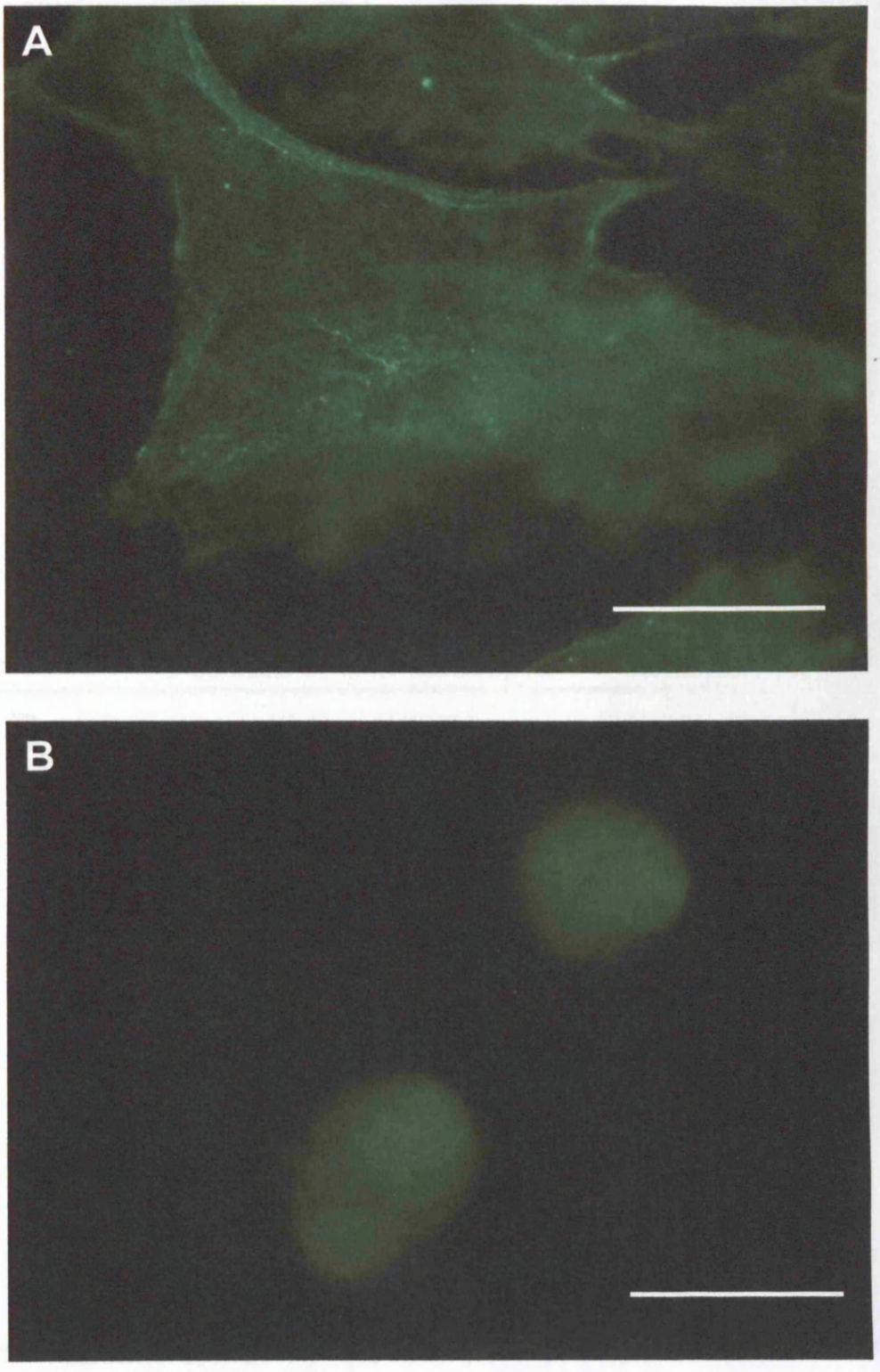

Figure 5.3 Calcifying vascular cells stain with the antibody 3G5. (a) Stained cells (x40, bar = 50μm); (b) control cells showing auto-fluorescence of nodules but not cells (x10, Bar = 200μm).

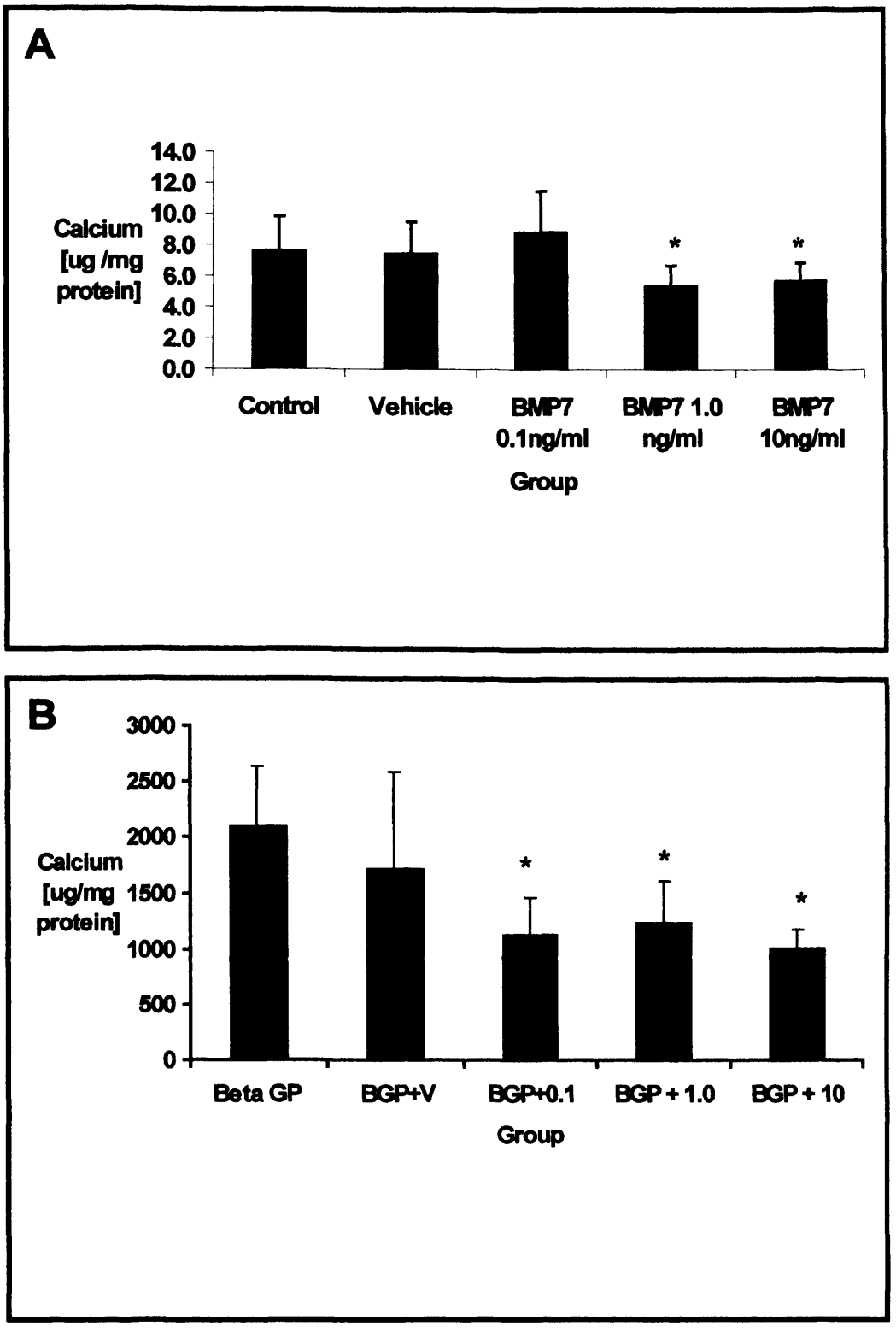

Figure 5.4 Calcification by calcifying vascular cells in response to BMP7 administration. (A) Cells cultured under basal conditions. (B) Medium supplemented with β-glycerophosphate to promote calcification. * $p < 0.05$ vs control.

5.5 Discussion

These experiments demonstrate that BMP-7 reduces calcification by CVCs, both in the presence and absence of an organic phosphate source, βGP. This finding supports the hypothesis that the benefits of BMP-7 on vascular calcification seen *in vivo* are mediated, at least in part, by direct effects on the vasculature, in addition to beneficial effects mediated through amelioration of renal bone disease and extracellular calcium and phosphate ion concentration. Since CVCs are in essence VSMCs selected over a number of passages in culture for their propensity to calcify spontaneously, they are likely to represent such cells at an advanced stage of osteoblastic transdifferentiation. Thus it is unlikely that BMP-7 is reducing calcification by preventing the transdifferentiation process itself, but rather is modifying the calcifying behaviour of differentiated cells. This may have importance when translating these findings to an *in vivo* or clinical setting, since it suggests that BMP7 may have the potential to ameliorate vascular calcification in settings where VC is already established, as well as preventing its initial emergence. The fact that the beneficial effects of BMP7 were also seen in the presence of concentrations

of βGP in the media selected to maximise calcification is also important, since phosphate is a strong promoter of VC in the clinical environment.

This effect of BMP7 on cells of vascular origin represents a novel effect of BMP7. While BMP7 expression in cardiovascular tissues is extensive in embryonic development, as discussed in section 2.2.4, its precise role is unclear, and no role is defined in the adult. This data supports the concept that BMP7 may act to sustain normal VSMC phenotype, although the mechanisms underlying this need further elucidation. It also suggests the possibility that BMP7 may benefit VC where it occurs in the absence of CKD and attendant renal osteodystrophy, where abnormalities of osteoblast biology are not necessarily relevant to the aetiology of VC.

One factor not investigated in these studies is the amount of TGFß expressed and secreted by these calcifying cells. This may influence the results of such experiments in a number of ways, particularly if there is variation between cell isolates. Firstly, as discussed in section 2, TGFß has been shown to promote VC by CVC [57]. Second, TGFß has been shown to promote changes in gene expression in VSMC in culture that are consistent with emergence of an osteoblastic phenotype [67], and thirdly in this latter study, it was shown that BMP7 is able to counteract these changes induced by TGFß. Thus the amount of calcification observed and the effect of a given dose of BMP7 in preventing it is likely to depend on the amount of TGFß expression by the cells under study. This will need further clarification in future studies, in parallel with studies to clarify the interaction between BMP7 and VSMCs and related cells such as CVCs as a whole.

Section 6

Conclusions and future directions

6.1 Conclusions

Recently there has been a significant increase in clinical and academic interest in vascular calcification (VC), following the publication of studies linking this phenomenon to adverse cardiovascular outcomes [13-16, 34]. Such increased interest has been particularly apparent in relation to renal disease, where VC is a particularly striking clinical problem in patients with chronic and end-stage renal failure [17], and where cardiovascular morbidity and mortality are extremely high [11].

Accordingly, VC is considered to be an active process with strong parallels to endochondral bone mineralization [12], orchestrated by a population of cells in the vessel wall expressing an osteoblastic phenotype. These cells appear to be derived from vascular smooth muscle cells by a process of transdifferentiation. In the particular setting of renal failure, but not necessarily elsewhere, VC also seems to be linked to abnormalities of bone mineral metabolism inherent in renal osteodystrophy (ROD) [12, 17], particularly hyperphosphataemia [4]. Nevertheless, despite this increase in understanding, the

mechanisms underlying the pathophysiology of VC remain unclear. Thus VC remains a considerable challenge to clinicians, since cardiovascular mortality is persistently high despite improvements in the management of many aspects of CRF and ESRD, and the life-expectancy of ESRD patients remains shortened. Indeed, evidence suggests that VC may in part be an iatrogenic problem in this setting, since severity of VC has been correlated radiologically to the use of several common therapies used in the treatment of ROD such as calcium-containing phosphate binders and Vitamin D analogues [17, 19]. In support of this, recent studies have suggested that Sevelamer, a newer phosphate binder that does not contain calcium, may prevent progression of VC in patients in established ESRF over six to twelve months follow-up [128, 129]; however this data has not as yet been linked to improved survival, and it is important to note that the use of Sevelamer has been associated with a failure of progression of VC rather than a regression of established disease.

At the same time as awareness of the clinical significance of VC has grown, CRF has become characterised as a state of relative deficiency of the growth factor Bone Morphogenetic Protein 7 (BMP7) [130]. Reduced expression of BMP7 occurs soon after renal injury [75, 76], and administration of exogenous BMP7 is beneficial to several aspects of renal failure in a number of animal models, including progressive interstitial fibrosis [91], diabetic nephropathy [92] and renal osteodystrophy [94, 95] . This concept may also be relevant to the pathophysiology and treatment of VC.

It was hypothesised that VC may also be a manifestation of relative BMP7 deficiency in CRF, and that administration of exogenous BMP7 might therefore improve or prevent it. Although the role of BMP7 in the adult cardiovascular system is not understood, *in vitro* data suggests BMP7 may prevent changes in gene expression consistent with osteoblastic

transdifferentiation seen in VSMCs following exposure to TGFß [67]. Thus the relative absence of BMP7 in CRF may facilitate these changes, and its replacement should reverse them. In addition, the beneficial effects of BMP7 on bone biology demonstrated in the context of ROD would also be expected to benefit VC by normalising calcium and phosphate ion metabolism and thereby removing an important stimulus for VC. Such a hypothesis, if confirmed, would strongly support a clinical role for BMP7-based therapy.

In contrast, it was also possible to hypothesise that exogenous BMP7 might have precisely the opposite effect and exacerbate VC, by promoting the osteoblastic transdifferentiation of VSMCs that seems to be central to the pathogenesis of VC. This argument is supported by the observation of BMP2 expression in the context of VC that is proposed to be an initiating event [39], and also the role of BMP7 in promoting maturation and function of osteoblasts in normal endochondral bone [80, 125]. If this were the case, the adverse impact of worsened VC on cardiovascular mortality could outweigh the benefits of exogenous BMP7 administration on other aspects of CRF, and significantly limit its therapeutic potential. The studies in this thesis were designed to evaluate the relative merits of these two paradoxical, though not necessarily mutually exclusive, hypotheses.

In section 3, *ldlr*$^{-/-}$ mice were used as a model of vascular calcification. While this is a complex model of atherosclerosis onto which uraemia was superimposed, its elements are directly comparable to the complex clinical setting for many patients with chronic renal failure, with dyslipidaemia and mild glucose intolerance included. Rodent species are generally resistant to VC, but arterial mineralization occurs spontaneously in these mutant animals, albeit at low levels. The study successfully demonstrated that

superimposition of uraemia worsened VC on histological grounds, and that administration of BMP7 prevented its occurrence almost entirely. We can conclude that BMP7 prevents VC in the setting of CRF. In addition, the data on osteocalcin expression are consistent with the conclusion that BMP7 treatment prevents the emergence of a cell in the vessel wall expressing an osteoblastic phenotype. Nevertheless, this study leaves open the question as to whether these beneficial effects of BMP7 are attributable to direct effects on the vasculature , indirect effects on bone and mineral metabolism or a combination of the two.

In section 4, further studies in the *ldlr*$^{-/-}$ model of VC in CKD used a chemical assay of total aortic calcium content to confirm the histological finding that BMP7 administration reduces VC. In addition, bone histomorphometry clearly demonstrates that uraemic *ldlr*$^{-/-}$ mice develop an adynamic bone disease. This was an unexpected finding, since uraemia is usually associated with a high bone turnover state, and these mice were not receiving treatment that could be expected to induce an adynamic picture. On the other hand, it is possible to hypothesise that the reduction of BMP7 expression that occurs soon after renal injury may lead to reduced bone anabolism at a stage of CKD when mineral ion homeostasis and vitamin D concentrations may still be relatively normal. This reduction in anabolism may then in turn be a stimulus for the initiation of hyperparathyroidism and Osteitis Fibrosa, since PTH is able to promote osteoblastic maturation, albeit aberrantly [74, 131]. Clearly this hypothesis is based on animal data and requires confirmation in humans

In addition, the low bone turnover state seen in this model may conceivably be attributed to the dyslipidaemia that characterises the *ldlr*$^{-/-}$ mutation. Previous clinical observations have linked vascular calcification and osteoporosis (another low-turnover bone disease)

[132, 133], and *in vitro* data attributes to certain lipid moieties both the ability to increase calcification by vascular cells and to impair maturation of osteoblastic cells [134]. In addition, adynamic bone disease is more commonly seen in diabetic patients, and the mild glucose intolerance of these animals may thus be contributory. Nevertheless, while the bone findings are somewhat unexpected, they still fall within the documented clinical spectrum of ROD, and are expected to contribute to the pathogenesis of VC through elevations in plasma calcium and phosphate ion concentrations. While elevations in the concentrations of these ions may occur through release from bone by increased resorption in high turnover forms of ROD, similar abnormalities may occur in adynamic states through different mechanisms. ABD is associated with a reduced Rapidly Diffusible Ion Pool in proportion to a reduced mineralising area, and this reduces the capacity to buffer extracellular calcium and phosphate ions. Thus, exaggerated fluctuations of these ions may occur, particularly post-prandially, and this may be a potent stimulus to VC. The histomorphometry data in this study clearly show normalisation of bone parameters in the BMP7-treated uraemic animals, in parallel with improvement in vascular calcification, which agrees with data from a study in a specific model of ABD [74] which also showed normalisation of bone histomorphometry parameters in response to BMP7 treatment. It also complements a study of the effects of BMP7 on a high turnover model of ROD [94]. From the point of view of the hypotheses relevant to this thesis, it is possible to conclude that BMP7 administration causes improvements in VC in parallel with changes in bone physiology likely to reduce factors known to promote its pathogenesis.

The studies described in section 5 address the question of whether or not BMP7 has direct effects of cells of vascular origin that might contribute to the reduction in VC seen in the previous experiments. Calcifying Vascular Cells (CVCs) are well established as cells

that have all the characteristics of smooth muscle cells but also display an osteoblastic phenotype and spontaneously mineralise their extracellular matrix. Our studies demonstrate that BMP7 is able to reduce calcification by CVCs under basal culture conditions and also when the growth medium is supplemented with β-glycerophosphate to maximise mineralization. It should also be noted that this represents a different therapeutic strategy to the previous studies, in that here the cells being treated are already established in their osteoblastic phenotype, whereas the timing of BMP7 administration in the animal studies exposes vascular tissues to BMP7 as soon as uraemia is established and before significant transdifferentiation could be expected to occur. In addition, the cell model does not include a uraemic component, and thus suggests that BMP7 may benefit VC in other situations than CRF.

In summary, the conclusion of this thesis is that that exogenous BMP7 administration reduces or prevents vascular calcification in a murine model of CRF, dyslipidaemia and atherosclerosis, and that this benefit is likely to reflect direct effects on vascular tissues as well as indirect effects on mineral metabolism mediated through normalisation of bone structure and function.

6.2 Future directions

It is clear that a number of questions arise from the results of these studies, some specific to these experiments and some more general.

Firstly, data in section 5 demonstrate an interaction between BMP7 and CVCs, which are cells of vascular origin with characteristics of VSMCs but which also express an osteoblastic phenotype. While the role of BMP7 in normal osteoblast biology is established, a role in normal VSMC biology, if any, is undefined. Thus the mechanisms underlying the observed effects on extracellular mineralization are unclear at present, and are a key area for further investigation. There is evidence to suggest that BMP7 may interact with TGFß in an antagonistic way at the level of Smad signalling [130], and data discussed in the appendix also suggest that interactions with Wnt signalling channelled by LRP5 through β-Catenin may be important. LRP5 is a member of the Low Density Lipoprotein Receptor family of cell surface receptors, and is essential for normal osteoblast function [135]. Single-nucleotide mutations in this gene have been linked to

striking bone mineral abnormalities in human disease [136-140]. Both activating and inactivating mutations are described, and are associated with extremely dense, mechanically strong bones [136-139] or juvenile osteoporosis respectively [140]. As demonstrated in the appendix, expression of LRP5 is increased in vascular tissues in both *ldlr*$^{-/-}$ and wild type animals fed the high cholesterol diet, and this protein may thus represent a link between VC and both the genetic mutation in our model and the general condition of dyslipidaemia and atherosclerosis.

A further point for future exploration concerning LRP expression and the use of BMP7 as a therapeutic agent concerns the potential impact of another member of this family, LRP1, on the pharmacokinetics of BMP7. BMP7 is bound to the plasma protein α2 macroglobulin in the circulation, and is removed in the liver by combining with LRP1, which is expressed on the surface of hepatocytes. As outlined in the Appendix, expression of LRPs may be altered in the response to high cholesterol diet, in the context of the *ldlr*$^{-/-}$ genotype and other genetic models of dyslipidaemia [122]. In particular, there is evidence that liver expression of LRP1 may be increased, raising the possibility that the half-life of BMP7 in the circulation may be reduced in hyperlipidaemic states. Clearly, this may be an important consideration if BMP7 therapy is developed into the clinical arena, and pharmacodynamic studies will need to be performed.

In addition, recent evidence suggests that modulation of extracellular matrix glycosaminoglycans such as hyaluronan may be relevant to the mechanism of interaction of BMP7 with VSMCs or CVCs. It has been shown that BMP7 may modulate haluronan synthesis in renal mesangial cells and modify cell behaviour by doing so [141]. Hyaluronans bind to and signal within cells through the cell surface protein CD44. The fact that mesangial cells may be regarded as modified smooth muscle cells suggests that

similar effects may occur in VSMCs, and the fact that VSMCs increase expression of CD44 when adopting the osteoblastic phenotype, as evidenced by the staining of CVCs with the anti-CD44 antibody 3G5 (Figure 5.3), suggests that altered interactions between these cells and hyaluronan in the extracellular matrix may be important to their emergence as cells with calcifying potential.

Finally, in general terms it is clear that demonstrable efficacy of exogenous BMP7 administration in improving so many aspects of renal failure in such a wide variety of models offers the exiting prospect that mortality associated with chronic kidney disease and end-stage renal failure and its consequences may be preventable or treatable for many patients in the future. BMP7 has already been used in clinical orthopaedic studies looking at its role in promoting fracture healing [142], and synthetic and modified BMP7 analogues are under investigation that may be suitable for evaluation in human studies [143]. It may even be the case that BMP7 has a role to play in treating vascular calcification outside the context of renal failure, with potential benefits to cardiovascular morbidity and mortality in the population at large.

Section 7

References

1. United States Renal Data System (USRDS), *2002 annual data report.* 2004, National Institutes of Health: Bethesda, MD.

2. Raine A.E., Margreiter R. and Bruner K.P. Report of the management of renal failure in Europe xxii 1991. *Nephrol Dial Transplant*, 1992; 7: 7-35.

3. Muntner P., He J., Hamm L., Loria C. and Whelton P. Renal insufficiency and subsequent death resulting from cardiovascular disease in the United States. *J Am Soc Nephrol*, 2002; 13: 745-753.

4. Block G. A. and Port F. K. Re-evaluation of risks associated with hyperphosphatemia and hyperparathyroidism in dialysis patients: Recommendations for a change in management. *Am J Kidney Dis*, 2000; 35: 1226-1237.

5. Lindner A., Charra B., Sherrard D. and Scribner B. Accelerated atherosclerosis in prolonged maintenance hemodialysis. *N Engl J Med*, 1974; 290: 697-701.

6. Chen J., Muntner P., Hamm L., Jones D., Batuman V., Fonseca V., et al. The metabolic syndrome and chronic kidney disease in U.S. Adults. *Ann Int Med*, 2004; 140: 167-174.

7. Nicholls A., Catto G., Edward N., Engeset J. and Macleod M. Accelerated atherosclerosis in long-term dialysis and renal-transplant patients: Fact or fiction? *Lancet*, 1980; 1: 276-278.

8. Ibels L., Alfrey A., Huffer W., Craswell P., Anderson J. and Weil R. 3rd. Arterial calcification and pathology in uremic patients undergoing dialysis. *Am J Med*, 1979; 66: 790-796.

9. Burke J. F., Jr., Francos G. C., Moore L. L., Cho S. Y. and Lasker N. Accelerated atherosclerosis in chronic-dialysis patients--another look. *Nephron*, 1978; 21: 181-185.

10. Thomas F. T. and Lee H. M. Factors in the differential rate of arteriosclerosis (as) between long surviving renal transplant recipients and dialysis patients. *Ann Surg*, 1976; 184: 342-351.

11. Foley R. N., Parfrey P. S. and Sarnak M. J. Clinical epidemiology of cardiovascular disease in chronic renal disease. *Am J Kidney Dis*, 1998; 32: S112-119.

12. Davies M.R. and Hruska K.A. Pathophysiological mechanisms of vascular calcification in end-stage renal disease. *Kidney Int*, 2001; 60: 472-479.

13. Margolis J. R., Chen J., Kong Y., Peter R. H., Behar V. S. and Kisslo J. A. The diagnostic and prognostic significance of coronary artery calcification. A report of 800 cases. *Radiology*, 1980; 137: 609-616.

14. London G. M., Guerin A. P., Marchais S. J., Metivier F., Pannier B. and Adda H. Arterial media calcification in end-stage renal disease: Impact on all-cause mortality. *Nephrol Dial Transplant*, 2003; 18: 1731-1740.

15. Raggi P., Boulay A., Chasan-Taber S., Amin N., Dillon M., Burke S. K., et al. Cardiac calcification in adult hemodialysis patients. A link between end-stage renal disease and cardiovascular disease? *J Am Coll Cardiol*, 2002; 39: 695-701.

16. Wong N. D., Hsu J. C., Detrano R. C., Diamond G., Eisenberg H. and Gardin J. M. Coronary artery calcium evaluation by electron beam computed tomography and its relation to new cardiovascular events. *Am J Cardiol*, 2000; 86: 495-498.

17. Goodman W. G., Goldin J., Kuizon B. D., Yoon C., Gales B., Sider D., et al. Coronary-artery calcification in young adults with end-stage renal disease who are undergoing dialysis. *N Engl J Med*, 2000; 342: 1478-1483.

18. Block G. A., Klassen P. S., Lazarus J. M., Ofsthun N., Lowrie E. G. and Chertow G. M. Mineral metabolism, mortality, and morbidity in maintenance hemodialysis. *J Am Soc Nephrol*, 2004; 15: 2208-2218.

19. Milliner D.S., Zinsmeister A.R., Lieberman E. and Landing B. Soft tissue calcification in pediatric patients with end-stage renal disease. *Kidney Int*, 1990; 38: 931-936.

20. Nicolosi A. C., Pohl L. L., Parsons P., Cambria R. A. and Olinger G. N. Increased incidence of radial artery calcification in patients with diabetes mellitus. *J Surg Res*, 2002; 102: 1-5.

21. Wexler L., Brundage B., Crouse J.,Detrano R., Fuster V., Maddahi J., et al. Coronary artery calcification: Pathophysiology, epidemiology, imaging methods, and clinical implications. A statement for health professionals from the American Heart Association. Writing group. *Circulation*, 1996; 94: 1175-1192.

22. Edmonds M. E. Medial arterial calcification and diabetes mellitus. *Z Kardiol*, 2000; 89: 101-104.

23. Kieffer P., Robert A., Capdeville-Atkinson C., Atkinson J. and Lartaud-Idjouadiene I. Age-related arterial calcification in rats. *Life Sci*, 2000; 66: 2371-2381.

24. Fitzgerald P. J., Ports T. A. and Yock P. G. Contribution of localized calcium deposits to dissection after angioplasty. An observational study using intravascular ultrasound. *Circulation*, 1992; 86: 64-70.

25. Letsov G.V., Baldwin J.C. and Westaby S. *Surgery for coronary artery disease*, in The Oxford Textbook of Surgery (Morris P.J. and Malt R., Editors). 1994, Oxford University Press: Oxford.

26. London G. M., Guerin A. P., Marchais S. J., Pannier B., Safar M. E., Day M., et al. Cardiac and arterial interactions in end-stage renal disease. *Kidney Int*, 1996; 50: 600-608.

27. Blacher J., Pannier B., Guerin A. P., Marchais S. J., Safar M. E. and London G. M. Carotid arterial stiffness as a predictor of cardiovascular and all-cause mortality in end-stage renal disease. *Hypertension*, 1998; 32: 570-574.

28. Guerin A. P., London G. M., Marchais S. J. and Metivier F. Arterial stiffening and vascular calcifications in end-stage renal disease. *Nephrol Dial Transplant*, 2000; 15: 1014-1021.

29. Mackenzie I., Wilkinson I. and Cockcroft J. Assessment of arterial stiffness in clinical practice (review). *Q J Med*, 2002; 95: 67-74.

30. Shoji T., Emoto M., Shinohara K., Kakiya R., Tsujimoto Y., Kishimoto H., et al. Diabetes mellitus, aortic stiffness, and cardiovascular mortality in end-stage renal disease. *J Am Soc Nephrol*, 2001; 12: 2117-2124.

31. Mourad J. J., Pannier B., Blacher J., Rudnichi A., Benetos A., London G. M., et al. Creatinine clearance, pulse wave velocity, carotid compliance and essential hypertension. *Kidney Int*, 2001; 59: 1834-1841.

32. Tozawa M., Iseki K., Iseki C., Oshiro S., Yamazato M., Higashiuesato Y., et al. Evidence for elevated pulse pressure in patients on chronic hemodialysis: A case-control study. *Kidney Int*, 2002; 62: 2195-2201.

33. Klassen P. S., Lowrie E. G., Reddan D. N., DeLong E. R., Coladonato J. A., Szczech L. A., et al. Association between pulse pressure and mortality in patients undergoing maintenance hemodialysis. *JAMA*, 2002; 287: 1548-1555.

34. Lindberg J.S., Moe S.M., Goodman W.G., Coburn J.W., Sprague S.M., Blaisdell P.W., et al. The calcimimetic AMG 073 reduces parathyroid hormone and calcium x phosphorus in secondary hyperparathyroidism. *Kidney Int*, 2003; 63: 248-254.

35. Virchow R, *Cellular pathology: As based upon physiology and pathophysiology*. 1971, New York: Dover. 404-408.

36. Shioi A., Mori K., Jono S., Wakikawa T., Hiura Y., Koyama H., et al. Mechanism of atherosclerotic calcification. *Z Kardiol*, 2000; 89: 75-79.

37. Bostrom K. I. Cell differentiation in vascular calcification. *Z Kardiol*, 2000; 89: 69-74.

38. Hunt J. L., Fairman R., Mitchell M. E., Carpenter J. P., Golden M., Khalapyan T., et al. Bone formation in carotid plaques: A clinicopathological study. *Stroke*, 2002; 33: 1214-1219.

39. Bostrom K., Watson K. E., Horn S., Wortham C., Herman I. M. and Demer L. L. Bone morphogenetic protein expression in human atherosclerotic lesions. *J Clin Invest*, 1993; 91: 1800-1809.

40. Kockx M. M., Muhring J., Bortier H., De Meyer G. R. and Jacob W. Biotin- or digoxigenin-conjugated nucleotides bind to matrix vesicles in atherosclerotic plaques. *Am J Pathol*, 1996; 148: 1771-1777.

41. Kim K. M. Calcification of matrix vesicles in human aortic valve and aortic media. *Fed Proc*, 1976; 35: 156-162.

42. Reynolds J., Joannides A., Skepper J. N., McNair R., churgers L., Proudfoot D., et al. Human vascular smooth muscle cells undergo vesicle-mediated calcification in response to changes in extracellular calcium and phosphate concentrations: A potential mechanism for accelerated vascular calcification in ESRD. *J Am Soc Nephrol*, 2004; 15: 2857-2867.

43. Rekhter M. D., Zhang K., Narayanan A. S., Phan S., Schork M. A. and Gordon D. Type I collagen gene expression in human atherosclerosis. Localization to specific plaque regions. *Am J Pathol*, 1993; 143: 1634-1648.

44. Hirota S., Imakita M., Kohri K., Ito A., Morii E., Adachi S., et al. Expression of osteopontin messenger RNA by macrophages in atherosclerotic plaques. A possible association with calcification. *Am J Pathol*, 1993; 143: 1003-1008.

45. O'Brien E. R., Garvin M. R., Stewart D. K., Hinohara T., Simpson J. B., Schwartz S. M., et al. Osteopontin is synthesized by macrophage, smooth muscle, and endothelial cells in primary and restenotic human coronary atherosclerotic plaques. *Arterioscler Thromb*, 1994; 14: 1648-1656.

46. Shanahan C. M., Cary N. R., Metcalfe J. C. and Weissberg P. L. High expression of genes for calcification-regulating proteins in human atherosclerotic plaques. *J Clin Invest*, 1994; 93: 2393-2402.

47. Ikeda T., Shirasawa T., Esaki Y., Yoshiki S. and Hirokawa K. Osteopontin mRNA is expressed by smooth muscle-derived foam cells in human atherosclerotic lesions of the aorta. *J Clin Invest*, 1993; 92: 2814-2820.

48. Fitzpatrick L. A., Severson A., Edwards W. D. and Ingram R. T. Diffuse calcification in human coronary arteries. Association of osteopontin with atherosclerosis. *J Clin Invest*, 1994; 94: 1597-1604.

49. Shanahan C. M., Proudfoot D., Tyson K. L., Cary N. R., Edmonds M. and Weissberg P. L. Expression of mineralisation-regulating proteins in association with human vascular calcification. *Z Kardiol*, 2000; 89: 63-68.

50. Shioi A., Nishizawa Y., Jono S., Koyama H., Hosoi M. and Morii H. Beta-glycerophosphate accelerates calcification in cultured bovine vascular smooth muscle cells. *Arterioscler Thromb Vasc Biol*, 1995; 15: 2003-2009.

51. Wada T., McKee M. D., Steitz S. and Giachelli C. M. Calcification of vascular smooth muscle cell cultures: Inhibition by osteopontin. *Circ Res*, 1999; 84: 166-178.

52. Jakoby M. G. 4th and Semenkovich C. F. The role of osteoprogenitors in vascular calcification. *Curr Opin Nephrol Hypertens*, 2000; 9: 11-15.

53. Stein G. S., Lian J. B., Stein J. L., Van Wijnen A. J. and Montecino M. Transcriptional control of osteoblast growth and differentiation. *Physiol Rev*, 1996; 76: 593-629.

54. Watson K. E., Parhami F., Shin V. and Demer L. L. Fibronectin and collagen I matrixes promote calcification of vascular cells in vitro, whereas collagen IV matrix is inhibitory. *Arterioscler Thromb Vasc Biol*, 1998; 18: 1964-1971.

55. Tintut Y., Parhami F., Bostrom K., Jackson S. M. and Demer L. L. cAMP stimulates osteoblast-like differentiation of calcifying vascular cells. Potential signaling pathway for vascular calcification. *J Biol Chem*, 1998; 273: 7547-7553.

56. Ducy P., Zhang R., Geoffroy V., Ridall A. L. and Karsenty G. Osf2/cbfa1: A transcriptional activator of osteoblast differentiation. *Cell*, 1997; 89: 747-754.

57. Watson K. E., Bostrom K., Ravindranath R., Lam T., Norton B. and Demer L. L. TGF-beta 1 and 25-hydroxycholesterol stimulate osteoblast-like vascular cells to calcify. *J Clin Invest*, 1994; 93: 2106-2113.

58. Schor A. M., Allen T. D., Canfield A. E., Sloan P. and Schor S. L. Pericytes derived from the retinal microvasculature undergo calcification in vitro. *J Cell Sci*, 1990; 97: 449-461.

59. Mori K., Shioi A., Jono S., Nishizawa Y. and Morii H. Dexamethasone enhances in vitro vascular calcification by promoting osteoblastic differentiation of vascular smooth muscle cells. *Arterioscler Thromb Vasc Biol*, 1999; 19: 2112-2118.

60. Balica M., Bostrom K., Shin V., Tillisch K. and Demer L. L. Calcifying subpopulation of bovine aortic smooth muscle cells is responsive to 17 beta-estradiol. *Circulation*, 1997; 95: 1954-1960.

61. Yamagishi S., Fujimori H., Yonekura H., Tanaka N. and Yamamoto H. Advanced glycation end-products accelerate calcification in microvascular pericytes. *Biochem Biophys Res Commun*, 1999; 258: 353-357.

62. Okada H., Moriwaki K., Konishi K., Kobayashi T., Sugahara S., Nakamoto H., et al. Tubular osteopontin expression in human glomerulonephritis and renal vasculitis. *Am J Kidney Dis*, 2000; 36: 498-506.

63. Massfelder T., Dann P., Wu T. L., Vasavada R., Helwig J. J. and Stewart A. F. Opposing mitogenic and anti-mitogenic actions of parathyroid hormone- related protein in vascular smooth muscle cells: A critical role for nuclear targeting. *Proc Natl Acad Sci U S A*, 1997; 94: 13630-13635.

64. Jono S., Nishizawa Y., Shioi A. and Morii H. Parathyroid hormone-related peptide as a local regulator of vascular calcification. Its inhibitory action on *in vitro* calcification by bovine vascular smooth muscle cells. *Arterioscler Thromb Vasc Biol*, 1997; 17: 1135-1142.

65. Jono S., Nishizawa Y., Shioi A. and Morii H. 1,25-dihydroxyvitamin D3 increases *in vitro* vascular calcification by modulating secretion of endogenous parathyroid hormone-related peptide. *Circulation*, 1998; 98: 1302-1306.

66. Katagiri T., Yamaguchi A., Komaki M., Abe E., Takahashi N., Ikeda T., et al. Bone morphogenetic protein-2 converts the differentiation pathway of C2C12 myoblasts into the osteoblast lineage. *J Cell Biol*, 1994; 127: 1755-1766.

67. Dorai H., Vukicevic S. and Sampath T. K. Bone morphogenetic protein-7 (osteogenic protein-1) inhibits smooth muscle cell proliferation and stimulates the expression of markers that are characteristic of SMC phenotype in vitro. *J Cell Physiol*, 2000; 184: 37-45.

68. Jono S., McKee M. D., Murry C. E., Shioi A., Nishizawa Y., Mori K., et al. Phosphate regulation of vascular smooth muscle cell calcification. *Circ Res*, 2000; 87: E10-17.

69. Llach F. and Bover J., *Renal osteodystrophies*, in The Kidney (Brenner, B.M., Editor), p. 2103-2186. WB Saunders Company: Philadelphia, 2000.

70. Hamdy N. The spectrum of renal bone disease. *Nephrol Dial Transplant*, 1995; 10: 14-18; discussion 37-43.

71. Ganesh S. K., Stack A. G., Levin N. W., Hulbert-Shearon T. and Port F. K. Association of elevated serum PO_4, Ca x PO_4 product, and parathyroid hormone with cardiac mortality risk in chronic hemodialysis patients. *J Am Soc Nephrol*, 2001; 12: 2131-2138.

72. Couttenye M.M., D'Haese P.C., Verschoren W.J., Behets G.J., Schrooten I. and De Broe M.E. Low bone turnover in patients with renal failure. *Kidney Int*, 1999; supplement: S70-76.

73. Fournier A., Hardy-Yverneau P., Hue P. and Said S. Adynamic bone disease in patients with uremia. *Curr Opin Nephrol Hypertens*, 1999; 3: 396-410.

74. Lund R.J., Davies M.R., Brown A.J. and Hruska K.A. Successful treatment of an adynamic bone disorder with bone morphogenetic protein-7 in a renal ablation model. *J Am Soc Nephrol*, 2004; 15: 359-369.

75. Simon M., Maresh J. G., Harris S. E., Hernandez J. D., Arar M., Olson M. S., et al. Expression of bone morphogenetic protein-7 m-RNA in normal and ischemic adult rat kidney. *Am J Physiol*, 1999; 276: F382-389.

76. Wang S. N., Lapage J. and Hirschberg R. Loss of tubular bone morphogenetic protein-7 in diabetic nephropathy. *J Am Soc Nephrol*, 2001; 12: 2392-2399.

77. *Endocrine regulation of calcium and phosphate metabolism*, in Physiology (Berne, R.M., Levy, M.N., Koeppen, B.M., and Stanton, B.A., Editors),p. 849., Mosby: St Louis 1998.

78. London G. M., Marty C., Marchais S. J., Guerin A. P., Metivier F. and de Vernejoul M-C. Arterial calcification and bone histomorphometry in end-stage renal disease. *J Am Soc Nephrol*, 2004; 15: 1943-1951.

79. Hogan B. L. Bone morphogenetic proteins: Multifunctional regulators of vertebrate development. *Genes Dev*, 1996; 10: 1580-1594.

80. Ducy P. and Karsenty G. The family of bone morphogenetic proteins. *Kidney Int*, 2000; 57: 2207-2214.

81. Urist M.R., Iwata H., Ceccotti P.L., Dorfman R.L., Boyd S.D., McDowell R.M., et al. Bone morphogenesis in implants of insoluble bone gelatin. *Proc Natl Acad Sci U S A*, 1973; 70: 3511-3515.

82. Helder M. N., Ozkaynak E., Sampath K. T., Luyten F. P., Latin V., Oppermann H., et al. Expression pattern of osteogenic protein-1 (bone morphogenetic protein- 7) in human and mouse development. *J Histochem Cytochem*, 1995; 43: 1035-1044.

83. Jena N., Martin-Seisdedos C., McCue P. and Croce C. M. BMP7 null mutation in mice: Developmental defects in skeleton, kidney, and eye. *Exp Cell Res*, 1997; 230: 28-37.

84. Luo G., Hofmann C., Bronckers A. L., Sohocki M., Bradley A. and Karsenty G. BMP-7 is an inducer of nephrogenesis, and is also required for eye development and skeletal patterning. *Genes Dev*, 1995; 9: 2808-2820.

85. Piscione T. D., Phan T. and Rosenblum N. D. BMP7 controls collecting tubule cell proliferation and apoptosis via Smad1-dependent and -independent pathways. *Am J Physiol Renal Physiol*, 2001; 280: F19-33.

86. Dudley A. T. and Robertson E. J. Overlapping expression domains of bone morphogenetic protein family members potentially account for limited tissue defects in BMP7 deficient embryos. *Dev Dyn*, 1997; 208: 349-362.

87. Kim R. Y., Robertson E. J. and Solloway M. J. BMP6 and BMP7 are required for cushion formation and septation in the developing mouse heart. *Dev Biol*, 2001; 235: 449-466.

88. Solloway M. J. and Robertson E. J. Early embryonic lethality in BMP5;BMP7 double mutant mice suggests functional redundancy within the 60a subgroup. *Development*, 1999; 126: 1753-1768.

89. Kopp J. B. BMP receptors in kidney. *Kidney Int*, 2000; 58: 2237-2238.

90. Vukicevic S., Basic V., Rogic D., Basic N., Shih M. S., Shepard A., et al. Osteogenic protein-1 (bone morphogenetic protein-7) reduces severity of injury after ischemic acute renal failure in rat. *J Clin Invest*, 1998; 102: 202-214.

91. Hruska K. A., Guo G., Wozniak M., Martin D., Miller S., Liapis H., et al. Osteogenic protein-1 prevents renal fibrogenesis associated with ureteral obstruction. *Am J Physiol Renal Physiol*, 2000; 279: F130-143.

92. Wang S., Chen Q., Simon T.C., Strebeck F., Chaudhary L, Morrissey J., et al. Bone morphogenic protein-7 (BMP-7), a novel therapy for diabetic nephropathy. *Kidney Int*, 2003; 63: 2037-2049.

93. Zeisberg M., Bottiglio C., Kumar N., Maeshima Y., Strutz F., Muller G., and Kalluri R.. Bone morphogenic protein-7 inhibits progression of chronic renal fibrosis associated with two genetic mouse models. *Am J Physiol Renal Physiol*, 2003;285:F1060-7

94. Gonzalez E.A., Lund R.J., Martin K.J., McCartney J.E., Tondravi M.M., Sampath T.K., et al. Treatment of a murine model of high-turnover renal osteodystrophy by exogenous BMP7. *Kidney Int*, 2002; 61: 1322-1331.

95. Lund R.J, Davies M.R., Brown, A.J.,Hruska, K.A. Successful treatment of an adynamic bone disorder with bone morphogenetic protein-7 in a renal ablation model. *J Am Soc Nephrol.* 2004; 15: 359-69.

96. Schneider M.D., Gaussin V. and Lyons K.M. Tempting fate: BMP signals for cardiac morphogenesis. *Cytokine & Growth Factor Reviews*, 2003; 14: 1-4.

97. Lane K. B., Machado R. D., Pauciulo M. W., Thomson J. R., Phillips J. A., 3rd, Loyd J. E., et al. Heterozygous germline mutations in BMPR2, encoding a TGF-beta receptor, cause familial primary pulmonary hypertension. The international PPHconsortium. *Nat Genet*, 2000; 26: 81-84.

98. Thomson J. R., Machado R. D., Pauciulo M. W., Morgan N. V., Humbert M., Elliott G. C., et al. Sporadic primary pulmonary hypertension is associated with germline mutations of the gene encoding BMPR2, a receptor member of the TGF- beta family. *J Med Genet*, 2000; 37: 741-745.

99. Runo J.R. and Loyd J.E. Primary pulmonary hypertension. *Lancet*, 2003; 361: 1533-1544.

100. Zhang S., Fantozzi I., Tigno D.D., Yi E.S., Platoshyn O., Thistlethwaite P.A., et al. Bone morphogenetic proteins induce apoptosis in human pulmonary vascular smooth muscle cells. *Am J Physiol Lung Cell Mol Physiol*, 2003; 285: L740-L754.

101. Galvin K. M., Donovan M. J., Lynch C. A., Meyer R. I., Paul R. J., Lorenz J. N., et al. A role for Smad6 in development and homeostasis of the cardiovascular system. *Nat Genet*, 2000; 24: 171-174.

102. Towler D. A., Bidder M., Latifi T., Coleman T. and Semenkovich C. F. Diet-induced diabetes activates an osteogenic gene regulatory program in the aortas of low density lipoprotein receptor-deficient mice. *J Biol Chem*, 1998; 273: 30427-30434.

103. Qiao J. H., Xie P. Z., Fishbein M. C., Kreuzer J., Drake T. A.,Demer L. L., et al. Pathology of atheromatous lesions in inbred and genetically engineered mice. Genetic determination of arterial calcification. *Arterioscler Thromb*, 1994; 14: 1480-1497.

104. Price P. A., Faus S. A. and Williamson M. K. Warfarin causes rapid calcification of the elastic lamellae in rat arteries and heart valves. *Arterioscler Thromb Vasc Biol*, 1998; 18: 1400-1407.

105. Price P. A., Faus S. A. and Williamson M. K. Warfarin-induced artery calcification is accelerated by growth and vitamin D. *Arterioscler Thromb Vasc Biol*, 2000; 20: 317-327.

106. Fraser J. D. and Price P. A. Induction of matrix GLA protein synthesis during prolonged 1,25-dihydroxyvitamin D3 treatment of osteosarcoma cells. *Calcif Tissue Int*, 1990; 46: 270-279.

107. Fraser J. D., Otawara Y. and Price P. A. 1,25-dihydroxyvitamin D3 stimulates the synthesis of matrix gamma-carboxyglutamic acid protein by osteosarcoma cells.

Mutually exclusive expression of vitamin K-dependent bone proteins by clonal osteoblastic cell lines. *J Biol Chem*, 1988; 263: 911-916.

108. Coates T., Kirkland G. S., Dymock R. B., Murphy B. F., Brealey J. K., Mathew T. H., et al. Cutaneous necrosis from calcific uremic arteriolopathy. *Am J Kidney Dis*, 1998; 32: 384-391.

109. Stehbens WE., *Atherosclerosis and degenerative diseases of blood vessels*, in Vascular Pathology (Stehbens WE., Lie JT., Editors), Chapman: London, 1995.

110. Watson K. E., Abrolat M. L., Malone L. L., Hoeg J. M., Doherty T., Detrano R., et al. Active serum vitamin D levels are inversely correlated with coronary calcification. *Circulation*, 1997; 96: 1755-1760.

111. Doherty T. M., Tang W., Dascalos S., Watson K. E., Demer L. L., Shavelle R. M., et al. Ethnic origin and serum levels of 1 alpha,25-dihydroxyvitamin D3 are independent predictors of coronary calcium mass measured by electron-beam computed tomography. *Circulation*, 1997; 96: 1477-1481.

112. Gagnon R. F. and Duguid W. P. A reproducible model for chronic renal failure in the mouse. *Urol Res*, 1983; 11: 11-14.

113. Gagnon R. F. and Gallimore B. Characterization of a mouse model of chronic uremia. *Urol Res*, 1988; 16: 119-126.

114. Parfitt A. M. , Drezner M. K., Glorieux F. H. , Kanis J. A. , Malluche H. H. ,Meunier P.J., et al. Bone histomorphometry: Standardization of nomenclature, symbols and units. *J Bone Miner Res*, 1987; 2: 595-610.

115. Eriksen E.F., Axelrod D.W. and Melson F., *Bone histomorphometry.*, New York: Raven Press 1994.

116. Wozniak M., Fausto A., Carron C. P., Meyer D. M. and Hruska K. A. Mechanically strained cells of the osteoblast lineage organize their extracellular

matrix through unique sites of alphavbeta3-integrin expression. *J Bone Miner Res*, 2000; 15: 1731-1745.

117. Hierck B. P., Iperen L. V., Gittenberger-De Groot A. C. and Poelmann R. E. Modified indirect immunodetection allows study of murine tissue with mouse monoclonal antibodies. *J Histochem Cytochem*, 1994; 42: 1499-1502.

118. Moe S. M., O'Neill K. D., Duan D., Ahmed S., Chen N. X., Leapman S. B., et al. Medial artery calcification in ESRD patients is associated with deposition of bone matrix proteins. *Kidney Int*, 2002; 61: 638-647.

119. Desbois C., Hogue D. A. and Karsenty G. The mouse osteocalcin gene cluster contains three genes with two separate spatial and temporal patterns of expression. *J Biol Chem*, 1994; 269: 1183-1190.

120. Ducy P., Desbois C., Boyce B., Pinero G., Story B., Dunstan C., et al. Increased bone formation in osteocalcin-deficient mice. *Nature*, 1996; 382: 448-452.

121. Worcester E. M., Nakagawa Y., Wabner C. L., Kumar S. and Coe F. L. Crystal adsorption and growth slowing by nephrocalcin, albumin, and Tamm-Horsfall protein. *Am J Physiol*, 1988; 255: F1197-1205.

122. Umans L., Overbergh L., Serneels L., Tesseur I. and Van Leuven F. Analysis of expression of genes involved in apolipoprotein E-based lipoprotein metabolism in pregnant mice deficient in the receptor-associated protein, the low density lipoprotein receptor, or apolipoprotein E. *Biol Reprod*, 1999; 61: 1216-1225.

123. Sanchez C.P., Kuizon B.D., Abdella P.A., Juppner H., Salusky I.B. and Goodman W.G. Impaired growth, delayed ossification, and reduced osteoclastic activity in the growth plate of calcium-supplemented rats with renal failure. *Endocrinology*, 2000; 141: 1536-1544.

124. Parhami F., Garfinkel A. and Demer L. L. Role of lipids in osteoporosis. *Arterioscler Thromb Vasc Biol*, 2000; 20: 2346-2348.

125. Rosen V. and Wozney J.M., *Bone morphogenetic proteins*, in Principles of bone biology (Belizikian JP., Raisz.L., Rodan GA, Editors), p. 919-928., Academic Press: San Diego, 1996

126. Zeisberg M., Bottiglio C., Kumar N., Maeshima Y., Strutz F., Muller G. A., et al. Bone morphogenetic protein-7 inhibits progression of chronic renal fibrosis associated with two genetic mouse models. *Am J Phyiol Renal Physiol*, 2003; 285: 1060-1067.

127. Davies M.R., Lund R.J. and Hruska K.A. Bmp-7 is an efficacious treatment of vascular calcification in a murine model of atherosclerosis and chronic renal failure. *J Am Soc Nephrol*, 2003; 14: 1559-1567.

128. Chertow G. M., Burke S. K. and Raggi P. Sevelamer attenuates the progression of coronary and aortic calcification in hemodialysis patients. *Kidney Int*, 2002; 62: 245-252.

129. Braun J., Asmus H., Holzer H., Brunkhorst R., Krause R., Schulz W., et al. Long-term comparison of a calcium-free phosphate binder and calcium carbonate--phosphorus metabolism and cardiovascular calcification. *Clin Nephrol*, 2004; 62: 104-115.

130. Lund R. J., Davies M. R. and Hruska K. A. Bone morphogenetic protein-7: An anti-fibrotic morphogenetic protein with therapeutic importance in renal disease. *Curr Opin Nephrol Hypertens*, 2002; 11: 31-36.

131. R.J. Lund, Gonzalez E.A., Martin K.J. and Hruska K.A. Efficacy of BMP-7 therapy in high turnover renal osteodystrophy, at *The American Society of Nephrology*. 2001. San Francisco: Journal of the American Society of Nephrology.

132. Boukhris R. and Becker K. Calcification of the aorta and osteoporosis. *JAMA*, 1972; 219: 1307-1311.

133. Ouchi Y., Akashita M., De Souza A., Nakamura T. and Orimo H. Age-related loss of bone mass and aortic/aortic valve calcification: Reevaluation of recommended dietary allowance ofcalcium in the elderly. *Ann N Y Acad Sci*, 1993; 676: 297-307.

134. Parhami F., Morrow A. D., Balucan J., Leitinger N., Watson A. D., Tintut Y., et al. Lipid oxidation products have opposite effects on calcifying vascular cell and bone cell differentiation. A possible explanation for the paradox of arterial calcification in osteoporotic patients. *Arterioscler Thromb Vasc Biol*, 1997; 17: 680-687.

135. Kato M., Patel M., Levasseur R., Lobov I., Chang B., Glass D. 2nd., et al. Cbfa1-independent decrease in osteoblast proliferation, osteopenia, and persistent embryonic eye vascularization in mice deficient in LRP5, a wnt coreceptor. *J Cell Biol*, 2002; 157: 303-314.

136. Babij P., Zhao W., Small C., Kharode Y., Yaworsky P., Bouxsein M., et al. High bone mass in mice expressing a mutant LRP5 gene. *J Bone Miner Res*, 2003; 18: 960-974.

137. Boyden L. M., Mao J., Belsky J., Mitzner L., Farhi A., Mitnick M. A., et al. High bone density due to a mutation in ldl-receptor-related protein 5. *N Engl J Med*, 2002; 346: 1513-1521.

138. Ferrari S., Deutsch S., Choudhury U., Chevally T., Bonjour J. P., Dermitzakis E., et al. Polymorphisms in the low-density lipoprotein receptor-related protein 5 (LRP5) gene are associated with variation in vertebral bone mass, vertebral bone size and stature in whites. *Am J Hum Genet*, 2004; 74: 866-875.

139. Little R. D., Carulli J. P., Del Mastro R. G., Dupuis J., Osborne M., Folz C., et al. A mutation in the LDL receptor-related protein 5 gene results in the autosomal dominant high-bone-mass trait. *Am J Hum Genet*, 2002; 70: 11-19.

140. Gong Y., Slee R. B., Fukai N., Rawadi G., Roman-Roman S., Reginato A. M., et al. LDL receptor-related protein 5 (lrp5) affects bone accrual and eye development. *Cell*, 2001; 107: 513-523.

141. Selbi W., de la Motte C., Hascall V. and Phillips A. O. BMP-7 modulates hyaluronan-mediated proximal tubular cell-monocyte interaction. *J Am Soc Nephrol*, 2004; 15: 1199-1211.

142. Issack P. and DiCesare P. Recent advances toward the clinical application of bone morphogenetic proteins in bone and cartilage repair. *Am J Orthop*, 2003; 32: 429-436.

143. Oppermann H., Tai M-S. and Hilly J. Enhanced biological and physical properties of variants of OP-1 and related BMPs, at *2nd European Conference on Bone Morphogenetic Proteins*. 2002. Zagreb.

144. Nykjaer A. and Willnow T. The low-density lipoprotein receptor gene family: A cellular swiss army knife? *Trends Cell Biol*, 2002; 12: 273-280.

145. Niehrs C. Developmental biology. Solving a sticky problem. *Nature*, 2001; 413: 787-788.

146. Nusse R. Developmental biology. Making head or tail of Dickkopf. *Nature*, 2001; 411: 255-256.

147. Coen G., Mazzaferro S., Ballanti P., Sardella D., Chicca S.,Manni M., et al. Renal bone disease in 76 patients with varying degrees of predialysis chronic renal failure: A cross-sectional study. *Nephrol Dial Transplant*, 1996; 11: 813-819.

148. Urano T., Shiraki M., Ezura Y., Fujita M., Sekine E., Hoshino S., et al. Association of single nucleotide polymorphism in low-density lipoprotein receptor-related protein 5 gene with bone mineral density. *J Bone Miner Metab*, 2004; 22: 341-345.

149. Hussein S., Duff E. and Sirard C. Smad4 and beta-catenin co-activators functionally interact with lymphoid-enhancing factor to regulate graded expression of MSX2. *J Biol Chem*, 2003; 278: 48805-48814.

150. Figueroa D. J., Hess J. F., Ky B., Brown S. D., Sandig V., Hermanowski-Vosatka A., et al. Expression of the type I diabetes-associated gene LRP5 in macrophages, vitamin a system cells, and the islets of Langerhans suggests multiple potential roles in diabetes. *J Histochem Cytochem*, 2000; 48: 1357-1368.

151. Ducy, P. Cbfa1: a molecular switch in osteoblast biology. *Dev Dyn*, 2000; 219: 461-71.

152. Revell, P. A. Histomorphometry of bone. *J Clin Pathol*, 1986;36:1323-1331.

Appendix A

The potential role of low density lipoprotein receptor-related protein 5 (LRP5) in the aetiology of vascular calcification in the *ldlr*$^{-/-}$ mouse

A.1 Aim

One question that arises from the studies described in the foregoing sections is whether or not the *ldlr*$^{-/-}$ genotype can itself directly affect bone and vascular mineralisation. The LDLR is a member of a larger family of structurally similar cell surface receptors, and there is evidence to suggest that expression of other members of the LDLR family may change in response to the *ldlr*$^{-/-}$ lesion. One member of this family, low-density lipoprotein receptor related-protein 5 (LRP5) has recently been shown to play a role in determining bone density, and so changes in LRP5 expression may be particularly relevant to the emergence of abnormal bone and vascular mineralisation patterns in this model.

The preliminary studies described in this section were designed to provide initial data to clarify this issue, by assaying levels of mRNA expression for LRP5 in *ldlr*$^{-/-}$ and wild type (WT) mice, when fed either standard chow or the high fat, high cholesterol diet previously discussed. The studies used Reverse Transcription Polymerase Chain Reaction

(RT-PCR) and Real-Time RT-PCR to quantify relative mRNA levels in a number of tissues from these animals. The preliminary nature of the data from these studies is emphasised, and explains their inclusion as an appendix rather than in the body of this thesis.

A.2 Background and hypothesis

The LDLR is a member of a family of structurally similar but functionally disparate cell surface receptors that includes a number of LDLR-related proteins, or LRPs [144]. In contrast to LDLR, which serves primarily as a receptor for low density lipoproteins, LRPs interact with a variety of extracellular ligands. The expression of a number of members of this family, including LRP1, have been shown to be increased in liver and other tissue of a number of models of hyperlipidaemia including *ldlr*$^{-/-}$, under certain conditions [122]. This observation suggests the possibility that abnormal patterns of LRP expression may also occur in this genetic model of vascular calcification. One factor that may be particularly relevant to both bone and vascular calcification is LRP5. This protein acts as a co-receptor with members of the Frizzled family of receptors for the Wnt family of ligands [145], and may direct signalling related to these ligands through the canonical, β-Catenin-dependant intracellular pathway. In addition, LRP5 is able to bind extracellular inhibitors of Wnt/Frizzled, including members of the Dickkopf (Dkk) family of proteins [146].

LRP5 has emerged as an important factor in normal bone mineralisation, and is expressed by osteoblasts [147]. Functional activation of LRP5 due to single point mutation has been associated with abnormally dense, but structurally normal bones in two large human kindreds [137, 139]]. Individuals with the activating mutation have extremely high bone density on dual energy x-ray absorbtiometry (DEXA) scanning that is two standard deviations or more beyond the population mean, giving Z scores at a single site of 2 or more, and combined Z scores at two sites of 4 or more. While life expectancy is normal and there is no significant morbidity associated with the lesion, it is interesting to note that traumatic fractures are virtually unheard of throughout these extensive kindreds. In addition, this phenotype has been successfully reproduced in a transgenic animal model [136]. Other studies supporting a key role of LRP5 in determining bone mineral density and strength is the description of an inactivating mutation of this same gene associated with a syndrome of juvenile osteoporosis, Osteoporosis Pseudoglioma syndrome (OPPS) [140], and the association of polymorphisms of LRP5 with bone density in Caucasian and Japanese populations [138, 148].

Relevant to the studies described in this thesis, it is further possible to hypothesise a link between LRP5 function and BMP7 signalling at a cellular level. Cooperativity between Wnt and BMP signalling pathways has been shown in at least in the setting of embryological development [149]. In this example, both pathways may simultaneously act on the same target gene, as well as influencing the expression levels of moieties in the other pathway. Nevertheless, there is no direct evidence at present for interaction between BMP7 and LRP5 signalling specifically.

Thus functional changes attributable to changes in expression of LRP5 may be relevant to the abnormal calcification seen in the *ldlr* $^{-/-}$ phenotype, both in terms of normal bone mineralisation and pathological VC, and further, may influence the therapeutic response to BMP7 in this setting. It was hypothesised that LRP5 expression would be increased in vascular tissues of *ldlr* $^{-/-}$ mice, and influenced by the hyperlipidaemia associated with the high cholesterol, high fat diet used in the studies described in sections 4 and 5.

A.3 Methods

A.3.1 Animals and diets

Experiments were conducted according to the guidelines of the Washington University Animal Care committee (http://medicine.wustl.edu/~acu). *ldlr*$^{-/-}$ mice were fed a chow diet until 10 weeks of age, then either continued to receive chow or were fed high fat high cholesterol diet as used in previous studies for two weeks. Ten week old wild type (WT) C57/Bl6 mice purchased from Harlan Teklad were fed either standard laboratory chow or the same high fat, high cholesterol diet for two weeks. All animals had access to water *ad libitum*. After two weeks on their respective diets, animals were sacrificed under anaesthesia (intraperitoneal xylazine 13mg/kg and ketamine 87mg/kg), and their internal organs rapidly dissected, then flash-frozen in dry ice / ethanol slurry. Samples were then immediately processed for mRNA extraction or stored at – 80 °C.

A.3.2 Messenger RNA extraction

RNA extraction was performed using 'RNAqueous™-4PCR' Kit (Ambion, Austin, TX) according to manufacturer's instructions. Briefly, total RNA was extracted from tissue samples by homogenisation in a buffer containing guanidinium thiocyanate, a denaturant that lyses cell membranes and inactivates cellular ribonucleases. The lysate is then mixed with 64% ethanol solution, and applied to a silica-based filter that selectively and quantitatively binds messenger RNA (mRNA) and larger ribosomal RNA but not transfer RNA (tRNA) or smaller ribosomal RNAs. The filter is washed to remove residual DNA and protein contaminants, and mRNA eluted from the filter in nuclease-free water containing 0.1mM EDTA to chelate heavy metal ions. Trace amounts of DNA contamination were removed by DNase I treatment of the eluate, followed by DNase inactivation. Quantification of the product was confirmed by absorbtiometry at 260nm.

A.3.3 RT-PCR

Reverse transcription to generate cDNA from the RNA isolated above used the Onestep RT-PCR kit (Qiagen, Valencia, CA), according to manufacturer's instructions. Expression of LRP5 was compared with the housekeeping gene GAPDH using the primers shown in table 7.1. LRP5 primers were as described [150], and GAPDH derived from Genbank sequences. Reaction mixtures variously included 20 - 100 ng template, based on eluate concentrations of mRNA derived by absorbtiometry, above. The

following cycles were used: Step One: 1 cycle of 30 minutes at 50 °C; Step Two: 1 cycle of 15 minutes at 95 °C; Step Three: 35 cycles of 1 minute at 94 °C, 1 minute at 54 °C, and 1 minute at 72 °C; Step Four: 1 cycle of 10 minutes at 72 °C; then hold at 4 °C.

	Primer	Sequence (5' - 3')	Product size
Lrp5	Sense	AAG CTC AGC TTC ATC CAC CG	900 bp
	Antisense	TCC CGT CTA TGT TGA TCA CCT CG	
Gapdh	Sense	AAC GGA TTT GGC CGT ATT GGC CGC	300 bp
	Antisense	CCT GCA TCT GCC CAT TTG ATG TTG	

Table A.1 Characteristics of primers for LRP5 and GAPDH used for Reverse transcription polymerase chain reaction (RT-PCR). See text for full explanation.

A.3.4 Real Time RT-PCR

To quantify RNA expression change in response to fat diet in aortic tissues, real time RT-PCR was performed using the reaction conditions given above, using 40 cycles of step 3. SYBR ® green, a fluorescent dye that binds selectively to double-stranded DNA, was added to the reaction mixture in place of an equal volume of dH_2O to enable identification of the amplification product. Fluorescence was detected with an ABI prism 5700 sequence detection system (PE Biosystems). The threshold cycle (C_T), which is defined as the cycle number at which the amount of amplified product reaches a fixed threshold, was obtained for LRP5 and GAPDH as a reference gene. The expression ratio of mRNA under various experimental conditions was calculated from the general formula:

Expression ratio = ER = $2^{-\Delta\Delta Ct}$.

To estimate LRP5 ER in relation to diet for the two genotypes, the following equations were used to calculate ΔΔCt:

1. $\Delta\Delta C_{TLDLR} = \Delta C_T(LRP5_{LDLRFat}) - \Delta C_T(LRP5_{LDLRChow})$,
2. $\Delta\Delta C_{TWT} = \Delta C_T(LRP5_{WTFat}) - \Delta C_T(LRP5_{WTChow})$

To estimate LRP5 ER in relation to genotype for the two diets, the following equations were used:

and $\Delta C_T(LRP5_{Fat}) = C_T(LRP5_{Fat}) - C_T(GAPDH_{Fat})$.

3. $\Delta\Delta C_{TChow} = \Delta C_T(LRP5_{WTChow}) - \Delta C_T(LRP5_{LDLRChow})$,
4. $\Delta\Delta C_{TFat} = \Delta C_T(LRP5_{WTFat}) - \Delta C_T(LRP5_{LDLRFat})$,

where $\Delta C_T(LRP5_{LDLRFat}) = C_T(LRP5_{LDLRFat}) - C_T(GAPDH_{LDLRFat})$

$\Delta C_T(LRP5_{LDLRChow}) = C_T(LRP5_{LDLRChow}) - C_T(GAPDH_{LDLRChow})$

$\Delta C_T(LRP5_{WTFat}) = C_T(LRP5_{WTFat}) - C_T(GAPDH_{WTFat})$

and $\Delta C_T(LRP5_{WTChow}) = C_T(LRP5_{WTChow}) - C_T(GAPDH_{WTChow})$

The C_T value for each genotype and diet was measured in triplicate, and the mean C_T used for analysis.

Primers were modified to generate smaller products for LRP5 and GAPDH, in the optimal size-range for real time RT-PCR of 50-150 bp. Reaction conditions were optimised accordingly.

	Primer	Sequence (5' - 3')	Product size
LRP5	Sense	CTA GAT GGG AGA GAT CGG CA	138 bp
	Antisense	TCC CGT CTA TGT TGA TCA CCT CG	
Gapdh	Sense	AAC GGA TTT GGC CGT ATT GGC CGC	150 bp
	Antisense	GTG CCG TTG AAT TTG CCG TGA GTG	

Table A.2 Characteristics of primers for LRP5 and GAPDH used for Real Time RT-PCR. See text for full explanation.

Aortic samples from two *ldlr* $^{-/-}$ animals fed chow, three *ldlr* $^{-/-}$ animals fed high fat, and three WT animals fed each diet were analysed for LRP5 and GAPDH (11 animals in all). Each sample was analysed in triplicate. For each sample, expression of LRP5 was normalised to the expression of GAPDH by comparing the mean difference in number of cycles required to reach a preset amplification threshold for each product. The mean of these normalised values was derived for each of the four animal groups defined by genetic lesion and diet. The normalised values for fat-fed animals were then expressed as a ratio relative to chow-fed animals for each genotype.

A.4 Results

RT-PCR was used to define the expression of LRP5 if any in tissues of *ldlr*$^{-/-}$ mice in relation to high fat diet or feeding with regular chow. Widespread expression of LRP5 was confirmed in a number or organs of animals fed high fat diets, including spleen, kidney liver and aorta (Figure A.1). Aortic expression of LRP5 was detected in none of the chow-fed animals, but all (3/3) of the animals on the high fat diet. Expression was not detected in lung, liver or colon, even with higher amounts of mRNA template and more cycles, irrespective of diet. Tissue assays by RT-PCR were not performed on sample from WT animals.

Further quantification of these findings was performed in aortic tissues by Real time RTPCR. This showed increased expression of LRP5 in aorta from both *ldlr*$^{-/-}$ and WT animals when fed the high fat diet (Figure A.2A). In *ldlr*$^{-/-}$ the increase was estimated to be 1600-fold, and in WT animals 200-300 fold. While the standard deviations of these estimates are large, reflecting sample size, they do not span zero, and suggest that an up-

regulation is occurring. The high ratio for *ldlr*$^{-/-}$ tissue may in part reflect the low levels seen in chow-fed animals. When comparing the effect of genotype on LRP5 expression under each dietary condition, WT animals surprisingly appeared to have higher levels of expression with both high fat and chow. However, the ratios are not large, and standard deviations overlap zero, such that confidence in these findings must be low.

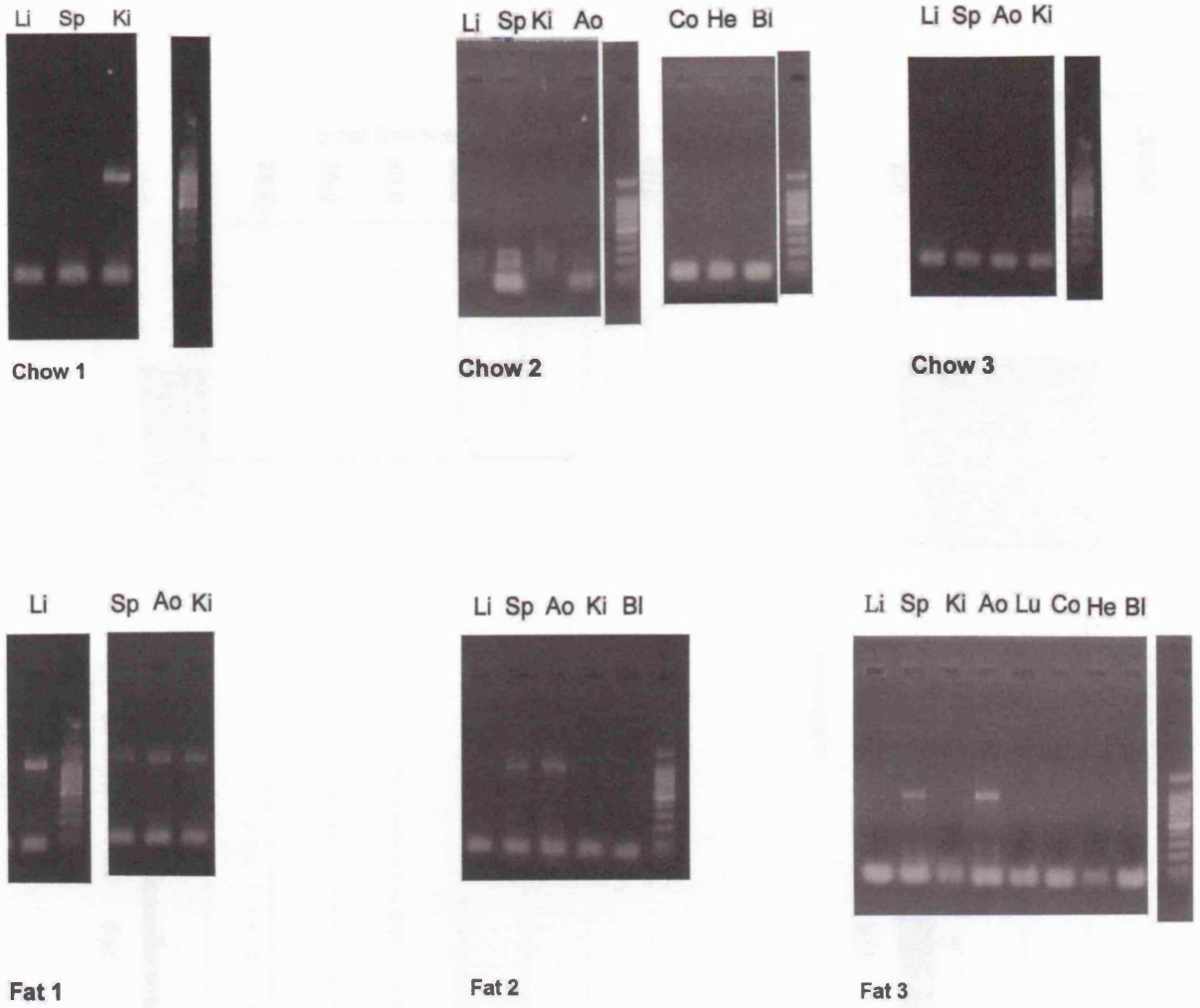

Figure A.1 Representative RT-PCR gels showing LRP5 mRNA expression in *ldlr*$^{-/-}$ mice. Bands are seen at 900bp in liver and kidney of one chow fed animal, and in liver, spleen and aorta variously in fat-fed animals. Aortic expression is seen in all three of these animals. All lanes containing template demonstrated bands for GAPDH (Not shown) Li, liver; Sp, spleen; Ki, kidney; Ao, aorta; Co, colon; He, heart; Lu, lung; Bl, blank.

A

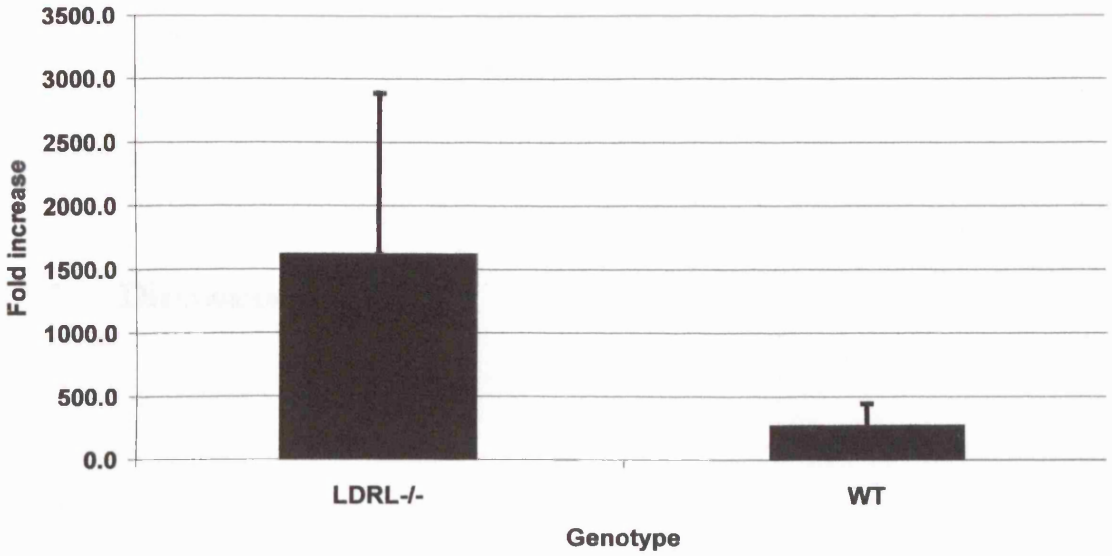

B

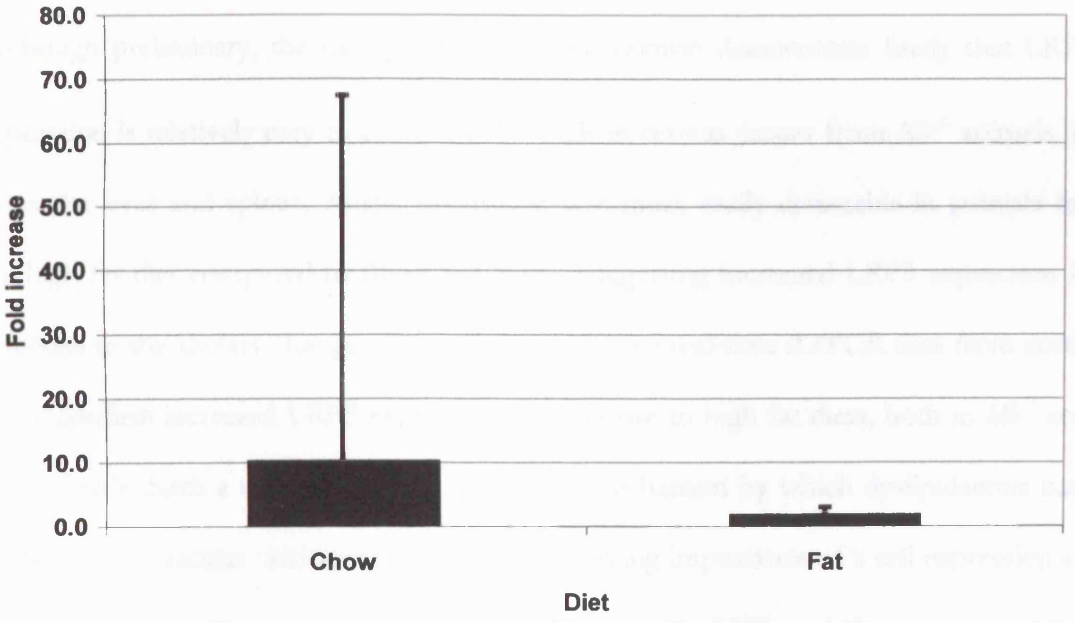

Figure A.2 Quantitative estimates of increase in LRP5 expression in Aortic tissue. A. Comparison between Fat-fed and chow fed animals in each genotype. **B.**Comparison between Wild type and *ldlr*$^{-/-}$ mice with diet. Each data point expressed as mean ± SD, n=3

A.5 Discussion

Although preliminary, the data presented in this section demonstrate firstly that LRP5 expression is relatively easy to detect by RT-PCR in certain tissues from *ldlr*$^{-/-}$ animals, in particular liver and spleen. Aortic expression was more easily detectable in animals fed the high fat diet compared to those fed chow, suggesting increased LRP5 expression in response to this dietary change. Secondly, quantitative real-time RTPCR data from aortic tissue confirm increased LRP5 expression in response to high fat diets, both in *ldlr*$^{-/-}$ and WT animals. Such a change suggests a possible mechanism by which dyslipidaemia may contribute to vascular calcification, given the emerging importance of a cell expressing an osteoblastic phenotype in the vasculature in the context of VC, and the requirement for LRP5 expression in normal osteoblast function. Further, the links between Wnt and BMP signalling pathways suggests that LRP5 expression may be relevant both to the manifestation of BMP7 deficiency in the context of CRF and to the response to therapy. It is known that cooperativity exists between Wnt and TGFß superfamily signalling in models of renal fibrosis, through augmentation of the nuclear effects of co-Smad4.

Changes in Wnt signalling mediated by changes in LRP5 expression would be expected to exaggerate any imbalance between TGFß and BMP7 in this setting, and equally may augment the biological response to BMP7 administration for similar reasons.

While these data are preliminary in nature, and care needs to be taken in drawing conclusions, it seems reasonable to conclude that LRP5 expression occurs in aortic tissues and that diet may influence the regulation of this, and as such control of LRP5 expression and function seems to be an area deserving further investigation

Appendix B

Publications and presentations to major meetings resulting from this thesis

B.1 Publications

1. **Davies M.R**. and Hruska K.A. Pathophysiological mechanisms of vascular calcification in end-stage renal disease. *Kidney Int*, 2001; 60: 472-479.
2. Lund R. J., **Davies M. R**. and Hruska K. A. Bone morphogenetic protein-7: An anti-fibrotic morphogenetic protein with therapeutic importance in renal disease. *Curr Opin Nephrol Hypertens*, 2002; 11: 31-36.
3. **Davies M.R.**, Lund R.J. and Hruska K.A. BMP-7 is an efficacious treatment of vascular calcification in a murine model of atherosclerosis and chronic renal failure. *J Am Soc Nephrol*, 2003; 14: 1559-1567.
4. Lund R.J., **Davies M.R.**, Brown A.J. and Hruska K.A. Successful treatment of an adynamic bone disorder with bone morphogenetic protein-7 in a renal ablation model. *J Am Soc Nephrol*, 2004; 15: 359-369.
5. **Davies M. R.**, Lund, R.J., Mathew, S., Hruska, K. A. Low Turnover Osteodystrophy and Vascular Calcification are Amenable to Skeletal Anabolism in an Animal Model of Chronic Kidney Disease and the Metabolic Syndrome. *J Am Soc Nephrol*, 2005. 16: 917-928.

B2 Presentations and Abstracts

Presenting author underlined.

1. **Davies M.R.**, Petrosova T. and Hruska K.A. BMP-7 is an effective treatment for vascular calcification in chronic kidney disease (CKD), at the annual meeting of *The American Society of Nephrology*, 2001. San Francisco CA: J Am Soc of Nephrol. (Poster)

2. **Davies M.R.**, Lund R.J. and Hruska K.A. BMP-7 reduces vascular calcification and improves hypertension in a murine model of uremia, at the annual meeting of *The American Society of Nephrology*, 2002. Philadelphia, PA: J Am Soc Nephrol.(Oral presentation)

3. **Davies M.R.** and Hruska K.A. Bmp-7 reduces calcification by calcifying vascular cells, at the annual meeting of *The American Society of Nephrology*, 2002. Philadelphia PA: J Am Soc Nephrol (Poster)

4. Hruska K.A., **Davies M.**, Lund R., Chen Q., Wang S., Petrosova T., et al. Replacement of bmp-7, a renal hormone deficient in chronic kidney disease, at the *1st European Conference on Bone Morphogenetic Proteins,* 2001. Zagreb (Oral presentation).

5. Lund R., **Davies M.**, Huq N. and Hruska K. Chronic kidney disease (CKD) directly produces an adynamic bone disorder which can be successfully treated with BMP-7, at the annual meeting of *American Society of Bone and Mineral Research.* 2002. San Antonio TX (Oral presentation).